Summer 7-2020

# The Role of Postnatal Adrenergic Manipulation in the Mediation of Fetal Programming Adaptions in Growth and Skeletal Muscle Glucose Metabolism That Persist in the Juvenile IUGR-born Lamb

Rachel L. Gibbs
*University of Nebraska - Lincoln*, rachel.gibbs@huskers.unl.edu

# THE ROLE OF POSTNATAL ADRENERGIC MANIPULATION IN THE MEDIATION OF FETAL PROGRAMMING ADAPTIONS IN GROWTH AND SKELETAL MUSCLE GLUCOSE METABOLISM THAT PERSIST IN THE JUVENILE IUGR-BORN LAMB

by

Rachel L. Gibbs

A THESIS

Presented to the Faculty of

The Graduate College at the University of Nebraska

In Partial Fulfillment of Requirements

For the Degree of Master of Science

Major: Animal Science

Under Supervision of Professor Dustin T. Yates

Lincoln, Nebraska

July 2020

# THE ROLE OF POSTNATAL ADRENERGIC MANIPULATION IN THE MEDIATION OF FETAL PROGRAMMING ADAPTIONS IN GROWTH AND SKELETAL MUSCLE GLUCOSE METABOLISM THAT PERSIST IN THE JUVENILE IUGR-BORN LAMB

Rachel LeeAnn Gibbs, M.S.

University of Nebraska, 2020

Advisor: Dustin T. Yates

Our 1st study assessed growth deficits in IUGR juvenile lambs and the benefits of treatment with adrenergic and inflammatory mediators. Growth metrics including bodyweight, rate of gain, and crown-rump length were diminished by placental insufficiency-induced IUGR through 2 mo. of age but were recovered by daily clenbuterol or curcumin supplementation. Body composition metrics indicated by bioelectrical impedance, proximate analysis, and loin size revealed that fat-free lean mass, specific muscle group sizes, and protein-to-fat ratios were reduced in unsupplemented IUGR lambs but recovered to or even past controls in clenbuterol-supplemented lambs. From these findings, we conclude that IUGR impairs postnatal growth and body composition through the juvenile stage, but postnatal treatment with clenbuterol or curcumin effectively recovered some aspects of diminished growth and improved body composition in IUGR lambs.

Our 2nd study determined whether IUGR-induced fetal programming previously observed in skeletal muscle glucose metabolism and pancreatic β cell function progressed in juvenile-aged offspring and whether postnatal adrenergic modification via daily clenbuterol injection improves these deficits. Juvenile IUGR lambs continued to exhibit

reduced skeletal muscle glucose oxidation and glucose-stimulated insulin secretion (GSIS). Clenbuterol effects on glucose metabolism in IUGR muscle varied. *In vivo* hindlimb glucose uptake and oxidation were improved by clenbuterol, but *ex vivo* glucose uptake was not improved and *ex vivo* glucose oxidation was further reduced in clenbuterol-supplemented IUGR primary muscle. Clenbuterol also recovered GSIS in IUGR lambs. Thus, results suggest that IUGR adaptions in insulin-stimulated glucose metabolism progress through the juvenile age. Furthermore, clenbuterol supplementation is effective when administered daily but loses its effect when removed.

Our 3rd study sought to determine the impact of stress on BIA-estimated body composition in neonatal IUGR-born lambs and in heat-stressed feedlot wethers. The BIA successfully detected changes in fat-free mass and fat-free soft tissue in IUGR neonatal lamb at 25 d of age and in heat-stressed wethers but not in IUGR lambs at 3 d of age. The BIA, however did not detect differences in nutrient or specific muscle group mass in either cohort. Thus, we conclude that BIA reasonably estimates stress-induced changes in lamb body composition, except in very young animals.

**Acknowledgments**

Never would I have imagined the experience and knowledge I would gain as a graduate student in the Yates lab. This opportunity has been an incredible journey that I am blessed to be able to continue. I would like to express my greatest gratitude to my major advisor Dr. Dustin Yates for his unwavering support. Dustin, despite all of your corny dad jokes, you are remarkable mentor, leader, and advisor and I feel lucky to be able to learn from one of the best. Don't worry, I'll make sure to have your red pen drawer stocked. You'll need it!

I would also like to thank my committee members Dr. James Wilson and Dr. Ty Schmidt for their guidance and support throughout my program. Both Dr. Wilson and Dr. Schmidt provided essential assistance with various techniques that were a large part of my metabolic and body composition research. I also appreciate their willingness to reach out to ensure my success in and outside of the classroom.

To my fellow lab mates and graduate students, I would never be able to thank each of you enough for your unending support, dedication, and guidance. Countless nights spent feeding baby lambs and weekends full of research are only a couple of times where I'm sure you wanted to kill me, but I can assure you that your hard work and dedication to my success were never unnoticed. I'm grateful to know each of you and will always cherish all the memories that were made and those that will be made.

Finally, no group of people deserve this gratitude more than my family. I have been blessed with an incredible support system that fuels my determination and hard work. Dad, thank you for being an incredible role model and instilling in me the drive and passion to follow my dreams. God bless Cindy for keeping you in line while I'm 12 hours away, lol!

Trevor, even though you never call me… I know you miss me! Lastly, Kyle you have put up with way more than one ever should and continue to stand by me every day. Thank you for always finding a way to make me laugh (even when I'm irrationally angry) and loving me endlessly.

# Table of Contents

## Chapter 1: Literature Review

# List of Figures

## Chapter 1



## Chapter 2

## Chapter 3

# List of Tables

## Chapter 2



## Chapter 4

# Chapter 1

# Literature Review

## Introduction

Maternofetal stress during critical windows of fetal development alters intrauterine conditions, restricts fetal and neonatal growth, and programs metabolic thrift due to the deficient nutritional environment in which fetal development occurs. Prenatal programing was first described by Hales and Barker (1992) in their "Thrifty Phenotype Hypothesis," which states that a poor intrauterine environment causes adaptive developmental programming that leads to decreased birthweight and an increased risk of metabolic diseases in adulthood. Subsequently, researchers have strived to understand the underlying mechanisms for developmental programming of growth and metabolic deficits associated with low birthweight, but the gap in knowledge remains. Intrauterine growth restriction (IUGR) is the result of nutrient-sparing metabolic and growth adaptations by the fetus in response to prenatal stress. These adaptions aid fetal survival at the expense of less vital peripheral tissues such as skeletal muscle. This leads to disruptions in muscle growth, glucose metabolism, insulin signaling, and body composition, all of which contribute poor postnatal growth and metabolic health (Limesand et al., 2007a; Brown et al., 2015; Yates et al., 2016; Cadaret et al., 2018; Posont et al., 2018). Fetal adaptions that stem from IUGR continue to be evident throughout the neonatal stage by consistently reduced muscle mass and poor oxidative metabolism (Cadaret et al., 2018; Cadaret et al., 2019b; Cadaret et al., 2019c). Using a well-characterized IUGR ovine model, we have reported that previously identified fetal

growth and metabolic pathologies persist in the neonate, but the progression of these deficits between the neonatal and juvenile growth stages are unclear, and there is limited information about potential avenues for postnatal treatment of IUGR pathologies.

## Intrauterine Growth Restriction

### *Placental Insufficiency Induces IUGR*

Intrauterine conditions that result in IUGR elicit *in utero* fetal programming that impairs peripheral insulin sensitivity and insulin secretion. This impairment leads to an increased risk for early onset obesity, hypertension, and Type II diabetes later in life (Hales et al., 1991). Together, these adaptions lead to 18-fold greater likelihood of Metabolic Syndrome for IUGR-born individuals (Barker et al., 1993; Gatford et al., 2010).

Placental insufficiency can be the result of a multitude of different maternal factors related to stress, such as harsh environmental conditions for livestock and poor dietary lifestyle choices in humans and is the most common cause for IUGR (Yates et al., 2018b). Placental insufficiently is characterized by changes in placental function and structure that reduce nutrient transfer to the fetus including 1) decreased placental oxygen permeability (Limesand et al., 2018), 2) reduced placental transporters for glucose and amino acids (Brown et al., 2011; Lin et al., 2014), and 3) poor vascularity and increased placental vasculature resistance (Baschat et al., 2001; Cheema et al., 2006). The effects of placental insufficiency on the fetus increase as the pregnancy progresses through the third trimester because the fetus increasingly outgrows the capacity of the stunted placenta (Limesand et al., 2018). With the fetus nutritional needs inadequate for optimal

development, the fetus becomes increasingly hypoxemic and hypoglycemic (Yates et al., 2018b). This in turn causes chronic fetal stress, which is characterized by increased secretion of catecholamines (norepinephrine and epinephrine) from the fetal adrenal medulla (Yates et al., 2014) and greater circulating inflammatory cytokines such as tumor necrosis factor α (TNFα) (Cadaret et al., 2019b) and Interleukin-6 (IL-6) (Raghupathy et al., 2011). Increased circulating norepinephrine and epinephrine in IUGR fetuses induces the redistribution of fetal blood flow and nutrients to vital organs such as the brain, heart, and lungs and away from less vital tissues such as skeletal muscle (Alexander et al., 1987; Morrison, 2008). This redistribution decreases hindlimb blood flow by almost 50% (Rozance et al., 2018), ultimately decreasing nutrient availability for muscle growth and energy production. Diminished prenatal muscle mass contributes to low birthweight and furthermore is correlated with reduced percentage of lean mass later in life (Gibbs et al., 2019; Gibbs et al., 2020). Greater circulating fetal catecholamines also decrease pancreatic islet development by reducing β cell mass (Limesand et al., 2005). This reduction in β cell mass impairs the secretion of insulin, and thus hypoinsulinemia is also present in IUGR fetuses (Leos et al., 2010; Macko et al., 2016a). Following parturition, nutrient and oxygen availability is restored and catecholamine and cytokine blood concentrations are less elevated. Consequently, IUGR neonates become transiently hyperinsulinemic, which causes the dangerous perinatal hypoglycemic condition in IUGR newborns (Camacho et al., 2017; Limesand et al., 2018) and necessitates glucose supplementation (Camacho et al., 2017).

*IUGR Reduces Survival & Value in Livestock*

In all livestock species, IUGR increases neonatal mortality and morbidity due to diminished vigor at birth (Wu et al., 2006). Intrauterine growth restriction has been reported to occur in approximately 10% of livestock, but the frequency can increase substantially during certain conditions (Wu et al., 2006). Entire herds of livestock may be affected by IUGR during chronic heat stress events, forage toxicity, or environmental drought, whereas shorter-term stress events may only affect pregnant animals that are within certain critical windows for fetal development at the time of stress. Regardless, IUGR has far-reaching implications for animal welfare and economic sustainability due to the increase in perinatal death loss and the diminished health and vigor of surviving offspring (Mellor, 1983). Producers are even more economically impacted by poor growth performance and carcass merit in surviving IUGR offspring (Smith et al., 1995; Gardner et al., 1998). Livestock impacted by IUGR exhibit increased fat deposition and decreased muscle growth (Greenwood et al., 1998) leading to carcasses with smaller high-value cuts and increased fat trim (Greenwood et al., 2000). Increased visceral fat deposition is independent of reductions in muscle mass (Desai and Ross, 2011), the latter of which is limited by reduced muscle stem cell function (Yates et al., 2014; Posont et al., 2018) and subsequent muscle fiber hypertrophy (Yates et al., 2016). Rather, increased adipose deposition is likely due to an upregulation of the adipogenic PPARγ pathway (Desai and Ross, 2011) and/or disruption of fatty acid mobilization, both of which can lead to increased circulating free fatty acids (Beard et al., 2018). Along with poor carcass merit, IUGR livestock have decreased growth efficiency and rates of gain, leading to the need for extended time on feed to reach optimal harvest weight (Hegarty and Allen,

1978; Gondret et al., 2005; De Blasio et al., 2007). As such, IUGR-born livestock compound the challenge described by Canton & Hess (2010) that results when body weight and age are the only available measurements to determine dietary rations and time of harvest for groups of livestock. Nutritional management decisions based on these limited criteria can lead to a wide variation in body composition under normal conditions but are particularity ineffective for IUGR-born animals. When nutrition is not reconciled with thrifty IUGR metabolic programming, increased fat-to-muscle ratios and wasted feed input occur (Wigmore and Stickland, 1983).

Less-than-desirable body composition and product uniformity in IUGR livestock lead to costly merit and yield discounts for producers at harvest, which can impede economic sustainability of a production system (Boleman et al., 1998). On average, IUGR-born offspring cost the US livestock industry 8% of its total annual product, which includes death loss of over 3 million beef calves, 930,000 dairy calves, and 580,000 lambs (Wu et al., 2006) and lost revenue of up to $12.1 billion each year (USDA, 2017). Despite the well-documented economic impact of IUGR, minimal advancements have been made toward prevention or treatment strategies to offset growth and metabolic deficits in IUGR-born livestock.

*Sheep Are a Valuable Model for IUGR*

Intrauterine growth restriction has a multi-factorial etiology that impacts essentially all mammalian species, and our understanding of IUGR has benefitted from the many different animal models used to study the associated pathologies and mechanisms (Beede et al., 2019). Early research in the field utilized smaller animals such

as rabbits and rodents models, but most of the recent advancements in our understanding of IUGR has been gained through the use of ovine models. Sheep prove to be an efficient and effective dual-purpose model for biomedical and agricultural intrauterine research due to relative similarities in fetal developmental milestones compared to both humans and beef cattle (Yates et al., 2011a; Yates et al., 2012a; Posont et al., 2018; Yates et al., 2018b; Beede et al., 2019). The ovine fetus also tolerates *in utero* surgical and experimental manipulation, making sheep the ideal species for fetal research (Yates et al., 2011a; Yates et al., 2012a; Posont et al., 2018; Yates et al., 2018b; Beede et al., 2019). Researchers have developed a multitude of techniques to induce fetal and placental growth restriction in order to develop models that best suit their research needs.

*PI-IUGR.* Maternal hyperthermia-induced placental insufficiency (PI) is the most common and best-characterized sheep model for IUGR. To create this model, pregnant ewes are exposed to ambient temperatures of 40°C with a relative humidity of 35% during peak placental development from the 40$^{th}$ to the 95$^{th}$ day of gestational age (dGA) (Cadaret et al., 2019b). This model reliably and consistently stunts the placenta, causing up to a 60% reduction in fetal growth at term (Brown et al., 2015; Macko et al., 2016a; Limesand et al., 2018). It is important to note that placental stunting in this model is due to the natural development of poor placental vasculature and restricted placentome size rather than decreased number of placentomes, which leads to the increased fetal-to-placenta mass ratio (Morrison, 2008). Reduced placental size combined with reductions in placental vasculature and nutrient transporters leads to the severity of this model, which can be controlled by the number of days for which ewes are exposed to hyperthermia (Galan et al., 2005).

*MI-IUGR.* Maternofetal inflammation (MI), a model recently developed in sheep by our lab, has been used to mimic the sustained inflammation associated with conditions such as obesity or illness during gestation (Cadaret et al., 2018; Posont et al., 2018; Cadaret et al., 2019b). It is created via serial maternal IV injections of the bacterial endotoxin, *E.coli* lipopolysaccharide (LPS), every 72 hours during the first 15 days of the 3rd trimester (Cadaret et al., 2019b). This stimulates a chronic maternal and fetal inflammatory response that is marked by increased circulating leukocytes and Tumor Necrosis Factor alpha (TNFα) concentrations that persist well after LPS injections are discontinued (Cadaret et al., 2019b). As one response to maternofetal inflammation, fetuses near term exhibit an increase in skeletal muscle cytokine receptors and pathway sensitivity that appear to contribute to the impaired capacity for muscle growth and metabolism (Posont et al., 2018; Cadaret et al., 2019b). Growth restriction in this model (~24% fetal growth restriction at term) is typically less severe when compared to the maternal hyperthermia model, but metabolic deficiencies are similar (Beede et al., 2019).

*Over/Under Nutrition.* Poor nutrition (excess or deficiency) during critical windows for placental and fetal development can stunt placental and fetal growth, although in some cases overnutrition causes fetal overgrowth (Caton and Hess, 2010) Two ovine models have been used to study the effects of maternal over and undernutrition, respectively, during gestation. The overnourished adolescent ewe model creates fetal growth restriction by supplying newly-pubertal ewes (made pregnant by embryo transfer) with 200% of the ewe's normal dietary energy requirements (Carr et al., 2012). This model causes placental insufficiency via decreased placental size rather than by reduced expression and activity of placental glucose and amino acid transporters

(Wallace et al., 2003). Placental insufficiency in this model is further compounded by increased nutrient demand of the growing adolescent dam, which also restricts nutrient availability for the fetus. In mature dams, however, the overnutrition model results in inconsistencies between fetal growth restriction and fetal overgrowth, making it difficult to model IUGR for research. At the other end of the spectrum, the nutrient restriction model is created by supplying pregnant ewes with only 60% of the ewe's normal dietary energy requirements (Lemley et al., 2011). Implementation of long-term (i.e. early through late gestation) nutrient restriction reduces fetal weights by 10-20% without obvious effects on placental development or function (Wallace, 1948; Mellor and Murray, 1982; Lemley et al., 2011).

*Surgical Placental Reduction.* Researchers also utilize surgical and mechanical techniques to reduce placental function and induce IUGR, which can offer more control of severity. The endometrial carunclectomy model involves the surgical removal of all but four of the 60 to 90 uterine caruncles prior to breeding. This reduces the number of placental attachment sites, which leads to diminished nutrient transfer and fetal growth restriction of ~26% (Zhang et al., 2016). Another surgical model uses single umbilical artery ligation (SUAL) performed in the last trimester to reduce umbilical blood flow and nutrient transfer, leading to fetal growth restriction of ~22% (Oh et al., 1975; Supramaniam et al., 2006). Finally, placental embolization can be created by embedding microspheres into the placental vasculature via placental capillary infusion, which leads to placental blood flow reduction, increased placental vasculature resistance, and fetal growth restriction of up to 66% (Lang et al., 2000; Bhide et al., 2016).

*IUGR Pathologies: Reduced Growth Capacity & Metabolic Dysfunction*

When fetal nutrient demand is not met, the fetus must adapt its developmental trajectory in order to survive. Because they alter development, these adaptive programming mechanisms have life-long consequences on growth and metabolic function, and in IUGR-born offspring these adaptions increase the risk of life-threatening health deficits (Thorn et al., 2011; Camacho et al., 2017). Studies in PI-IUGR lambs show that offspring are hallmarked by consistently-exhibited pathologies, including reduced muscle mass, asymmetric growth patterns, impaired skeletal muscle glucose metabolism, and β-cell dysfunction (Limesand et al., 2007a; Limesand et al., 2018; Yates et al., 2018b). Nutrient-sparing developmental mechanisms that cause these pathologies are critical for maintaining vital organ growth and function even though it is at the expense of skeletal muscle, which normally accounts for as much as 85% of insulin-stimulated glucose utilization (Brown, 2014). When nutrient supply is restricted, the growth of skeletal muscle facilitated by progenitor cells known as myoblasts is subsequently impaired. This is reflected in reduced myoblast function and decreased sensitivity of myogenic stimulation in IUGR-born offspring (Yates et al., 2014). Impaired hypertrophic muscle growth is evident in the near-term fetus (Yates et al., 2016) and the neonate (Posont et al., 2018; Cadaret et al., 2019b). In addition to myoblast dysfunction, protein degradation pathways are upregulated in IUGR fetuses, which mobilize amino acids to be used as energy substrates rather than for protein synthesis and accretion (Rozance et al., 2018). Restricted muscle growth is accompanied by increased glycolytic-to-oxidative fiber proportions (Yates et al., 2016), reflecting a shift in muscle metabolism that favors glycolytic lactate production rather than glucose oxidation (Limesand et al.,

2007a; Brown et al., 2015). This is supported by studies performed by our lab in which IUGR fetuses and neonates exhibited diminished skeletal muscle glucose oxidation independently of their capacity for glucose uptake or utilization (Cadaret et al., 2019b; Cadaret et al., 2019c; Posont, 2019). Glucose metabolism in IUGR offspring is further compromised by reduced pancreatic β-cell mass and islet function. Proper glucose-stimulated insulin secretion from β-cells is critical for insulin-stimulated glucose metabolism and glucose homeostasis. However, IUGR pancreatic islets are characterized by decreased size and β-cell proliferation (Limesand et al., 2005), impaired development of islet microvasculature (Lee and Hennighausen, 2005; Kostromina et al., 2013), reduced islet insulin content (Limesand et al., 2006; Limesand et al., 2007a), and reduced capacity for glucose-stimulated insulin secretion (Limesand et al., 2006; Limesand et al., 2007a). Adaptions affecting skeletal muscle growth and metabolism in the IUGR fetus contribute to poor later-life health, but it has yet to be determined how these pathologies progress between the neonatal and the juvenile stages and whether the latter is an effective window for postnatal intervention.

## ***Components of Body Composition***

### *Skeletal Muscle Development*

Body composition is an important parameter of health in humans and livestock. In addition, body composition is also a determining factor in the carcass value of livestock. It is largely dependent on proper development of skeletal muscle and adipose tissues. Skeletal muscle is a dynamic tissue that not only facilitates structural movement of the body but also plays a key role in glucose homeostasis and metabolic efficiency (Brown,

2014). Skeletal muscle mass accounts for roughly 40% of body mass in humans and 50% of in livestock, and primarily consists of the muscles that make up the head, limbs, and trunk of the body (Gunn, 1989; Kim et al., 2016). Myogenesis is the multistep physiological process in which muscle develops during fetal development for most mammalian species, although it continues into the neonatal stage for some litter-bearing species (Bentzinger et al., 2012). Myogenesis involves sequential expression of a series of myogenic regulatory factors (MRF) that are transcription factors that specifically regulate myogenic gene expression responses (Soto et al., 2017). These factors also serve as biomarkers for regulating the progression of myoblast stages. This process is activated during embryonic development by signaling from surrounding tissue, primarily the dermomyotome or neural tube, and begins with the expression of paired box transcription factors including Pax 7 within certain somite cells (Buckingham and Relaix, 2015). These Pax $7^{+}$ cells migrate from the somite to muscle development sites in the embryo where cells proliferate until exiting the cell cycle for myogenic differentiation (Buckingham and Relaix, 2015). Pax $7^{+}$ expression is then co-expressed with the initial expression of myogenic factor 5 (Myf5) and the later expression of myogenic determining factor 1 (MyoD) that mark these cells as muscle precursors (Du et al., 2010). The expression of Myf5 and MyoD resign these formerly multipotent cells to a myogenic fate by committing the cell into muscle stem cells or myoblasts (Haldar et al., 2008). Proliferating myoblasts exit the cell cycle following the increased expression of MyoD and myogenin, which signify terminal differentiation of the myoblast. Differentiated myoblasts are capable of fusion into multinucleated myofibers within early embryonic development (Edmondson and Olson, 1993). As myoblasts differentiate in preparation for

fusion, myoblasts begin production of desmin, a type III myofilament. Desmin contributes to the structural integrity and sarcomere development of myofibers (Li et al., 1997) and is also a hallmark biomarker of fully-differentiated myoblasts.

*Skeletal Muscle Fiber Types*

Skeletal muscle fibers can be classified in several ways. One common categorization is by their metabolic properties that correspond to the myosin heavy chain (MyHC) isoform that they express. In mammals, most skeletal muscle groups have heterogeneous populations of the three fiber types: Types I, IIa, and IIx, (IIb is the fourth fiber type observed in rodents). Fibers of different types are differentiated by contractile speed and metabolic function, and over time fibers can transition between types in order to maintain appropriate metabolic function (Pette and Staron, 1997; Brown, 2014). Type I fibers are slow twitch red fibers and contain elevated amounts of myoglobin that contribute to Type I high oxidative capacity. Type I fibers utilize oxidative phosphorylation as the primary pathway for metabolism, which is ideal for low-input, high duration contractile activity (Scott et al., 2001). Type IIx fibers are white, fast twitch fibers that rely primarily on glycolytic metabolism, providing power but are inefficient and highly susceptible to fatigue (Schiaffino and Reggiani, 2011).Type IIa fibers are fast twitch, red fibers that posess both glycolytic and oxidative metabolic capability. Type IIa fibers represent an intermediate form between Type I and Type IIx fibers and are the most dynamic regarding the utilization of energy sources during short duration, high contractile activity (Pette and Staron, 1990).

*Skeletal Muscle Growth*

The completion of muscle hyperplasia prior to birth limits postnatal muscle growth to hypertrophy (i.e. increased diameter and length) of existing myofibers (Gollnick et al., 1981; White et al., 2010). Postnatal muscle growth (hypertrophy) requires the establishment of muscle stem cell populations during fetal myogenesis. A subset of myoblasts do not differentiate but rather become quiescent satellite cells (Schultz, 1989). These satellite cells migrate to the basal lamina of myofibers and remain in the quiescent state until activated (Collins et al., 2005). To facilitate muscle growth, quiescent satellite cells are activated and return to the cell cycle (*i.e.* proliferate), differentiate, and eventually fuse with existing muscle fibers (Gibson and Schultz, 1983; Collins et al., 2005; Zammit et al., 2006). This increases the fiber's myonuclear content and thus its capacity for protein synthesis and growth. A subset of activated cells self-renew the muscle stem cell pool following proliferation by again becoming quiescent satellite cells (Zammit et al., 2006).

Protein cycling is the combined fluxes of protein synthesis and protein degradation that help to balance fiber size with nutrient availability. These fluxes are determined by nutrient levels, growth factors, and activity of skeletal muscle (Paul and Rosenthal, 2002; Lai et al., 2004). Skeletal muscle hypertrophy occurs when protein synthesis exceeds protein degradation, leading to structural protein accumulation (Adams and Haddad, 1996). Protein synthesis is particularly responsive to insulin and insulin growth factor I (IGF-I), which signal in part through mammalian target of rapamycin (mTOR)-mediated pathways (Vandenburgh et al., 1991; Rommel et al., 2001). When insulin or IGF-I bind to respective tyrosine kinase receptors on the plasma membrane of

muscle, it results in phosphorylation of insulin receptor substrate 1, which initiates the activation sequence of phosphoinositide 3-kinase and then protein kinase B (Akt) (Sandri et al., 2013). Akt stimulates mTOR complex 1 (mTORC-1), which in turn activates ribosomal protein S6 kinase to increase protein synthesis and thus myofiber growth (Bodine et al., 2001; Rommel et al., 2001). mTORC-1 also inhibits kinases involved in muscle protein degradation (Zhang et al., 2014). Protein degradation is a mechanism for providing amino acids as substrates for metabolism when availability of carbohydrates or fatty acids is diminished. It is primarily facilitated by the ubiquitin proteasome pathway that marks proteins for degradation by attaching ubiquitin chains (Rock et al., 1994). This "flagging" step initiates the ATP-dependent catabolic reactions that break down large proteins into small peptides and, ultimately, into individual amino acids (Hadari et al., 1992). Once amino acids are deaminated, the carbon skeleton can then be used by the muscle cell as an energy substrate. Amino acids often affect protein fluxes via negative feedback. For example, when the branched-chain amino acid leucine begins to accumulate due to use as an energy substrate wanes, its increased binding of leucyl-tRNA synthetase activates the downstream transcription factor RAG GTPase (Han et al., 2012), which signals via mTORC-1 to inhibit further protein degradation (Han et al., 2012).

*Adipose Tissue Development*

Adipose tissue develops from two different linages of adipocytes, brown and white, which are equally prominent within the perirenal-abdominal region during proliferative phases in early fetal development. However, the unilocular lipid-rich (white) adipocyte progress in greater abundance than the multilocular mitochondria-rich (brown)

adipocytes near term and after birth (Clarke et al., 1997; Pope et al., 2014). As adipocytes mature, brown adipocyte activation for growth and thermogenesis function is regulated by the expression of uncoupling protein 1 (UCP1) (Gemmell et al., 1972), whereas white adipocyte activation is regulated by leptin expression (Yuen et al., 2002). Adipose tissue accounts for only a small percentage of body weight at birth, but its role perinatal thermoregulation is vital. Brown adipose tissue is particularly important for thermoregulation during the perinatal period to prevent hypothermia. Heat production by brown adipose tissue is facilitated by increased UCP1 abundance in response to stimulatory factors such as increased catecholamine, cortisol, and/or prolactin concentrations near term (Symonds et al., 2000; Mostyn et al., 2002; Mostyn et al., 2003). UCP1 expression peaks shortly after birth and then gradually diminishes along with the reduction of brown adipose depots, as other thermoregulatory mechanisms such as shivering take their place (Clarke et al., 1997; Mostyn et al., 2002). The progressive loss of brown adipose tissue coincides with increased abundance of white adipose tissue under the skin and around organs (Gemmell et al., 1972; Symonds et al., 1992). The expansion of white adipose tissue may occur through hypertrophy or hyperplasia based on diet, environment, and metabolic factors. Visceral white adipose tissue predominately increases by hypertrophy of existing adipocytes (Wang et al., 2013). However, this is often linked to adipose insulin resistance and an increased risk for obesity, cardiovascular disease, and metabolic syndrome (Miyazaki and DeFronzo, 2009). Conversely, subcutaneous fat depots typically expand by hyperplasia, which is an increase in adipocyte number rather than size (McLaughlin et al., 2011). Subcutaneous white adipose tissue expansion is inversely associated with the development of insulin resistance.

Further research is warranted to determine how prenatal stress impacts white adipose tissue expansion postnatal and whether differences in visceral and subcutaneous adipocyte expansion is a factor in adipose-driven compensatory growth in IUGR-born livestock.

*Fatty Acid Mobilization & Utilization for Energy*

Adipose tissue is a reservoir for energy that the body utilizes in situations of negative energy balance. During conditions such as fasting or hypoglycemia, lipids are mobilized by the breakdown of stored triglycerides into free fatty acids (FFA), which are then released into circulation and utilized by tissues (Lafontan and Langin, 2009). Under low-nutrient conditions, increased catecholamine secretion mediates a β adrenergic response that stimulates FFA mobilization (Beard et al., 2018). In skeletal muscle, fatty acid binding proteins facilitate FFA uptake, which are oxidized upon insulin stimulation to provide energy (Pan et al., 1997). However, when FFA accumulate in muscle tissues due to being taken up at a greater rate than they are metabolized, a toxic intracellular environment is created that impairs skeletal muscle insulin signaling (Ghosh et al., 2007). Similar FFA accumulation in pancreatic islets reduces glucose-stimulated insulin secretion from β-cells (Sako and Grill, 1990), which further contributes to insulin resistance and obesity (Lelliott and Vidal-Puig, 2004).

*Bioelectrical Impedance Analysis of Body Composition*

Body condition scoring is the most common method of estimating body composition in livestock. However, this method is highly subjective and limited to

exterior assessment of fat deposition and muscle mass, which doesn't account for visceral fat depots. Quantitative measurements by bioelectrical impedance analysis (BIA) offer a more objective and repeatable method to estimate differences in whole-body protein and fat content, allowing the ability to predict the mass of whole or specific muscle groups (Berg et al., 1996). This tool is complimentary to body mass index tests in humans and has been shown to be an effective non-invasive technique. Bioelectrical impedence analysis utilizes resistance and reactance of electrical stimulation through body tissue rather than tissue biopsy to estimate whole body composition (Berg et al., 1996; Bohuslavek et al., 2002; Avril et al., 2013). More specifically, BIA has been used to predict the body composition indicators of fat-free mass (FFM), fat-free soft tissue (FFST), nutrient composition, and mass of specific muscle groups in many mammalian species (Berg et al., 1996; Bohuslavek et al., 2002; Avril et al., 2013). However, it is important to note that BIA is an estimation tool that relies on accurate species and age-specific prediction equations developed from known measurements determined by morphometric analysis.

### *Skeletal Muscle Glucose Metabolism*

Proper skeletal muscle development and growth is essential in maintaining homeostatic glucose concentrations, as skeletal muscle accounts for upward of 60% of whole-body glucose utilization, and 85% of insulin-stimulated glucose metabolism (Brown, 2014). Glucose is the primary energy substrate for muscle. Its utilization by muscle is tightly regulated by insulin, which is secreted in response to elevated blood glucose concentrations (Rommel et al., 2001; Limesand et al., 2007a). Insulin signaling

activates the canonical Akt/PI3-K pathway, which stimulates the translocation of the glucose transporter GLUT4 from the cytosol to the membrane. Once embedded, it creates a channel for glucose to enter the muscle cell down its concentration gradient (Bertacca et al., 2005) (Limesand et al., 2007a). When blood glucose is elevated, insulin also acts on the liver to inhibit hepatic gluconeogenesis (Saltiel and Kahn, 2001), further contributing to homeostatic glycemic levels. Once glucose is taken up by skeletal muscle from circulation, it is irreversibly converted to glucose 6-phosphate by hexokinase II, which prevents its flow back into circulation (da Justa Pinheiro et al., 2010). When energy demands are limited, glucose 6-phosphate is stored as glycogen, which provides a local source of energy to the skeletal muscle cell (Rozance et al., 2008; Jensen et al., 2011). When energy needs increase, glucose 6-phosphate molecules are mobilized from glycogen and converted to pyruvate through a cascade of enzymatic reactions known as glycolysis. This produces 2 net ATP (Nelson and Cox, 2008). In Type 1 fibers, pyruvate is primarily metabolized into acetyl-CoA via decarboxylation or oxaloacetate by oxidative phosphorylation, both of which enter the TCA cycle (Nelson and Cox, 2008). This produces NADH & $FADH_2$, which are essential electron carriers for oxidative phosphorylation by the electron transport chain (Scott et al., 2001; Nelson and Cox, 2008). Oxidative phosphorylation is the most efficient utilization of glucose, as it generates 36 net ATP, but also leaves nothing but the waste products, $H_2O$ and $CO_2$. In Type IIx fibers, pyruvate is primarily converted to lactate, which produces a much smaller amount of ATP but also creates a metabolic substrate that can be released into the blood stream for utilization by non-muscle tissue. Normal insulin signaling and oxidative capacity in Type I and IIa fibers is imperative for proper function of skeletal muscle

glucose metabolism. Glucose deficits can lead to a shift toward less efficient modes of skeletal muscle glucose metabolism and increased production of lactate.

### *The Adrenergic System*

The adrenergic system consists of a set of signaling pathways that mediate the involuntary physiological responses to catecholamines. Epinephrine and norepinephrine produced by the adrenal medulla serve as the systemic hormone ligands for the adrenergic system by binding 7-transmembrane G-protein coupled adrenoceptors. Adrenoceptors exist in nine subtypes that are expressed in various combinations by throughout most (if not all) tissues (Ciccarelli et al., 2017). In the fetus, norepinephrine is the predominant adrenal catecholamine, and the cortisol surge at parturition stimulates a shift to predominant epinephrine production by activating the phosphorylating enzyme phenylethanolamine N-methyltransferase (PNMT) (Anthony and Henry, 2015). Ahlquist (1948) originally identified two types of adrenoceptors, α and β, that have since been further divided into $\alpha_1$A, $\alpha_1$B, $\alpha_1$D, $\alpha_2$A, $\alpha_2$B, $\alpha_2$C, $\beta_1$, $\beta_2$, and $\beta_3$ subtypes. Ligand concentrations and binding affinities for individual subtypes determine which catecholamine is most likely to activate each adrenoceptor (Anthony and Henry, 2015). In response to acute stress, signals from the sympathetic nervous system stimulate chromaffin cells within the adrenal medulla to release catecholamines into the blood stream (De Diego et al., 2008). This process is initiated by the binding of acetylcholine to its receptor, which stimulates the opening of $Ca^{2+}$ channels on the plasma membrane. The resulting $Ca^{2+}$ influx increases intracellular cAMP and, ultimately, exocytosis of catecholamine-filled vesicles (García et al., 2006). Catecholamines then mediate

physiological responses including vasodilation and vasoconstriction as well as modification of insulin action, glucose and lipid metabolism, and pancreatic islet function (William Tank and Lee Wong, 2011).

*Adrenergic Regulation of Muscle Growth*

In skeletal muscle, the most prominent adrenoceptor subtype is $\beta_2$, but $\beta_1$ and $\beta_3$ subtypes are also expressed. $\beta_2$ adrenoceptors are typically excitatory and most commonly signal via $G\alpha_s$ proteins, activating adenylyl cyclase, which is responsible for intercellular cAMP production (Nonogaki, 2000; Yang and Tao, 2019). The accumulation of cAMP activates protein kinase A (PKA), which leads to physiological responses vital for muscle growth (**Figure 1-1**). Sustained $\beta_2$ activation increases lean muscle mass by stimulating protein synthesis and limiting protein degradation, resulting in a positive protein balance (Beermann, 2002). This is primarily accomplished through the activation of Akt and its downstream protein synthesis mediator, mTORC1 (Bodine et al., 2001). $\beta_2$ adrenoceptors also mediate vasodilation of arterioles in skeletal muscle, allowing for increased blood flow to supply the necessary nutrients for hypertrophy (Kaur et al., 2014).

*Adrenergic Regulation of Metabolism*

The adrenergic system also plays a role metabolic regulation. Adrenoceptors in pancreatic islets, skeletal muscle, and adipose tissues mediate changes in the metabolic fate of nutritional substrates (Nonogaki, 2000). Within skeletal muscle, acute activation of $\beta_2$ adrenoceptors decreases glucose uptake and increases glycogen breakdown by

glycogenolysis (Anthony and Henry, 2015). This is important in hypoglycemic conditions, as glucose mobilized by glycogenolysis can be used by the muscle or secreted as lactate and taken up by the liver for gluconeogenesis in a process known as the Cori Cycle (Rozance et al., 2008). Despite reducing glucose uptake, $\beta_2$ adrenoceptors stimulate skeletal muscle glucose oxidation both in the presence and in the absence of insulin (Cadaret et al., 2017). Signaling through $\beta_1$ and $\beta_3$ adrenoceptors in adipose tissue decreases glucose uptake in adipocytes and induces lipolysis, thus mobilizing free fatty acids that can be utilized by skeletal muscle and other tissues for β-oxidation (Beard et al., 2018; Yang and Tao, 2019). In the liver, activation of $\beta_1$ and $\beta_2$ receptors stimulate glycogenolysis and increase glucose production, fatty acid breakdown, and ketone body formation (Anthony and Henry, 2015). These metabolic shifts collectively result in increased blood glucose, ketone body, free fatty acid, lactate, and glycerol concentrations. This helps re-appropriate the supply of energy substrates to vital organs at the expense muscle and other peripheral tissues (Nonogaki, 2000).

In pancreatic islet β cells, α and β adrenoceptors play differing roles in maintaining glucose homeostasis. Under fasting conditions, elevated catecholamines inhibit insulin secretion predominantly via $\alpha_2$ adrenoceptors, which prevent adenylyl cyclase-induced exocytosis of insulin vesicles (Chen et al., 2017). In response to low blood glucose, $\beta_2$ adrenoceptors located on pancreatic islet α cells stimulate glucagon secretion to increase blood glucose through glycogenolysis, facilitating the return of homeostatic blood glucose levels (Limesand et al., 2006).

## *The Inflammatory System*

### *Inflammatory Signaling*

Inflammation is among the first defense mechanisms for the immune system but is also an important regulator of metabolism and other physiological functions. Inflammatory mediators initiate responses through a series of chemical intracellular signaling pathways (Chen et al., 2018). Toll-like receptors (TLR) on the surface of cells are activated by pathogen-associated molecular patterns (PAMPS) or other factors and modulate intracellular signaling necessary for phagocytosis and other responses associated with inflammation. Cytokines, which are small signaling proteins secreted by numerous cell and tissue types, are primary contributors to the inflammatory response by binding to specific receptors, which activate intracellular signaling pathways for inflammation (Chen et al., 2018). Key components of many inflammatory cytokine pathways include Nuclear Factor κ-B (NFκB), mitogen-activated protein kinase (MAPK), and Janus kinase (Jak)-signal transducer and activator of transcription (STAT) (Rawlings et al., 2004; Bollrath and Greten, 2009).

Nuclear Factor κ-B is a major hub of multiple inflammatory signaling pathways, including those initiated by TLR4, TLR2, and TLR6 as well as the cytokines interlukin-1β (IL-β), IL-6, and TNFα (Chen et al., 2018). Downstream proinflammatory mediator, NFκB, can be activated through two separate IκB kinase (IKK) complex subunits that respond to distinct stimulants and act on different regulatory complexes (Bollrath and Greten, 2009). The IKK complex consists of two kinase subunits, IKKα and IKKβ, coupled with a regulatory subunit IKKγ (Lawrence, 2009). The canonical NFκB pathway is preferentially activated by TNFα, IL-β, and TLR and is mediated by IKKβ and IKKγ.

The NFκB pathway ultimately increases cytokines and other inflammatory factors by activating RelA/p50 dimerization (Bollrath and Greten, 2009; Lawrence, 2009). TNFα-induced IKK activation is predominantly facilitated by TNF receptor 1 (TNFR1) signaling complex but can also be stimulated by a second receptor, TNFR2, in some tissues. Activation of TNFR1 stimulates the recruitment of adaptor proteins such as tumor necrosis factor receptor-associated factors (TRAF) and Tumor Necrosis Factor-Associated Death Domain (TRADD), which are necessary for the IKK phosphorylation that leads to canonical NFκB activation. The non-canonical pathway for NFκB activation is typically stimulated by other members of the TNF-superfamily such as TWEAK, lymphotoxin β (LB), or β-cell Activating Factor (BAFF) (Bollrath and Greten, 2009). The non-canonical NFκB pathway is mediated by the IKKα subunit and increases gene expression associated with long-term cell survival by activating RelB/p52 dimerization (Lawrence, 2009). Lipopolysaccharides can also activate the non-canonical NFκB pathway through TLR4 (Chow et al., 1999; Faure et al., 2001). This pathway involves the activation of mitogen-activated protein kinases, which are responsible for subsequent increases in cytokine production (Cadaret et al., 2019b).

### *Inflammatory Regulation of Muscle Growth*

Inflammatory factors including cytokine signaling contribute to the development, growth, and regeneration of skeletal muscle, but prolonged exposure to elevated cytokines disrupts these physiological processes. Two prominent inflammatory cytokines are secreted by skeletal muscle fibers and resident macrophages. Myoblast exposure to both TNFα and IL-6 reduce skeletal muscle growth, myoblast function, and protein

synthesis over time (Thoma and Lightfoot, 2018; Cadaret et al., 2019c; Posont, 2019). During fetal development, these cytokines regulate myogenesis by increasing proliferation of myoblasts (Posont et al., 2018). However, prolonged exposure of TNFα and IL-6, due to poor intrauterine conditions can lead to intrinsic deficits in myoblast function which persist after birth (Yates et al., 2014; Soto et al., 2017; Cadaret et al., 2019b). Elevated IL-6 and TNFα-induced NFκB activation disrupts terminal myoblast differentiation and inhibits protein synthesis (Langen et al., 2001). This is due to NFκB activation reducing expression for the differentiation factors MyoD and myogenin and the structural protein desmin (Langen et al., 2001; Posont et al., 2018). Myoblast dysfunction prenatal in turn reduces fetal muscle mass and further hypertrophic growth capacity (Cadaret et al., 2019b). Postnatal, acute increases in cytokine signaling via STAT3 pathways induce quiescent satellite cells to proliferate in order to facilitate hypertrophic muscle growth (Zhang et al., 2013). However, chronic activation of these regulatory pathways leads to myoblast dysfunction, increased protein degradation, muscle wasting, and ultimately reduced skeletal muscle mass (Yates et al., 2014; Brown and Hay Jr, 2016; Posont et al., 2018). This is particularly evident in fetuses exposed to chronically-elevated cytokines during peak myogenesis, which leads to intrinsic deficits in inflammatory regulation of postnatal muscle growth. This appears to be a result of adaptions in myoblast cytokine sensitivity, which is evidenced by reduced myoblast responsiveness to TNFα and IL-6 during proliferation and differentiation (Yates et al., 2016; Posont et al., 2018).

*Inflammatory Regulation of Metabolism*

The inflammatory system plays a role in metabolic regulation and substrate utilization via both acute and chronic changes. During normal physiological conditions, NFκB activation initiates transcription of genes for glycolysis, thus shifting glucose metabolism to a less efficient route of energy production (Tornatore et al., 2012). In skeletal muscle, TNFα and IL-6 act through both the canonical and non-canonical NFκB pathways to regulate basal and insulin-stimulated glucose metabolism. One mechanism for regulating energy utilization by skeletal muscle is inhibition of insulin-stimulated glucose uptake (del Aguila et al., 1999). Elevated inflammatory cytokines block insulin-stimulated Akt phosphorylation, which prevents the translocation of GLUT4 to the plasma membrane of the muscle cell (**Figure 1-3)** (Lorenzo et al., 2008) (Pirola et al., 2004). However, acute TNFα and IL-6 exposure in some conditions can also increase glucose uptake independently of insulin through the activation of the non-canonical NFkB pathway (Carey et al., 2006; Glund et al., 2007). In addition, cytokine exposure following acute stress is also effective in directly increasing skeletal muscle glucose oxidation in the absence of insulin and independently of glucose uptake (Cadaret et al., 2017).

In pancreatic islets, IL-6 signaling via JAK/STAT3 supports homeostatic glucose metabolism by promoting development of pancreatic islet microvasculature (Kostromina et al., 2010). When activated, STAT3 promotes the expression of Vascular Endothelial Growth Factor A (VEGF-A), which is critical for the proper development of microvasculature in the pancreatic islet cells (Kostromina et al., 2010). Poor islet microvasculature development can reduce insulin secretion and result in glucose

intolerance (Lee and Hennighausen, 2005; Kostromina et al., 2013). This form of glucose intolerance is a primary contributor to Type II diabetes and obesity (Cui et al., 2004). The temporal differences in TNFα and IL-6 action suggests that inflammatory regulation of metabolism relies on the duration of cytokine exposure. Chronic exposure during fetal development impairs postnatal regulation of glucose metabolism which is evidenced by reduced TNFα-stimulated skeletal muscle glucose oxidation (Cadaret et al., 2018).

### *Adaptive Programming of Adrenergic & Inflammatory Regulation in IUGR*

The consequences of IUGR on growth and metabolism stem in large part from adaptive programming mechanisms that alter inflammatory and adrenergic action. When fetal stress pathways are upregulated due to reduced glucose and oxygen availability, nutrient-sparing adrenergic adaptions disrupt muscle development, hypertrophic growth, and oxidative capacity (Yates et al., 2014; Yates et al., 2016). In addition, fetal pancreatic islet development is diminished, resulting in impaired insulin secretion in IUGR fetuses and offspring (Limesand et al., 2007a; Rozance et al., 2009; Limesand and Rozance, 2017b). These pathologies are in part due to the chronic exposure of fetal tissues to increased catecholamines and cytokines, which causes developmental changes in the nature of their signaling pathways and thus programs life-long dysfunction (**Figure 1-2)** (Yates et al., 2011a; Chen et al., 2017; Limesand and Rozance, 2017b; Posont et al., 2018). As IUGR offspring mature, it is important to understand the underlying mechanisms associated with these pathologies and when and how they can be mediated.

*Improving Adrenergic Pathologies of IUGR with β-agonists*

Thorough research has shown the effects of stimulating adrenergic activity with β adrenergic agonists on muscle growth and metabolic efficiency in multiple species of livestock. In fact, β agonists are utilized as feed additives in 70% to 90% of all cattle in US feedlots (Johnson et al., 2013; Johnson et al., 2014). The $\beta_2$ agonist clenbuterol HCl is particularly effective in enhancing muscle growth through increased protein synthesis and attenuation of muscle atrophy (Maclennan and Edwards, 1989; Hinkle et al., 2002). In addition, clenbuterol improves body composition by reducing adipose deposition (Ricks et al., 1984; Miller et al., 1988). The mechanisms by which clenbuterol acts are not fully elucidated, but it is clear that clenbuterol binds to $\beta_2$ adrenoceptors in skeletal muscle (Hinkle et al., 2002). The effects of clenbuterol are typically longer lasting than other β-agonists, making clenbuterol an ideal means for mediating chronically altered mechanisms such as those present in IUGR tissues although currently prohibited for use in livestock. Improvements in lean muscle mass and metabolic efficiency measured by increased carcass merit and feed-to-gain ratios have been achieved with β-agonists in uncompromised livestock, and we will seek to determine the effects of β-agonist supplementation on poor gain and altered body compositions in IUGR-born animals.

*Meditating Enhanced Inflammatory Sensitivity in IUGR*

The use of nonsteroidal anti-inflammatory drugs (NSAID) in the treatment of chronic inflammatory disorders is a common means to reduce cytokine action on tissues that contribute to systemic inflammation (Enthoven et al., 2016). However, prolonged use of these drugs and chronic suppression of inflammatory pathways can have severe

consequences on the regulatory properties of inflammation on muscle growth and metabolism. Inflammatory pathways provide key regulatory signals that when chronically impaired have the potential to disrupt the balance of protein cycling and energy substrate utilization. In addition, the chronic usage of NSAID have been correlated with the increased risk of gastrointestinal bleeding, renal disease, and cardiovascular disease (Bauer et al., 1996; Gooch et al., 2007; Verhaegh et al., 2016). Thus, alternatives to NSAID such as curcumin, a nutraceutical, are warranted. Curcumin is the bioactive polyphenol of the root of the Turmeric (*Curcuma longa*) plant. Cell culture studies indicate that curcumin has antioxidant and anti-inflammatory properties and is particularity effective in reducing TNFα/TNFR1-induced NFκB activation (Leclercq et al., 2004; Gonzales and Orlando, 2008; Sadeghi et al., 2018), which could reduce the impact of enhanced inflammatory pathways on skeletal muscle growth and metabolism in IUGR offspring.

### *Conclusion*

Our recent studies have connected fetal adaptions in adrenergic and inflammatory signaling pathways to reductions in neonatal growth and metabolic performance in IUGR-born offspring (Cadaret et al., 2019c; Posont, 2019; Yates et al., 2019a). Understanding how pathologies lead to these adaptions and progressively worsen throughout early life will help identify underlying mechanisms that could be targeted to improve later life health deficits. As such, the objective of the following studies were directed at determining if fetal and neonatal IUGR growth and metabolic deficits worsen

as these offspring enter the juvenile stage and whether these adaptive programming mechanisms can be treated through the use of adrenergic or inflammatory modifiers.

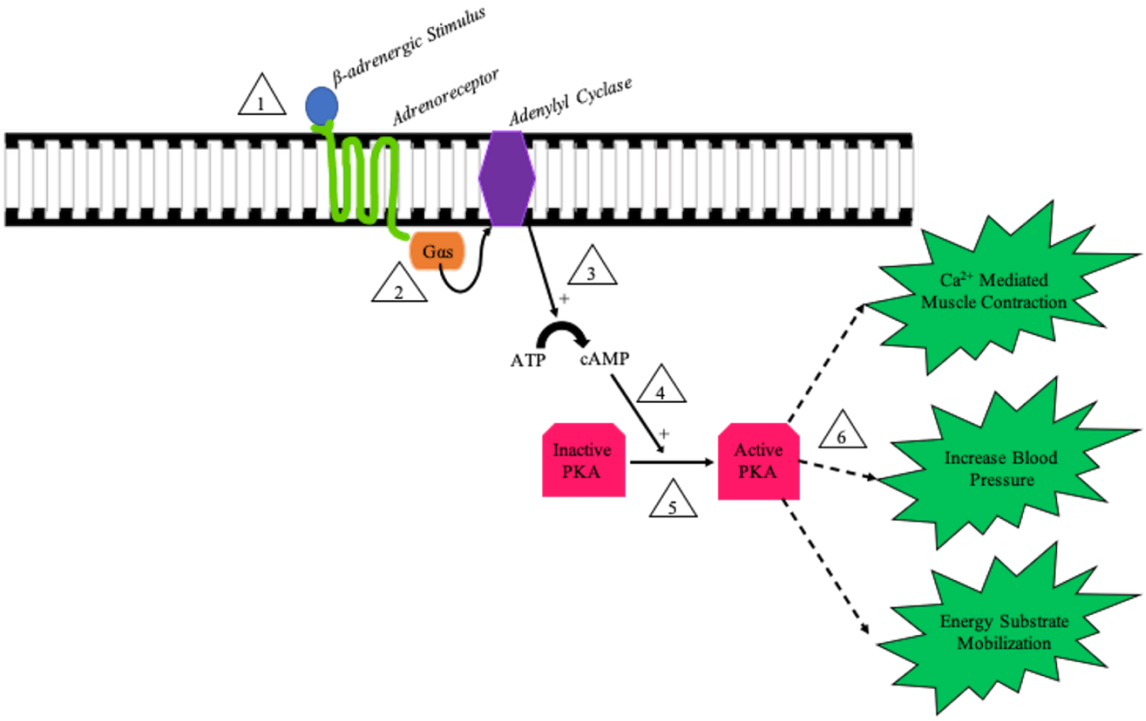


**Figure 1-1.** The modulation of intercellular cAMP production and action in response to β adrenoreceptor binding.

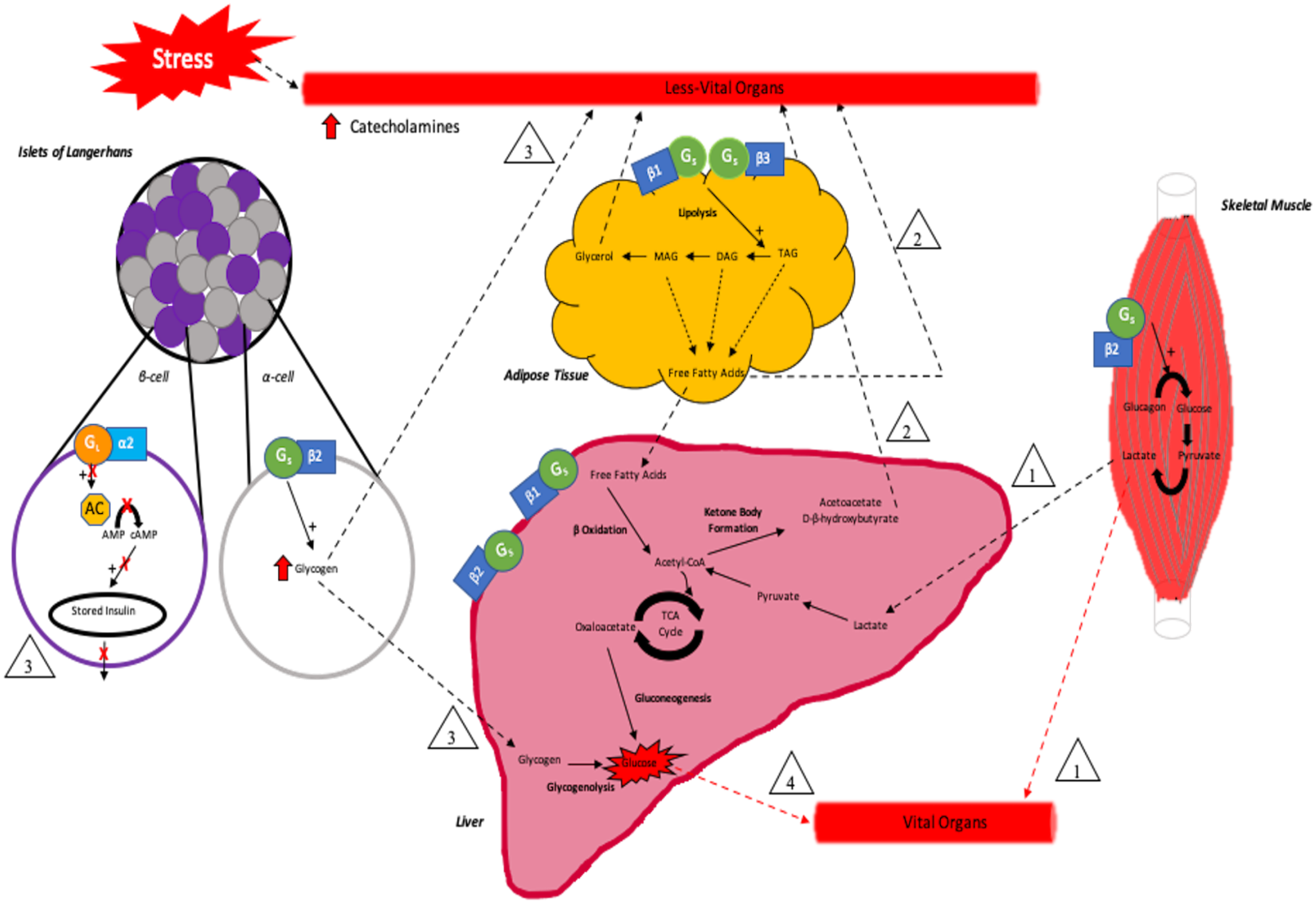


**Figure 1-2.** Illustration of the adrenergic activity of skeletal muscle, adipose tissue, pancreatic islet cells, and the liver in response to elevated catecholamines. 1. Skeletal muscle secretes lactate produced by aerobic glycolysis, which can used as an energy substrate for cardiac muscle or be shuttled to the liver for gluconeogenesis. 2. In adipose tissue, catecholamines mediate the breakdown of triglycerides through cAMP-mediated lipolysis, which mobilizes free fatty acids that can be used by peripheral tissues for energy or be shuttled to the liver for ketone body formation. 3. In the pancreatic islets, glycogen is secreted by alpha cells, which can be also be utilized by peripheral tissues or travel to the liver for glycolysis. The activation of adrenoreceptors in β cells is inhibited by elevated catecholamines, which reduces insulin secretion to preserve blood glucose concentrations. 4. Through various routes, the liver produces glucose, which is secreted to fuel vital tissues during a period of stress.

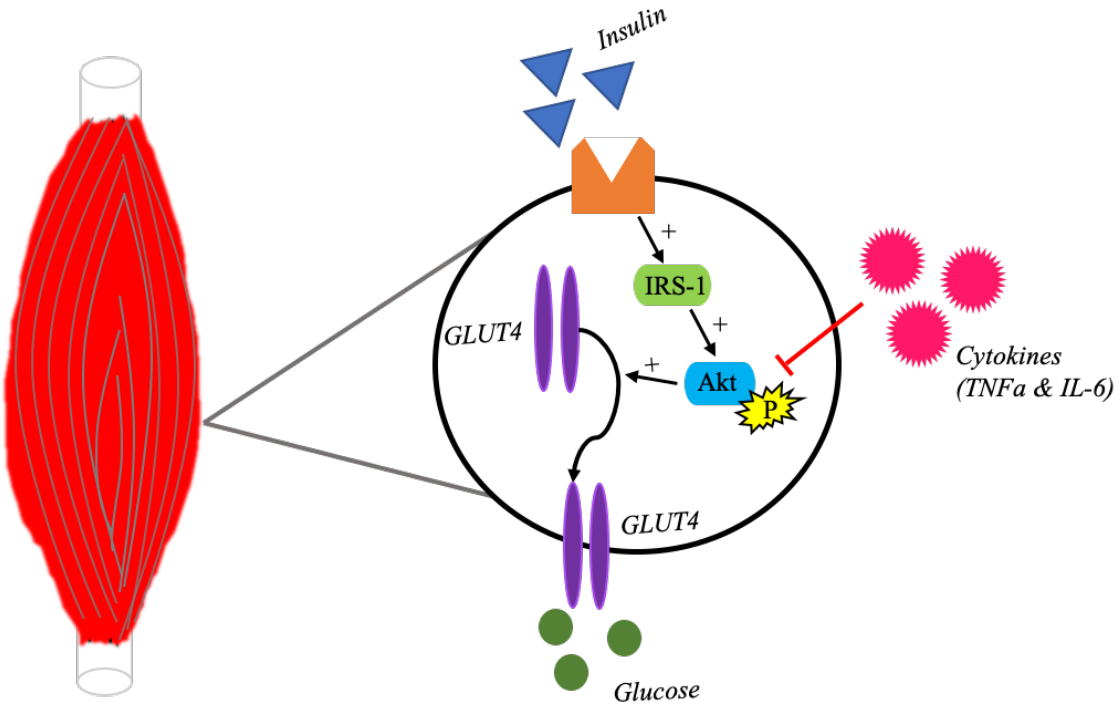


**Figure 1-3.** Illustration of the mechanisms involved in insulin-stimulated glucose uptake for skeletal muscle, which can be inhibited by elevated cytokine exposure.

# Chapter 2

## Deficits in growth, muscle mass, and body composition caused by placental insufficiency-induced intrauterine growth restriction persisted in lambs at 60 d of age but were improved by daily supplementation of clenbuterol or curcumin.[1]

[1]A version of this chapter containing minimal modification has been accepted for publication by *Translational Animal Science*.


## ABSTRACT

Placental insufficiency consistently induces intrauterine growth restriction (IUGR), and the consequences follow the individual through postnatal life. In meat animals, IUGR causes reduced muscle mass and asymmetric growth that favors of fat deposition. The resulting body composition is detrimental to carcass value at harvest. We hypothesized that IUGR fetal adaptions would continue to negatively impact postnatal growth and body composition of juvenile-aged lambs but that adrenergic and inflammatory modifiers would improve growth deficits at this age. Thus, the objective of this study was to assess the impact of IUGR in juvenile lambs to determine whether diminished growth and body composition could be recovered by daily postnatal treatment with clenbuterol or curcumin. IUGR lambs were produced by maternal hyperthermia-induced placental insufficiency and growth metrics were assessed over the 1$^{st}$ 60 d of age. At all assessed ages, bodyweight (BW) and average daily gain were diminished ($P <$ 0.05) and crown-to-rump tended to be reduced (P = 0.07) in unsupplemented IUGR lambs compared to controls, but IUGR lambs treated with clenbuterol or curcumin did

not differ from controls. Crown circumference, body girth, and crown circumference-to-body girth ratios were greater ($P < 0.05$) in curcumin-supplemented IUGR lambs than controls at birth, but crown circumference-to-body girth ratios were reduced ($P < 0.05$) in curcumin-supplemented IUGR lambs by 60 d. At necropsy, brain-to-BW ratio, hindlimb, heart, and flexor digitorum superficialis (FDS) muscle mass tended to be reduced ($P \leq 0.09$) in IUGR lambs compared to controls, but the FDS muscle mass did not differ between curcumin-supplemented IUGR lambs and controls. Lung and kidney mass, lung-to-BW ratio, and kidney-to-BW ratio were also diminished ($P < 0.05$) in IUGR lambs compared to controls. Kidney mass was further diminished ($P < 0.05$) in clenbuterol-supplemented and curcumin-supplemented IUGR lambs compared to unsupplemented IUGR lambs, but lung mass and lung-to-BW ratio in clenbuterol-supplemented IUGR lambs did not differ from controls. Regardless of experimental group, females exhibited larger ($P < 0.05$) hindlimb, heart, kidney, and liver masses compared to males, but males had larger ($P < 0.05$) lung-to-BW and brain-to-BW ratios. Group x age interactions were observed ($P < 0.05$) for BIA estimated body composition, nutrient composition, and muscle composition, which were not different among experimental groups at 30 d of age. Fat-free mass (FFM) and fat-free soft tissue (FFST) were also not different at 60 d of age, but estimated mass of several muscle groups were reduced ($P < 0.05$) in IUGR lambs compared to controls, clenbuterol-supplemented IUGR lambs, and curcumin-supplemented IUGR lambs. At necropsy, FFM, FFST, and mass of muscle groups were all less ($P < 0.05$) in unsupplemented IUGR lambs than in controls, clenbuterol-supplemented IUGR lambs, and curcumin-supplemented IUGR lambs. Estimated crude fat and nutrient composition values for moisture, protein, fat, and lean content were less

($P < 0.05$) in unsupplemented but not clenbuterol-supplemented or curcumin-supplemented IUGR lambs than controls. Actual loin eye area (REA) and loin protein content measured at necropsy were less ($P < 0.05$) in unsupplemented IUGR lambs but greater ($P < 0.05$) in clenbuterol-supplemented IUGR lambs compared to controls and curcumin-supplemented IUGR lambs. Loin fat content, fat-to-protein ratio, and caloric content were all greater ($P < 0.05$) in unsupplemented IUGR lambs compared to controls, clenbuterol-supplemented IUGR lambs, and curcumin-supplemented IUGR lambs. From these findings, we conclude that IUGR reduces postnatal growth performance and decreases body composition quality through 2 mo of age, but postnatal treatment with clenbuterol or curcumin was effective in recovering several aspects of poor growth, which allowed for improved body composition in IUGR lambs.

## INTRODUCTION

Low birthweight in livestock results from stress-induced intrauterine growth restriction (IUGR) of the fetus (Yates et al., 2018a). These animals exhibit diminished muscle mass at term that persists in the neonatal stage (Brown and Hay Jr, 2016; Cadaret et al., 2019b). When coupled with metabolic dysfunction, poor muscle growth leads to asymmetric body composition and decreased weight gain (Cadaret et al., 2019c). Ultimately, low birthweight pathologies result in poor carcass yield and merit at harvest (Greenwood et al., 1998), resulting in price discounts and reduced profitability for producers (Boleman et al., 1998). Poor performance and compromised wellbeing associated with low birthweight make it necessary to develop postnatal treatment strategies aimed at improving outcomes of IUGR. In this study, we examined the

potential benefits of daily supplementation of two bioactive compounds aimed at targeting adrenergic and inflammatory adaptations that we previously observed in IUGR muscle tissues (Posont et al., 2018; Yates et al., 2018a). First, adrenergic activity was manipulated by daily injections of clenbuterol, a pharmaceutical β2 adrenergic agonist that is a well-characterized stimulant of muscle growth and efficiency in livestock (Beermann, 2002). Second, inflammatory activity was manipulated by oral administration of curcumin, a nutraceutical extract of turmeric root that elicits anti-inflammatory properties by disrupting NFκB-mediated inflammatory pathways (Leclercq et al., 2004; Cho et al., 2007). We previously reported that IUGR diminished muscle growth and altered body composition at the neonatal stage (Cadaret et al., 2019c). In this study, we hypothesized that growth deficits would persist at the juvenile stage, manifesting in poor body composition and diminished carcass merit indicators. We also postulated that daily postnatal supplementation of clenbuterol and curcumin would at least partially recover growth and body symmetry in IUGR-born lambs at 60 d of age. The objective of this study was to test this hypothesis by determining the extent to which IUGR fetal adaptions impair growth capacity over the first 60 d of age. We also sought to determine whether clenbuterol or curcumin could improve IUGR-induced deficits in lean tissue growth to provide a more desirable body composition.

## MATERIALS & METHODS

### *Animals and Experimental Design*

These studies were approved by the Institutional Animal Care and Use Committee at the University of Nebraska-Lincoln, which is accredited by AAALAC International.

Placental insufficiency-induced IUGR lambs were produced from Polypay ewes as previously described (Cadaret et al., 2019). Briefly, timed-mated ewes (18 to 24 mo of age at breeding) were exposed to elevated ambient temperatures of 40°C with a relative humidity of 35% during peak placental development from the 40$^{th}$ to 95$^{th}$ d of gestational age. Ewes were returned to thermoneutral temperatures (25°C) alongside their pair-fed control counterparts following the 55-d exposure, and all ewes were allowed to lamb naturally. Nutritional management, housing, and husbandry for all ewes were practiced as previously described (Macko et al., 2016b). Following parturition, lambs were weaned at 12 h of age and hand-reared until 60 d of age. After being fed a minimum of 200 ml colostrum (pooled from multiple ewes) within the first 24 h, lambs were raised on milk replacer (Land O'Lakes Inc., Arden Hills, MN) for the first 30 d. Lambs were hand fed every four hours until trained to eat from stationary bottle hangers, typically within 5 d of birth. Milk bottles were replaced twice daily. Lambs were then transitioned to the *ad libitum* grain diet in **Table 2-1** beginning at 30 d of age, and milk replacer was discontinued at 45 d of age. IUGR lambs were randomly assigned at birth to receive one of the three daily treatments outlined in **Table 2-2** (IUGR: n=6; IUGR+Clenbuterol: n=7; IUGR+Curcumin: n=5). Control lambs (n=11) received both treatment placebos.

### *Growth Metrics*

Crown circumference, front cannon bone length, body girth just behind the shoulder blades, and crown-rump length were measured at birth and weekly thereafter for a total of 8 weeks. Lamb bodyweights (BW) and feed intake were recorded daily. Lambs were euthanized by double barbiturate overdose and necropsied at 60 d of age. Brain,

heart, lungs, kidneys, liver, and flexor digitorum superficialis muscles were weighed. Following necropsy, lamb carcasses were chilled for a minimum of 24 h and then split between the 12$^{th}$ and 13$^{th}$ rib where ribeye area (REA) was measured utilizing Iowa State University's Plastic Grid for Quick Measurement.

***In vivo Body Composition Estimations***

Bioelectrical impedance analysis was performed at 30 and 60 d of age in the live animal to estimate body composition. It was also performed on the longissimus dorsi muscle at necropsy. A four-terminal Quantum V (RJL Systems, Detroit, MI) was used to measure reactance (Xc), resistance (Rs), and phase angle (PA). Each BIA utilized two sets of equally spaced electrode terminals to transmit an electrical current across the tissues. Electrodes were connected to aluminum 20G MONOJECT needles (Covidien, Mansfield, MA) placed subcutaneous in live animals and intramuscular in the longissimus dorsi. The outer electrodes were placed 2.5 cm behind the point of the scapula and 5 cm in front of the hip bone, and the inner electrodes were placed 2.5 cm inside of these. Both sets were placed dorsally 1 cm to the right of the midline. Measurements were recorded for 30 sec, with one measurement every 5 sec, resulting in six total measurements that were averaged. Also at necropsy, the contralateral longissimus dorsi muscle was removed, frozen, and sent to Midwest Laboratories (Omaha, NE) for proximate analysis to determine muscle moisture, protein, fat, ash, carbohydrates, and caloric concentrations.

Ultrasonic measurements of the loin were performed at 60 d of age on a subset of lambs comprised of the control group for this study. Lambs were tightly sheared over the

12th and 13th ribs from the midline to the lower right flank of the animal. An IBEX PRO (E.I. Medical Imaging, Loveland, CO) ultrasound machine with a L6.2 12-cm linear transducer was used to measure REA, ribeye depth, and back fat thickness between the 12th and 13th rib. The transducer was placed at a 45° angle toward the head of the animal between the 12th and 13th rib following heavy application of vegetable oil as a couplant. REA, ribeye depth, and back fat thickness were then measured from a frozen image utilizing the caliper tracing mode.

### *Statistical Analysis*

Data were analyzed using SAS 9.4 (SAS Institute, Cary, NC). Necropsy and ultrasound data were analyzed for differences among experimental groups by ANOVA using the mixed procedure, and Fisher's LSD was used for mean separation. The main effect of sex was also examined, but interacting effects between group and sex were not included in the model due to insufficient power. Bodyweights, growth metrics, and estimated body composition data were likewise analyzed using the mixed procedure, with day as the repeated measure. For bioelectrical impedance data, readings over the 30-s period were averaged and the mean was used for the equations. Spearman correlation coefficients for ultrasound estimates and actual REA were determined with the correlation procedure of SAS. Lamb was considered the experimental unit for all outputs. Data are presented as means ± standard error. Significant differences were declared at $\alpha \leq 0.05$ and tendencies at $\alpha \leq 0.10$.

## RESULTS

### *Growth Metrics*

An experimental group x age interaction was observed ($P < 0.05$) for crown circumference/abdominal girth but not for BW, average daily gain (ADG), crown circumference, body girth, crown-rump length, or cannon bone length. Average BW was reduced ($P < 0.05$) for IUGR lambs compared to all other groups, regardless of age (**Figure 2-1A)**. ADG was reduced ($P \leq 0.05$) for unsupplemented, clenbuterol-supplemented, and curcumin-supplemented IUGR lambs compared to controls, whether determined at 30 d or 60 d (**Figure 2-1B)**. ADG between birth and the 30$^{th}$ d of age tended to be greater ($P = 0.10$) than between the 30$^{th}$ and 60$^{th}$ d for all lambs, regardless of experimental group (**Figure 2-1C)**. Crown circumference and abdominal girth were greater ($P \leq 0.05$) in curcumin-supplemented IUGR lambs compared to all other groups, regardless of age. Crown-rump length tended to be diminished ($P = 0.07$) in IUGR lambs compared to all other groups, regardless of age. Cannon bone length did not differ among experimental groups. At birth, crown circumference/abdominal girth was greater ($P \leq 0.05$) for IUGR and curcumin-supplemented IUGR lambs than for controls and clenbuterol-supplemented IUGR lambs. After 8 weeks, however, crown circumference/abdominal girth was less ($P \leq 0.05$) for curcumin-supplemented IUGR lambs than controls but not IUGR and clenbuterol-supplemented IUGR lambs. BW, ADG, and growth metrics did not differ between sexes.

At necropsy, hindlimb mass for IUGR lambs tended to be lighter ($P = 0.09$) than controls, but hindlimb mass for curcumin-supplemented and clenbuterol-supplemented

IUGR lambs did not differ from controls (**Table 2-3**). Female hindlimbs were heavier ($P \leq 0.05$) than male hindlimbs (**Table 2-4**). Hindlimb mass/BW did not differ among experimental groups or between sexes. The flexor digitorum superficialis muscle mass tended to be lighter ($P = 0.06$) for IUGR lambs than controls or curcumin-supplemented IUGR lambs, but its mass in clenbuterol-supplemented and curcumin-supplemented IUGR lambs did not differ from controls. Flexor digitorum superficialis muscle mass/BW did not differ among experimental groups or between sexes. Heart weights tended to be smaller ($P = 0.09$) in unsupplemented, curcumin-supplemented, and clenbuterol-supplemented IUGR lambs than in controls, and were heavier ($P \leq 0.05$) in females than males. Heart weight/BW did not differ among experimental groups or between sexes. Lung weight and lung weight/BW ratio were lower ($P \leq 0.05$) for IUGR lambs than for controls but did not differ among clenbuterol-supplemented IUGR lambs, curcumin-supplemented IUGR lambs, and controls. Lung weight/BW was greater ($P \leq 0.05$) in males than females. Liver weight and liver weight/BW did not differ among experimental groups, but liver weight tended to be higher ($P = 0.06$) in females than males. Kidney weight was lighter ($P \leq 0.05$) for IUGR lambs than for controls and was lighter ($P \leq 0.05$) for curcumin-supplemented and clenbuterol-supplemented IUGR lambs than for controls or unsupplemented IUGR lambs. Kidney weight was higher ($P \leq 0.05$) in females than males. Kidney weight/BW ratio did not differ between controls and unsupplemented IUGR lambs but was lower ($P \leq 0.05$) for curcumin-supplemented and clenbuterol-supplemented IUGR lambs than for controls or unsupplemented IUGR lambs. Brain weight was not different among experimental groups or between sexes. Brain weight/BW tended to be lower ($P = 0.07$) for unsupplemented, curcumin-

supplemented, and clenbuterol-supplemented IUGR lambs than for control lambs and was higher ($P \leq 0.05$) in males than females. Loin eye area was smaller ($P \leq 0.05$) in IUGR lambs than controls, larger ($P \leq 0.05$) in clenbuterol-supplemented IUGR lambs than controls, and did not differ between curcumin-supplemented IUGR lambs and controls. Loin eye area was also larger ($P \leq 0.05$) in females than in males.

***In vivo Body Composition Estimations***

Experimental group x age interactions were observed ($P \leq 0.05$) for all BIA estimates. No differences in any body composition, nutrient composition, or muscle composition estimated were observed among experimental groups at 30 d of age (**Table 2-5**). At 60 d of age, however, 1 of the 3 FFM equations (FFM1) indicated that FFM was lower ($P < 0.05$) in IUGR lambs but greater ($P \leq 0.05$) in curcumin-supplemented IUGR lambs compared to controls. This equation also indicated that FFM for clenbuterol-supplemented lambs did not differ from controls or curcumin-supplemented IUGR lambs but was still greater ($P \leq 0.05$) than IUGR lambs. The remaining FFM equations and all FFST equations did not indicate a difference among experimental groups at 60 d of age. The estimated sum of the leg, sirloin, rack, shoulder, neck, riblets, shank, and lean trim mass (SUM) as well as the sum of the leg, sirloin, loin, rack, and shoulder mass (LSRLS) and the sum of the leg, sirloin, and loin mass (LSL) were all less ($P < 0.05$) in IUGR lambs than in controls or curcumin-supplemented IUGR lambs at 60 d of age. In clenbuterol-supplemented IUGR lambs, these estimates were intermediate and did not differ from any of the other group. Nutrient composition estimations indicated no difference in moisture, lean mass, or protein content at 60 d of age. However, estimated

fat content was less ($P \leq 0.05$) for IUGR lambs than for controls or curcumin-supplemented IUGR lambs. Estimated fat content for clenbuterol-supplemented IUGR lambs was again intermediate and did not differ from any of the other experimental groups. Crude fat content (CF) indicated by the CF3 equation was likewise reduced ($P < 0.05$) in IUGR lambs compared to control and curcumin-supplemented IUGR lambs but not clenbuterol-supplemented IUGR lambs.

At necropsy, all equations indicated that FFM and FFST were reduced ($P \leq 0.05$) in IUGR lambs compared to controls and curcumin-supplemented IUGR lambs, and 2 of 3 equations for each parameter indicated that FFM and FFST were also reduced ($P \leq 0.05$) in IUGR lambs compared to clenbuterol-supplemented IUGR lambs. The remaining equations indicated that FFM and FFST were lower ($P \leq 0.05$) in clenbuterol-supplemented IUGR lambs than controls at necropsy. Estimated SUM and LSL at necropsy were less ($P \leq 0.05$) for IUGR lambs than for controls or curcumin-supplemented IUGR lambs but not different from clenbuterol-supplemented IUGR lambs. Estimated LSLRS at necropsy was less ($P \leq 0.05$) for IUGR lambs than controls but did not differ from curcumin-supplemented or clenbuterol-supplemented IUGR lambs. All equations indicated that CF was reduced ($P \leq 0.05$) in IUGR lambs compared to controls, and 2 of 3 equations indicated that CF was also less ($P \leq 0.05$) than in clenbuterol-supplemented IUGR lambs. The remaining equation indicated that CF in IUGR lambs did not differ from clenbuterol-supplemented IUGR lambs but was less ($P \leq 0.05$) than in curcumin-supplemented IUGR lambs. Nutrient composition estimations at necropsy indicated diminished ($P \leq 0.05$) moisture, protein, fat, and lean contents for IUGR lambs compared to all other groups. BIA estimated fat-to-protein ratios were

greater ($P \leq 0.05$) in IUGR lambs than controls and clenbuterol-supplemented IUGR but did not differ from curcumin-supplemented IUGR lambs. Proximate analysis of the contralateral loin muscle collected at necropsy showed no differences among experimental groups or between sexes for moisture, ash, and carbohydrate content but revealed less ($P \leq 0.05$) protein content for IUGR lambs compared to controls and greater ($P \leq 0.05$) protein content for clenbuterol-supplemented IUGR lambs compared to controls. Loins from males tended to have a higher (P = 0.08) protein content than females. Loin fat content was increased ($P \leq 0.05$) in IUGR lambs compared to controls but was not different among clenbuterol-supplemented IUGR lambs, curcumin-supplemented IUGR lambs, and controls. Loin fat content also did not differ between sexes. Loin fat-to-protein content was higher ($P \leq 0.05$) in IUGR lambs than in controls and in males compared to females but not different among clenbuterol-supplemented IUGR lambs, curcumin-supplemented IUGR lambs, and controls. Loin caloric content was higher ($P \leq 0.05$) in IUGR lambs than in controls but not different among clenbuterol-supplemented IUGR lambs, curcumin-supplemented IUGR lambs, and controls.

Correlations between ultrasound estimates of loin eye area, loin eye depth, and back fat thickness and actual loin eye measurements indicated that ultrasound-estimated loin eye depth was most strongly correlated to actual loin eye area with a correlation coefficient of 0.74 ($P \leq 0.05$). Ultrasound-estimated back fat thickness had a correlation coefficient with actual loin eye area of 0.58 ($P = 0.16$), and ultrasound-estimated loin eye area had a correlation coefficient with actual loin eye area of 0.48 ($P = 0.26$).

## DISCUSSION

In this study, we found that the repercussions of IUGR on postnatal growth and body composition were evident in juvenile-aged lambs and paralleled deficits observed at younger ages. We also found that daily postnatal treatment with injectable clenbuterol or oral curcumin recovered some aspects of diminished postnatal growth and improved body composition characteristics by 60 d of age. Specifically, juvenile lambs that were born IUGR exhibited morphometric measurements and lean tissue mass parameters that were consistent with asymmetrical growth patterns. This phenotype was compounded by decreased feed efficiency and rates of gain that coincided with greater fat-to-muscle ratios and poorer carcass merit indicators at necropsy. Postnatal supplementation of clenbuterol or curcumin recovered indicators of lean tissue mass in IUGR-born lambs, thus improving a major factor contributing to the hallmark asymmetric fat-to-protein ratios. Clenbuterol supplementation even improved estimated muscle mass beyond that of lambs that were not IUGR at birth. Together these finding show that the impact of IUGR persists through the juvenile stage but that postnatal supplementation of curcumin or clenbuterol can improve and even enhance soft tissue growth and body composition.

Impaired capacity for growth was present in juvenile-aged IUGR offspring, much like we had previously observed in the fetus (Yates et al., 2016) and neonatal offspring (Cadaret et al., 2019c; Posont, 2019). However, several of the diminished growth indicators were improved by daily administration of the injectable β2 adrenergic agonist clenbuterol or the oral anti-inflammatory nutraceutical curcumin to IUGR-born lambs over the 1$^{st}$ 60 d of life. Bodyweights and crown-rump lengths, which are metrics of total

body growth, were diminished in IUGR lambs at birth. This was expected based on our previous findings in IUGR lambs (Cadaret et al., 2019c) However, IUGR-born lambs gained weight less rapidly after birth and both bodyweights and crown-rump lengths continued to lag behind controls at 1 and 2 mo of age. This suggests that adipose-driven catch-up growth had not occurred over this timeframe, and thus juvenile growth patterns mirrored the diminished fetal and neonatal growth patterns observed in previous studies by us and others (De Blasio et al., 2007; Cadaret et al., 2019c). However, in a recent study using the same model of maternal hyperthermia, we found that IUGR lambs were 20% lighter than their control counterparts at 30 d of age (Cadaret et al., 2019). Here, we found that IUGR lambs were only 12% lighter at 60 d of age. We believe this to show that as IUGR offspring progress from the neonatal stage to the juvenile stage, the discrepancy in their growth rates may dwindle somewhat. Additionally, the slower rates of gain for all lambs in the 2$^{nd}$ mo of age compared to the 1$^{st}$ mo suggests less opportunity for growth as the animal ages, which would be consistent with previous findings (Thiruvenkadan et al., 2011). For IUGR offspring, this could mean less opportunity to recover diminished growth.

The impact of placental insufficiency-induced IUGR was not proportional among all morphometric parameters measured in this study. Cannon bone length, for example, was not diminished in IUGR lambs at birth or at the neonatal or juvenile stages. This indicates that the skeletal structure is protected from growth restriction similar to the way that growth of brain, heart, and other vital organs is spared. When these tissues are spared at the expense of muscle, fat, and other soft tissues, the result is an asymmetrical pattern of growth and body composition that is hallmark to the IUGR fetus (Yates et al., 2014;

Posont et al., 2018) and neonate (Cadaret et al., 2019c; Posont, 2019; Yates et al., 2019a). Additionally, the higher degree of bone maturity that would be expected at the time of fetal insult in this model shouldn't be ignored (Wu et al., 2006), as less-developed tissues (i.e. skeletal muscle) are more severely impacted by nutritional repartitioning. Nevertheless, when IUGR-born lambs were supplemented with clenbuterol or curcumin, their bodyweights and growth metrics were no longer impaired by 60 d of age. In fact, crown circumference-to-body girth ratios in IUGR-born juvenile lambs supplemented with curcumin indicate that the nutraceutical improved soft tissue-to-skeletal growth symmetry beyond that of our normal lambs. Furthermore, both supplements were effective in recovering poor weight gain in IUGR-born lambs, and curcumin supplementation recovered indicators of both skeletal and soft tissue growth. This shows that postnatal treatment with existing pharmaceuticals or nutraceuticals may be a viable strategy to increase feed efficiency, growth, and symmetrical body composition. This in turn could reduce the negative effects on wellbeing, metabolic efficiency, and carcass composition, thus recovering value in IUGR/low birthweight livestock. It is worth noting, however, that clenbuterol-supplemented and curcumin-supplemented IUGR lambs in this study did not exhibit the same reduction in birthweight as our unsupplemented IUGR lambs. In fact, curcumin-supplemented IUGR lambs had greater body girth, crown circumference, and crown circumference-to-body girth ratios than our controls at birth and maintained those advantages throughout the 60-d period. We speculate that this was due to the low power and inordinate number of singleton-born lambs relative to twins and triplets in these two groups.

At 60 d of age, the impact of IUGR on soft tissue growth was particularly evident postmortem. This was consistent with our observations at the neonatal stage (Cadaret et al., 2019c; Posont, 2019) and shows the persistent effect of nutrient repartitioning adaptions in the IUGR fetus on postnatal body composition. Nutrient repartitioning towards vital tissues is programmed by prenatal stress and leads to asymmetric growth (Alexander et al., 1987; Morrison, 2008) but is necessary to preserve vital organ function and prevent fetal death. Postnatal consequences of nutrient-sparing fetal adaptions are reflected in this study by the increased brain-to-bodyweight ratios in IUGR lambs at 60 d of age. Like bodyweight, however, clenbuterol and curcumin improved several key indicators of soft tissue-specific growth in IUGR lambs. Reduced lung-to-bodyweight ratios in IUGR juvenile lambs were recovered by clenbuterol supplementation, leading us to speculate that clenbuterol may improve growth of soft tissues beyond just muscle, as previously predicted (Von Deutsch et al., 2000). Unlike other metrics of asymmetry, however, brain-to-bodyweight ratios were not improved by postnatal clenbuterol or curcumin supplementation. Furthermore, kidney weights and kidney weight-to-bodyweight ratios were diminished by both supplements, perhaps suggesting a negative impact of these products on kidney growth and/or function. In a recent case study, excessive clenbuterol use by an athlete in training increased the subject's myoglobin in the bloodstream due to rhabdomyolysis, leading to secondary kidney damage (Grimmer et al., 2016). On the other hand, curcumin has been shown to improve chronic kidney disease in humans by preventing gut leakage of inflammatory biomolecules (Ghosh et al., 2014) and thus its effects on kidney size here were unexpected. At 30 d of age, body composition and nutrient components estimated in the live animals by bioelectrical

impedance were not different among any groups in our study, which was surprising considering our previous observation of diminished lean mass and fat content at 25 d (Gibbs et al., 2019). The present findings may indicate that mild catch up growth had occurred by 30 d of age and persisted at 60 d of age. It is more likely, however, that the differences among groups were meager enough that we were unable to detect them through our estimations.

As expected, loin muscle size and estimated lean mass was diminished in IUGR lambs at necropsy, which reflects the negative impact of prenatal stress on muscle growth capacity. Indeed, these observations were likely the product of reduced fetal myoblast proliferation (Yates et al., 2014) and impaired protein anabolism (Soto et al., 2017), which was clearly not recovered at the juvenile stage. Poor muscle growth at this stage helps to explain reduced yield and carcass merit that plagues IUGR/low birthweight livestock at harvest (Greenwood et al., 2000). However, clenbuterol supplementation increased the size of the loin in IUGR lambs, which provides some of the highest-value cuts in meat animals. This was perhaps not surprising, as it reflects the β2 agonist's documented ability to enhance muscle growth in beef cattle and sheep (Johnson et al., 2014). More surprisingly, however, was that estimated lean mass and loin size were also recovered by curcumin supplementation to IUGR lambs, although the mechanism by which it did so is not clear from these findings.

Fat content is an important consideration when assessing the effectiveness of a postnatal IUGR treatment. Although, IUGR-born juvenile lambs had less total fat mass, their percentage of soft tissue that was comprised of fat was actually greater than controls. Based on previous findings in IUGR rats (Cettour-Rose et al., 2005), we

speculate that if these IUGR lambs had been assessed beyond the juvenile stage, their fat deposition would eventually reach the point that live-animal estimations for fat mass would reflect the observed increases in fat percentage. Curcumin supplementation lowered fat mass in IUGR lambs, which reflects the nutraceutical's inhibitory effect on adipogenesis (Bradford, 2013). However, since bodyweight was not reduced at birth in supplemented IUGR lambs, differences in fat-to-protein ratios may more accurately represent body composition. Indeed, estimated and actual fat-to-protein ratios were increased in IUGR lambs, which reflects the adipose-driven pattern of postnatal catch up growth that arises from the reduced capacity for muscle growth (Cianfarani et al., 1999). Clenbuterol supplementation recovered estimated fat-to-protein ratios and increased protein content to the level of controls, which again reflects its ability to stimulate lean muscle growth (Johnson et al., 2014) and decrease lipogenesis (Miller et al., 1988). Despite its benefit to other growth indicators, curcumin supplementation did not elicit an effect on fat-to-protein ratios.

The findings of this study allow us to conclude that the impact of IUGR on growth extends beyond early life and continues to be detrimental to juvenile-aged offspring. Specifically, IUGR persistently diminished morphometric indicators of soft tissue growth, which in turn altered body composition and reduced estimates of carcass merit. However, daily postnatal treatment with clenbuterol or curcumin demonstrated potential avenues to recover poor muscle growth and weight gain in IUGR-induced low birthweight livestock. Together, these findings show the potential for supplement-driven strategies to improve IUGR outcomes and justify further research to develop a more comprehensive and definitive understanding of their benefit to low birthweight livestock.

## IMPLICATIONS

Lambs born with low birthweight due to IUGR continued to exhibit diminished bodyweight, muscle mass, feed efficiency, and carcass merit as juveniles. This shows that IUGR pathologies are persistent beyond early life. It also demonstrates the importance of developing preventative and therapeutic strategies to improve mechanisms of muscle growth and metabolic efficiency, which is perhaps the most effective approach to recovering value in low birthweight livestock. This study demonstrates that postnatal pharmaceutical and nutraceutical supplements may be a valid approach to improving diminished growth and body composition in IUGR offspring and warrant continued research.

**Table 2-1.** Sheep Balancer B136 Medicated Grain Diet.

| Ingredient | Amount |
|---|---|
| Crude Protein (Min)[a] | 36% |
| Crude Fat (Min) | 1% |
| Crude Fiber (Max) | 11.50% |
| Calcium (Ca) (Min) | 4.50% |
| Calcium (Ca) (Max) | 5.50% |
| Phosphorus (P) (Min) | 0.85% |
| Salt (NaCl) (Min) | 2.50% |
| Salt (NaCl) (Max) | 3.50% |
| Selenium (Se) (Min) | 1.30 ppm |
| Vitamin A (Min) | 2000 IU/lb |
| Lasalocid Sodium[b] | 136 g/ton |

[a]Includes not more than 4.00% equivalent crude protein from non-protein nitrogen .
[b]Active ingredient.

**Table 2-2.** Experimental groups assessed in this study.

| Group | n | Experimental Treatment | | Oral Carrier | | IV Carrier |
|---|---|---|---|---|---|---|
| | | Curcumin[a] (100mg/kg) | Clenbuterol[b] (0.08µg/kg) | Piperine[c] (20mg/kg) | Corn Oil[d] (1 ml) | Saline[e] (1ml) |
| Control | 11 | . | . | ✓ | ✓ | ✓ |
| IUGR | 6 | . | . | ✓ | ✓ | ✓ |
| IUGR + Curcumin | 5 | ✓ | . | ✓ | ✓ | ✓ |
| IUGR + Clenbuterol | 7 | . | ✓ | ✓ | ✓ | ✓ |

[a] HerbaDiet, Akure Health Care, Haryana, India.
[b] Mazola, ACH Food Companies Inc., Cordova, Tennessee 38016.
[c] VetOne, MWI Veterinary Supply, Boise, Idaho 83705.
[d] Puritan's Pride, Puritans Pride Inc., Oakdale, New York, 11769-9001.
[e] Sigma-Aldrich, St. Louis, Missouri, 63178.

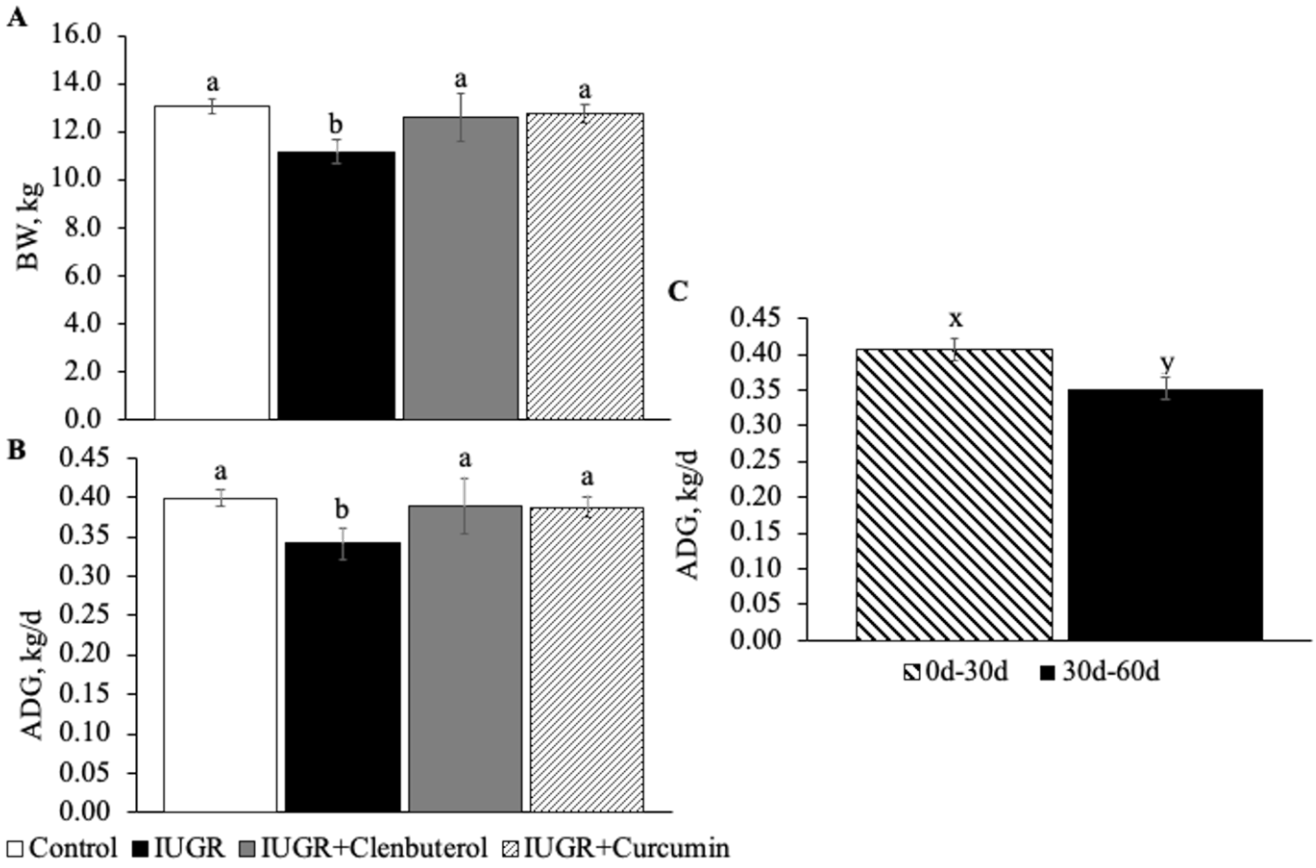


**Figure 2-1.** Bodyweight (A) and average daily gain (B) measured over the first 60d of life in Control (n=15), IUGR (n=10), IUGR+Clenbuterol (n=7), and IUGR+Curcumin (n=4) lambs. Age differences in average daily gain (C) between the neonatal and juvenile stage. a,b means with differing superscripts differ ($P<0.05$). x,y means with differing superscripts tend to differ ($P<0.10$).

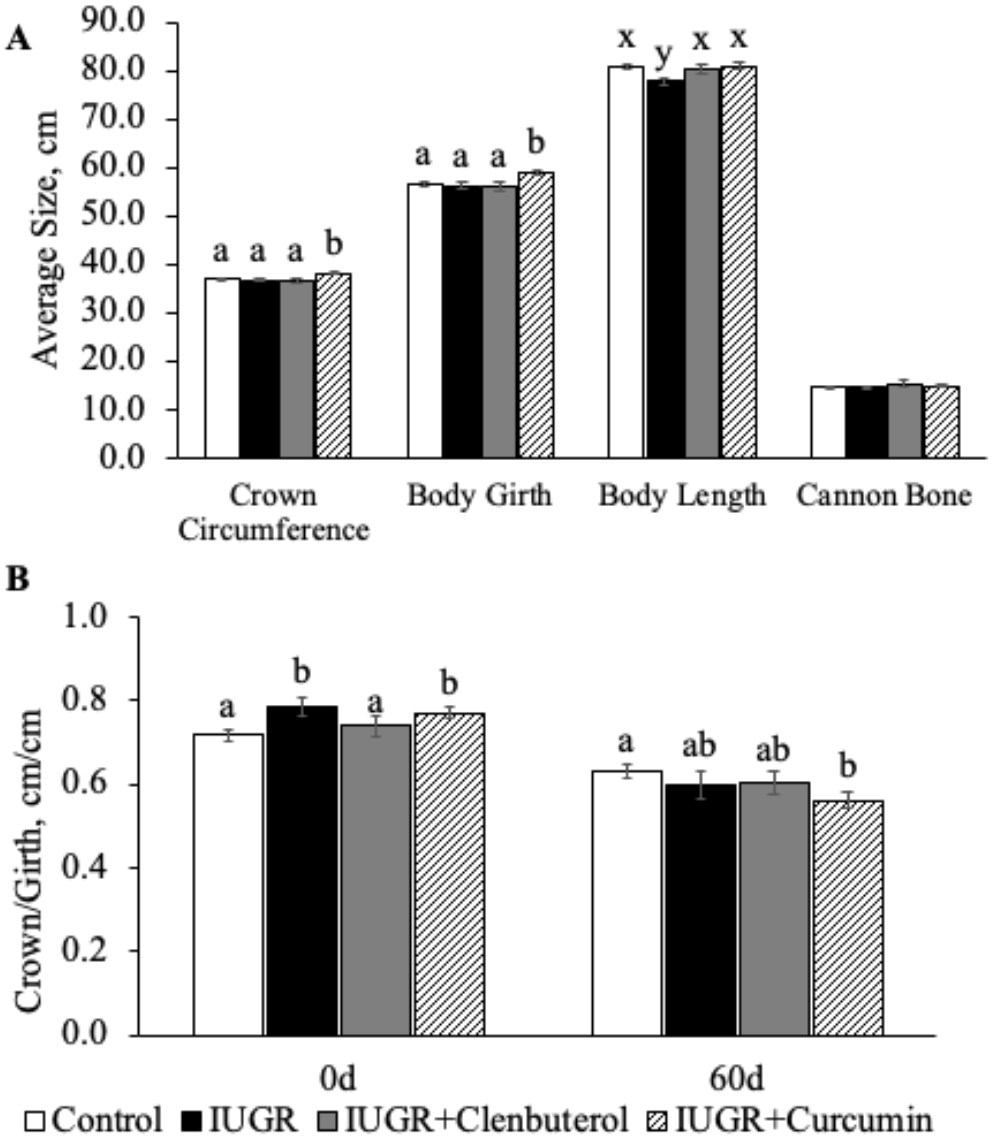


**Figure 2-2.** Average growth metric measured weekly (A) and crown-to-girth ratio at birth and 60d of age in Control (n=15), IUGR (n=10), IUGR+Clenbuterol (n=7), and IUGR+Curcumin (n=4) lambs. a,b means with differing superscripts differ ($P<0.05$). x,y means with differing superscripts tend to differ ($P<0.10$).

**Table 2-3.** Organ weights from IUGR lambs at 60 d of age.

| Variable | Experimental Group | | | | *P*-value |
|---|---|---|---|---|---|
| | Control | IUGR | IUGR+Clenbuterol | IUGR+Curcumin | |
| Hindlimb, g | 180 ± 10$^{x}$ | 150 ± 10$^{y}$ | 180 ± 30$^{x}$ | 180 ± 20$^{x}$ | 0.09 |
| Hindlimb/BW, g/kg | 82 ± 1 | 82 ± 3 | 83 ± 3 | 83 ± 3 | NS |
| FDS, g | 23.1 ± 1.2$^{x}$ | 18.0 ± 1.5$^{y}$ | 24.1 ± 4.8$^{xy}$ | 23.1 ± 1.6$^{x}$ | 0.06 |
| FDS/BW, g/kg | 1.04 ± 0.034 | 0.97 ± 0.082 | 1.12 ± 0.1 | 1.12 ± 0.091 | NS |
| Heart, g | 189 ± 13$^{x}$ | 135 ± 18$^{y}$ | 136 ± 17$^{y}$ | 93 ± 38$^{y}$ | 0.09 |
| Heart/BW, g/kg | 8.33 ± 0.33 | 8.72 ± 0.99 | 7.46 ±0.43 | 7.45 ± 1.51 | NS |
| Lungs, g | 468 ± 34$^{a}$ | 334 ± 22$^{b}$ | 408 ± 41$^{a}$ | 378 ± 57$^{ab}$ | 0.03 |
| Lungs/BW, g/kg | 21.43 ± 1.18$^{a}$ | 18.5 ± 0.49$^{b}$ | 20.51 ± 0.33$^{a}$ | 20.35 ± 1.59$^{ab}$ | 0.02 |
| Liver, g | 580 ± 34 | 503 ± 39 | 494 ± 57 | 492 ± 53 | NS |
| Liver/BW, g/kg | 25.92 ± 1.14 | 26.9 ± 1.61 | 23.79 ± 0.67 | 25.00 ± 1.86 | NS |
| Kidney, g | 71 ± 2$^{a}$ | 60 ± 4$^{b}$ | 45 ± 2$^{c}$ | 40 ± 7$^{c}$ | < 0.001 |
| Kidney/BW, g/kg | 3.2 ± 0.07$^{a}$ | 3.23 ± 0.15$^{a}$ | 2.32 ± 0.23$^{b}$ | 2.35 ± 0.19$^{b}$ | < 0.001 |
| Brain, g | 89 ± 2 | 86 ± 2 | 91 ± 3 | 93 ± 5 | NS |
| Brain/BW, g/kg | 4.04 ± 0.19$^{x}$ | 4.74 ± 0.17$^{y}$ | 4.64 ± 0.33$^{y}$ | 4.79 ± 0.18$^{y}$ | 0.07 |

Values are expressed as means ± SE; BW, bodyweight; FDS, flexor digitorum superficialis; IUGR, intrauterine growth restriction; NS, not significant.

**Table 2-4.** Sex differences in organ weight of 60 d lambs regardless of experimental group.

| Variables | Female | Male | *P*-value |
|---|---|---|---|
| Hindlimb, g | 200 ± 10[a] | 150 ± 10[b] | 0.006 |
| Hindlimb/BW, g/kg | 86 ± 2 | 82 ± 4 | NS |
| FDS, g | 23.6 ± 1.3 | 20.5.0 ± 2.1 | NS |
| FDS/BW, g/kg | 1.04 ± 0.04 | 1.08 ± 0.08 | NS |
| Heart, g | 175 ± 10[a] | 101 ± 29[b] | 0.04 |
| Heart/BW, g/kg | 7.30 ± 0.44 | 8.68 ± 0.88 | NS |
| Lungs, g | 414 ± 20 | 379 ± 36 | NS |
| Lungs/BW, g/kg | 17.92 ± 0.51[a] | 22.50 ± 0.69[b] | < 0.001 |
| Liver, g | 576 ± 24[a] | 458 ± 50[b] | 0.06 |
| Liver/BW, g/kg | 25.49 ± 0.69 | 25.29 ± 1.24 | NS |
| Kidney, g | 62 ± 2[a] | 45 ± 5[b] | 0.006 |
| Kidney/BW, g/kg | 2.73 ± 0.08 | 2.82 ± 0.19 | NS |
| Brain, g | 90 ± 1 | 89 ± 3 | NS |
| Brain/BW, g/kg | 3.97 ± 0.12[a] | 5.13 ± 0.23[b] | < 0.001 |

Values are expressed as means ± SE; BW, bodyweight; IUGR, intrauterine growth restriction; NS, not significant.

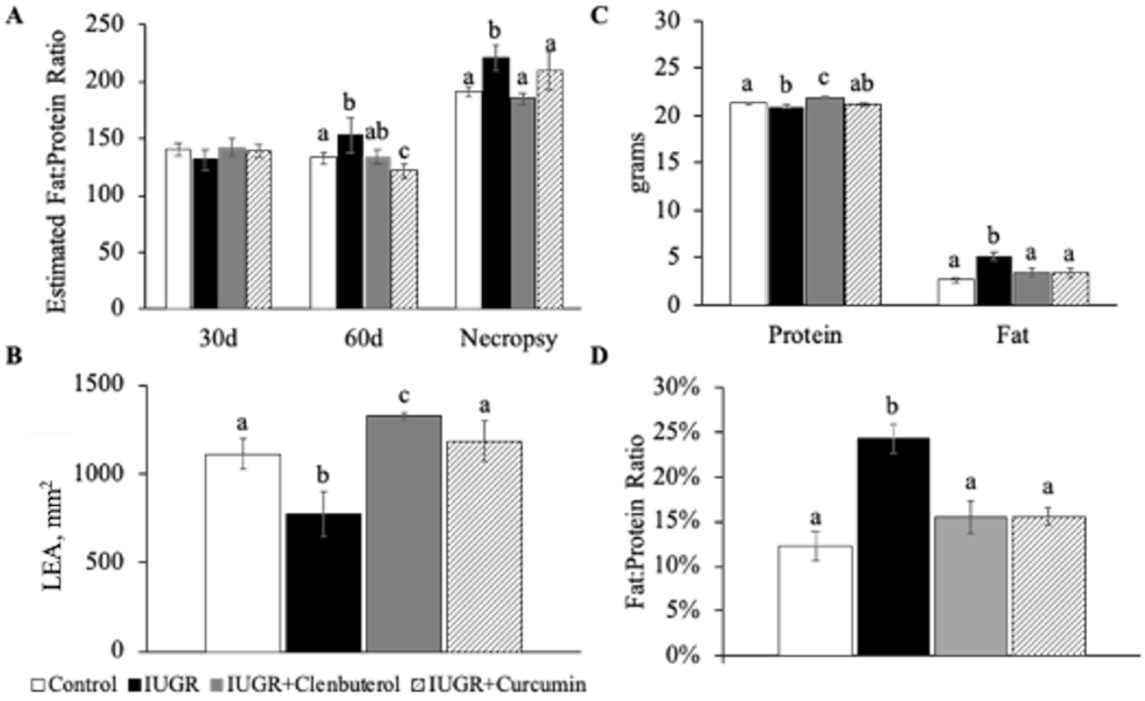


**Figure 2-3.** BIA estimated fat-to-protein ratio (A), loin-eye area (B), proximate analysis measured protein and fat content (C) and proximate analysis measured fat-to-protein ratio from Control (n=11), IUGR (n=5), IUGR+Clenbuterol (n=7), and IUGR+Curcumin (n=3) lambs. a,b means with differing superscripts differ ($P<0.05$). x,y means with differing superscripts tend to differ ($P<0.10$).

**Table 5.** Body composition at 30 and 60 d of age and carcass composition at necropsy estimated by BIA in IUGR lambs.

| Variables | Experimental Group | | | | *P*-value |
|---|---|---|---|---|---|
| | Control | IUGR | IUGR+Clenbuterol | IUGR+Curcumin | |
| **30 d of age** | | | | | |
| FFM, kg | 6.7 ± 1.11 | 6.32 ± 1.74 | 6.71 ± 1.1 | 6.78 ± 1.01 | NS |
| FFST, kg | 7.61 ± 0.99 | 7.26 ± 1.50 | 7.52 ± 1.01 | 7.55 ± 0.94 | NS |
| CF, g | 143.5 ± 2.6 | 140.6 ± 11.0 | 145.5 ± 9.6 | 139.5 ± 9.0 | NS |
| SUM, kg | 6.1 ± 0.35 | 5.40 ± 0.5 | 6.00 ± 0.65 | 5.74 ± 0.37 | NS |
| LSLRS, kg | 4.29 ± 0.25 | 3.82 ± 0.35 | 4.21 ± 0.44 | 4.04 ± 0.26 | NS |
| LSL, kg | 2.17 ± 0.18 | 1.91 ± 0.25 | 2.12 ± 0.28 | 2.02 ± 0.19 | NS |
| Moisture, kg | 8.79 ± 0.65 | 8.59 ± 0.82 | 8.94 ± 0.66 | 8.59 ± 0.61 | NS |
| Protein, kg | 2.49 ± 0.22 | 2.36 ± 0.33 | 2.64 ± 0.26 | 2.52 ± 0.19 | NS |
| Fat, kg | 1.61 ± 0.28 | 1.50 ± 0.35 | 1.65 ± 0.30 | 1.48 ± 0.27 | NS |
| Lean, kg | 10.11 ± 0.83 | 9.63 ± 1.26 | 10.76 ± 0.99 | 10.33 ± 0.70 | NS |
| **60 d of age** | | | | | |
| FFM, kg | 13.38 ± 0.97 | 10.09 ± 2.87 | 13.34 ± 2.19 | 14.77 ± 1.14 | NS |
| FFST, kg | 13.88 ± 0.88 | 10.74 ± 2.70 | 13.73 ± 2.04 | 15.05 ± 1.04 | NS |
| CF, g | 210.5 ± 9.5$^{a}$ | 183.7 ± 16.4$^{b}$ | 214.6 ± 25.2$^{ab}$ | 236.8 ± 19.8$^{a}$ | < 0.001 |
| SUM, kg | 10.19 ± 0.34$^{a}$ | 8.46 ± 0.5$^{b}$ | 9.97 ± 1.30$^{ab}$ | 10.20 ± 0.63$^{a}$ | < 0.001 |
| LSLRS, kg | 7.1 ± 0.24$^{a}$ | 5.96 ± 0.57$^{b}$ | 6.95 ± 0.9$^{ab}$ | 7.15 ± 0.42$^{a}$ | < 0.001 |
| LSL, kg | 4.0 ± 0.17$^{a}$ | 3.22 ± 0.42$^{b}$ | 3.91 ± 0.59$^{ab}$ | 4.11 ± 0.29$^{a}$ | < 0.001 |
| Moisture, kg | 13.48 ± 0.69 | 11.55 ± 1.28 | 13.88 ± 1.8 | 15.40 ± 1.38 | NS |
| Protein, kg | 4.09 ± 0.23 | 3.56 ± 0.40 | 4.32 ± 0.61 | 4.78 ± 0.41 | NS |
| Fat, kg | 3.77 ± 0.30$^{a}$ | 2.88 ± 0.56$^{b}$ | 3.89 ± 0.8$^{ab}$ | 4.57 ± 0.62$^{a}$ | < 0.001 |
| Lean, kg | 16.01 ± 0.83 | 14.15 ± 1.47 | 16.93 ± 2.23 | 18.59 ± 1.48 | NS |
| **Necropsy** | | | | | |
| FFM, kg | 18.50 ± 0.49$^{a}$ | 15.50 ± 0.55$^{b}$ | 18.68 ± 1.34$^{a}$ | 17.65 ± 0.78$^{a}$ | < 0.001 |
| FFST, kg | 21.68 ± 0.48$^{a}$ | 18.73 ± 0.58$^{b}$ | 21.77 ± 1.66$^{a}$ | 20.97 ± 0.87$^{a}$ | < 0.001 |
| CF, kg | 160.2.5 ± 3.0$^{a}$ | 137.2 ± 9.5$^{b}$ | 165.7 ± 17.6$^{a}$ | 156.8 ± 14.7$^{ab}$ | < 0.001 |
| SUM, kg | 23.59 ± 0.54$^{a}$ | 21.09 ± 0.74$^{b}$ | 23.19 ± 2.31$^{ab}$ | 22.96 ± 0.98$^{a}$ | < 0.001 |
| LSLRS, kg | 15.13 ± 0.37$^{a}$ | 13.44 ± 0.58$^{b}$ | 14.86 ± 1.51$^{ab}$ | 14.73 ± 0.65$^{ab}$ | < 0.001 |
| LSL, kg | 9.34 ± 0.22$^{a}$ | 8.34 ± 0.34$^{b}$ | 9.18 ± 0.91$^{ab}$ | 9.13 ± 0.37$^{a}$ | < 0.001 |
| Moisture, kg | 10.47 ± 0.27$^{a}$ | 8.75 ± 0.46$^{b}$ | 10.92 ± 1.29$^{a}$ | 10.38 ± 0.84$^{a}$ | < 0.001 |
| Protein, kg | 3.37 ± 0.10$^{a}$ | 2.73 ± 0.16$^{b}$ | 3.60 ± 0.45$^{a}$ | 3.43 ± 0.26$^{a}$ | < 0.001 |
| Fat, kg | 2.27 ± 0.11$^{a}$ | 1.54 ± 0.19$^{b}$ | 2.41 ± 0.55$^{a}$ | 2.14 ± 0.39$^{a}$ | < 0.001 |
| Lean, kg | 13.71 ± 0.39$^{a}$ | 11.31 ± 0.58$^{b}$ | 14.63 ± 1.66$^{a}$ | 14.02 ± 0.94$^{a}$ | < 0.001 |

Values are expressed as means ± SE; FFM, fat-free mass (kg); FFST, fat-free soft tissue; CF, crude fat; IUGR, intrauterine growth restriction; NS, not significant.

**Table 2-6.** Spearman Correlations of ultrasound estimations of loin size with actual loin eye area.

| | **Measurement** | **Ultrasound Estimates** | | |
|---|---|---|---|---|
| **Ultrasound Estimate** | Loin eye Area | Loin eye Area | Back Fat Thickness | Loin eye Depth |
| Loin eye Area | 0.48 | . | 0.01 | 0.74 |
| | *(0.26)* | . | *(0.99)* | *(0.05)* |
| Back Fat Thickness | 0.58 | 0.01 | . | 0.46 |
| | *(0.16)* | *(0.99)* | . | *(0.3)* |
| Loin eye Depth | 0.74 | 0.46 | 0.22 | . |
| | *(0.05)* | *(0.3)* | *(0.63)* | . |

Values are expressed as correlation coefficients with P-values italicized in parenthesis.

# Chapter 3

## Deficits in skeletal muscle glucose metabolism and pancreatic islet β cell function in the IUGR juvenile lamb are improved by daily treatment with the β2 adrenergic agonist, clenbuterol HCl.


### ABSTRACT

Fetal metabolic programming associated with intrauterine growth restriction (IUGR) has been linked to deficits in skeletal muscle glucose metabolism and pancreatic β cell dysfunction throughout the neonatal stage. These adaptions disrupt physiological mechanisms that regulate energy substrate utilization and tissue responsiveness to metabolic stimuli. We hypothesized that these fetal programing deficits persist and potentially worsen as IUGR-born offspring reach the juvenile stage. We also postulated that these deficits could be mitigated postnatal through β adrenergic manipulation. Thus, the objective of this study was to determine if muscle-centric deficits in glucose metabolism and pancreatic β cell dysfunction progressively worsen at the juvenile stage and whether daily treatment with the β agonist clenbuterol is an effective strategy to improve glucose homeostasis and metabolic health IUGR-born offspring. At 60 d of age, basal hindlimb glucose oxidation tended to be reduced ($P < 0.10$) and insulin-stimulated hindlimb glucose oxidation was reduced ($P < 0.05$) in placental insufficiency-induced IUGR lambs compared to controls and clenbuterol-supplemented IUGR lambs. Basal hindlimb glucose uptake did not differ among groups and insulin-stimulated hindlimb glucose uptake was greater ($P < 0.05$) in clenbuterol-supplemented IUGR lambs than controls or unsupplemented IUGR lambs. In isolated flexor digitalis superficialis and soleus muscle, basal glucose oxidation rates were diminished ($P < 0.05$) in IUGR lambs

compared to controls. In soleus, basal glucose oxidation in clenbuterol-supplemented lambs was intermediate between controls and unsupplemented IUGR lambs. Insulin-stimulated glucose oxidation rates were also diminished *(P* < 0.05) in both unsupplemented and clenbuterol-supplemented IUGR flexor digitalis superficialis and soleus muscle compared to controls. TNFα-stimulated glucose oxidation rates for isolated flexor digitalis superficialis did not differ between control and unsupplemented IUGR lambs but were less (*P* < 0.05) for clenbuterol-supplemented IUGR lambs than controls or unsupplemented IUGR lambs. TNFα-stimulated glucose oxidation rates for isolated soleus was less (*P* < 0.05) in IUGR lambs than controls and less (*P* < 0.05) in clenbuterol-supplemented IUGR lambs than unsupplemented IUGR lambs. Basal, insulin-stimulated, and TNFα-stimulated glucose uptake rates were all less (*P* < 0.05) in unsupplemented and clenbuterol-supplemented IUGR lambs than controls. Whole-body $O_2$ consumption rates tended to be less (*P* = 0.07) and $CO_2$ production was less (*P* < 0.05) in unsupplemented IUGR lambs than in controls or clenbuterol-supplemented IUGR lambs at 30 d of age, but neither differed among groups at 60 d of age. Basal insulin concentrations did not differ among groups at 60 d of age, but glucose-stimulated insulin secretion was reduced (*P* < 0.05) in unsupplemented IUGR lambs compared to controls and clenbuterol-supplemented IUGR lambs. This study shows that muscle-centric metabolic deficits and pancreatic islet dysfunction that persist in IUGR-born juvenile lambs can be improved by β adrenergic modification with daily clenbuterol treatment.

## INTRODUCTION

Intrauterine growth restriction (IUGR) is the result of a compilation of fetal adaptions that are essential for fetal survival of poor *in utero* conditions but that also lead to intrinsic deficits in growth and metabolic function after birth (Barker et al., 1993; Cadaret et al., 2019c; Yates et al., 2019a). This fetal programming includes reduced skeletal muscle glucose metabolism that is compounded by pancreatic β-cell dysfunction, both of which contribute to an 18-fold increase in the risk for Metabolic Syndrome in adulthood (Limesand et al., 2007a; Gatford et al., 2010; Yates et al., 2018b; Posont, 2019). Growth and metabolic adaptions can be attributed at least in part to changes in adrenergic and inflammatory signaling in muscle that continue even after the cessation of prenatal stress (Leos et al., 2010; Yates et al., 2011a). β2 adrenergic activity is a natural stimulant of skeletal muscle glucose oxidation (Cadaret et al., 2017) and is important for proper functional development of pancreatic islets (Macko et al., 2016a; Yates et al., 2019a). Thus, we speculate that postnatal adrenergic manipulation could be effective in improving skeletal muscle glucose metabolism in IUGR-born offspring. We previously found that IUGR impairs oxidative mechanisms of glucose metabolism in fetal and neonatal skeletal muscle (Cadaret et al., 2018; Cadaret et al., 2019c; Posont, 2019; Yates et al., 2019a). These deficits in skeletal muscle are further compounded by altered pancreatic islet development and function, which restricts proper insulin secretion and disrupts whole-body insulin sensitivity (Limesand et al., 2007a). Moreover, neonatal metabolic deficits occurred in the absence of adipose-driven postnatal catch-up growth. This suggests that deficient glucose metabolism and insulin signaling is likely not the result of greater fat deposition but instead is due to programming adaptions induced by

prenatal stress proper (Cadaret et al., 2019c). In this study, we hypothesized that developmental adaptions in skeletal muscle glucose metabolism and pancreatic β cells persist or even worsen in IUGR-born lambs between the neonatal and juvenile ages, but that daily treatment with clenbuterol HCl, an injectable β2 agonist, could correct postnatal adrenergic regulatory tone and thus improve their metabolic function. Therefore, the objective of this study was to test this hypothesis by assessing *in vivo* and *ex vivo* skeletal muscle glucose metabolism, whole body oxidative metabolic indicators, and pancreatic β-cell function in IUGR-born lambs at 60 d of age. We also sought to determine if daily treatment with clenbuterol HCl would recover aspects of diminished skeletal muscle glucose metabolism by increasing β2 adrenergic tone.

## MATERIALS & METHODS

### *Animals and Experimental Design*

These studies were approved by the Institutional Animal Care and Use Committee at the University of Nebraska-Lincoln, which is accredited by AAALAC International. Placental insufficiency-induced IUGR lambs were produced from Polypay crossbred ewes by the well-characterized maternal hyperthermia model described by Cadaret et al. (2019b) and Gibbs et al. (2020), and well as in the previous chapter. Briefly, timed-mated ewes were subjected to elevated ambient temperatures of 40°C with a relative humidity of 35% during peak placental development from the 40$^{th}$ to the 95$^{th}$ d of gestational age. Ewes were returned to thermoneutral temperatures (25°C) alongside their pair-fed control counterparts following the 55-d exposure, and all ewes were allowed to lamb naturally. At parturition, IUGR lambs were randomly assigned to receive 0.8μg/kg/d clenbuterol

HCl (i.m.) or a saline placebo of equal volume. All lambs were weaned at 12 hours of age and were hand-reared on milk replacer fed *ad libitum* for 30 days (Land O'Lakes Inc., Ardin Hills, MN) and then transitioned to the grain diet in **Table 2**. Milk replacer was discontinued by 45 d of age. At 55 d of age, lambs underwent surgical placement of indwelling catheters in the femoral artery and vein of one hindlimb as previously described (Yates et al., 2019a). A venous catheter and arterial perivascular blood flow probe were placed in the contralateral hindlimb. All catheters were exteriorized at the lamb's flank. Arterial blood samples were taken daily from 55 to 60 d of age. Whole blood was analyzed for complete blood counts with a HemaTrue Veterinary Chemistry Analyzer (Heska, Loveland, CO) and for blood gases and metabolites with an ABL90 Flex blood gas analyzer (Radiometer America, Bera, CA). Lambs were euthanized at 60 d of age by double barbiturate overdose.

***In vivo Metabolism***

*Indirect Calorimetry.* To estimate whole body oxidative metabolism, $O_2$ consumption rates and $CO_2$ production rates were determined by indirect calorimetry. At 30 and 58 d of age, a sealed clear-plastic chamber was secured over the head of the lamb. Atmospheric air was pumped into the chamber through an inlet hose at a constant rate of 110 L/min. $O_2$ and $CO_2$ content of air leaving the chamber through an outlet hose was measured with a Fox Box Respirometry System (Sable Systems, Las Vegas, NV). Measurements were obtained over two 30-min periods, each of which followed a 5-min baseline reading of atmospheric air. For the duration of this experiment, lambs were restrained in Panepinto slings to which they had been previously familiarized. Values for

$O_2$ consumption rate ($O_2CR$), $CO_2$ production ($CO_2P$), and metabolic rate (cal/hr) were averaged over the two periods.

*Glucose-Stimulated Insulin Secretion.* To measure β-cell function, glucose-stimulated insulin secretion was determined during a square-wave hyperglycemic clamp at 58 d of age as previously described (Camacho et al., 2017). Briefly, a series of three baseline arterial blood samples were taken in 5-minute intervals. Afterward, an intravenous glucose bolus (150 mg/kg, i.v.) was administered followed by a continuous, variable-rate glucose infusion until the target steady-state glucose concentration (2.5X baseline glucose) was achieved. During steady-state hyperglycemia, another three arterial blood samples were taken in 5-min intervals. Blood samples collected into EDTA syringes were centrifuged (14,000 x *g*, 2 min, 4°C) to isolate plasma, which was then stored at -80°C. Bovine insulin ELISA (Alpco, Salem, NH) were then used to measure insulin concentrations in all plasma samples. Inter- and intra-assay CV were below 10%. Blood samples collected into heparin-coated syringes were analyzed using an ABL90 Flex to measure glucose and lactate content.

*Hindlimb Glucose Metabolism.* At 59 d of age, hindlimb glucose metabolism was assessed during a hyperinsulinemic-euglycemic clamp (HEC) as previously described (Yates et al., 2019a). Briefly, lambs were bolused 2 ml of radiolabeled glucose tracer (18.75μCi/ml, U-[$^{14}$C]-glucose; Perkin-Elmer, Waltham, MA) followed by a constant infusion of U-[$^{14}$C]-glucose for 40 min at a rate of 2 ml/hr. Arterial and venous blood samples were simultaneously collected through femoral catheters in 5-minute intervals during the baseline period (4 total pairs of samples). Following baseline sample collection, a 6-ml glucose (150 mg/kg, i.v.) bolus and a 4-ml insulin (250 mU/kg;

Humulin-R, Eli Lilly, Indianapolis, IN) bolus were administered. Glucose was constantly infused at variable rates to maintain euglycemia (±10% baseline) and insulin was infused at a constant rate of 0.5 ml/hr/kg. Once steady-state HEC was achieved for 2 hours, four more pairs of simultaneously-collected arterial and venous blood samples were taken in 5-minute intervals. Plasma was collected and stored at -80°C and insulin concentrations were determined by Bovine Insulin ELISA. Blood samples were analyzed for blood gasses and metabolites. To measure hindlimb glucose oxidation, additional arterial and venous blood was placed in micro-centrifuge tubes containing 2M HCl and suspended within a 20-ml scintillation vial containing 1M NaOH at the bottom. These vials were sealed and incubated at room temperature. During a 24-hr incubation, HCl caused the release of $CO_2$ from the blood sample, which was then recaptured by the NaOH at the bottom of the scintillation vial. Following the incubation period, the blood-filled microcentrifuge tubes were removed, and scintillation vials were filled with UltimaGold scintillation fluid (Perkin-Elmer). Radiolabeled $CO_2$ ($^{14}CO_2$) concentrations were quantified using a Beckman-Coulter 1900 TA LC counter (Brea, CA). Glucose oxidation rates were then determined from the difference in $^{14}CO_2$ concentration between each arterial and venous blood sample pair. The amount of glucose oxidized was calculated in nmol using the specific activity of $^{14}C$ in the infusate, and these values were normalized to hindlimb mass and femoral artery blood flow rate at the time of sample collection. Hindlimb glucose uptake rates were estimated by the difference in arterial and venous glucose concentrations, normalized to hindlimb mass and blood flow rate.

***Ex vivo Skeletal Muscle Glucose Metabolism***

At 60 d of age, lambs were euthanized and the flexor digitorum superficialis and soleus muscles were collected for *ex vivo* metabolic analysis. Muscles were split tendon-to-tendon into 500 ± 50 mg strips. Strips were pre-incubated for 1 hr in Krebs-Heneslit Buffer (KHB) with no additive (basal), insulin (5 mU/ml Humulin-R), or TNFα (10 ng/ml). Following pre-incubation, muscle strips were washed in glucose-free KHB with the respective additive for 20 min. To measure glucose oxidation, muscle strips were placed in sealed dual-well chambers and incubated in KHB media containing the respective additive and 5 mM [$^{14}$C-U] D-glucose for 2 hr. The adjacent well of each chamber contained 1M NaOH. After 2 hr, chambers were cooled and wells containing muscle strips were injected with 2M HCl and allowed to incubate at 4°C for an additional 2 hr, during which bicarbonate-bound $^{14}CO_2$ was freed from the media and captured by the NaOH in the adjacent well. NaOH was collected and $^{14}CO_2$ concentration was determined by liquid scintillation. To measure glucose uptake, muscle strips were incubated in KHB media containing the respective additive and 1 mM [$^{3}$H]2-deoxyglucose for 20 min. After the 20 min incubation, muscle strips were cooled, washed, and lysed by incubation in 2M NaOH. The concentration of [$^{3}$H]2-deoxyglucose for each lysate was then determined by liquid scintillation.

***Statistical Analysis***

All data were analyzed using the Mixed procedure of SAS (SAS Institute, Cary, NC) with lamb as the experimental unit. Variables in GSIS, HEC, and *ex vivo* studies were analyzed for effects due to treatment, period (or incubation condition), and the

interaction, with period/incubation condition treated as repeated variables. For GSIS and HEC studies, samples within each period (technical replicates) were averaged for each lamb. Likewise, the 3 technical replications/condition for each lamb in *ex vivo* studies were averaged. Data are presented as means ± SEM.

## *RESULTS*

### *Hematology*

No experimental group x day interactions were observed for any hematology components. Total white blood cells (WBC), monocyte, lymphocyte, and granulocyte concentrations were not different among experimental groups (**Figure 3-1).** Hematocrit (**Figure 3-2A)**, red blood cell concentrations (**Figure 3-2B)**, and platelet concentrations (**Figure 3-2C)** were increased ($P < 0.05$) in unsupplemented IUGR lambs and reduced ($P < 0.05$) in clenbuterol-supplemented IUGR lambs compared to controls. Mean corpuscular volume (**Figure 3-2D)** and mean platelet volume (**Figure 3-2E)** were less ($P < 0.05$) in unsupplemented IUGR lambs but greater ($P < 0.05$) in clenbuterol-supplemented IUGR lambs compared to controls. Hemoglobin concentration did not differ between controls and unsupplemented IUGR lambs but were less ($P < 0.05$) in clenbuterol-supplemented IUGR lambs than controls (**Figure 3-3A**). Carbon dioxide-bound hemoglobin was greater ($P < 0.05$) in all IUGR lambs compared to controls but to a larger ($P < 0.05$) degree in clenbuterol-supplemented IUGR lambs (**Figure 3-3D).** Mean corpuscular hemoglobin concentration (**Figure 3-3B**) and oxygen bound hemoglobin concentration (**Figure 3-3C)** were not different among experimental groups.

***Blood Gases and Metabolites***

There were no differences in daily blood glucose (**Figure 3-4A**), plasma insulin (**Figure 3-4B**), glucose-to-insulin ratio (**Figure 3-4C**), or blood lactate concentrations (**Figure 3-4D**) among experimental groups. Blood pH did not differ between controls and unsupplemented IUGR lambs but was reduced ($P < 0.05$) in clenbuterol-supplemented IUGR lambs (**Figure 3-5C**). We also observed experimental group x day interactions for $CO_2$ partial pressure ($pCO_2$; **Figure 3-5D)**, $O_2$ partial pressure ($pO_2$; **Figure 3-5E**), $O_2$-bound hemoglobin (**Figure 3-3B)**, and $HCO_3$ concentrations (**Figure 3-5B)**. $pCO_2$ was lower ($P < 0.05$) in unsupplemented IUGR lambs than controls on d 56 and 57 but not on d 58, 59, and 60. $pCO_2$ in clenbuterol-supplemented IUGR lambs was lower *(*$P < 0.05$) than controls on d 56, greater *(*$P < 0.05$) on d 60, and not different on d 57, 58, and 59. $HCO_3$ concentrations were lower *(*$P < 0.05$) for both unsupplemented and clenbuterol-supplemented IUGR lambs than controls on d 57 but not different on d 56 and 60. $HCO_3$ was also less ($P < 0.05$) in clenbuterol-supplemented IUGR lambs than controls on d 59 and less ($P < 0.05$) than unsupplemented IUGR lambs on d 58. $pO_2$ was greater ($P < 0.05$) in unsupplemented IUGR lambs than controls on d 56, 57, 59, and 60 but not on d 58. $pO_2$ was also greater ($P < 0.05$) in clenbuterol-supplemented IUGR lambs compared to controls on d 56, 58, and 60, and was lower ($P < 0.05$) compared to unsupplemented IUGR lambs on d 60. $O_2$-bound hemoglobin was greater ($P < 0.05$) for both unsupplemented and clenbuterol-supplemented IUGR lambs compared to controls on each day. $O_2$-bound hemoglobin was also greater ($P < 0.05$) for clenbuterol-supplemented IUGR lambs than unsupplemented IUGR lambs on d 57 but less ($P < 0.05$)

on d 60. Potassium concentrations tended to be less ($P = 0.08$) in unsupplemented IUGR lambs compared to controls but did not differ between controls and clenbuterol-supplemented IUGR lambs. Sodium and calcium concentrations did not differ among experimental groups.

***Whole-body Oxidative Metabolism***

At 30 d of age, OCR tended to be less ($P = 0.07$) and $CO_2P$ was less ($P < 0.05$) in unsupplemented IUGR lambs compared to controls but did not differ between clenbuterol-supplemented IUGR lambs and controls (**Figure 3-6A)**. At 60 d of age, there were no differences among experimental groups for OCR or $CO_2P$. Metabolic rates did not differ among experimental groups at 30 or 60 d (**Figure 3-6A, 3-6B, 3-6C**). OCR, $CO_2P$, and metabolic rates were reduced ($P < 0.05$) at 60 d compared to 30 d of age, regardless of experimental group.

***Glucose-Stimulated Insulin Secretion***

An experimental group x day interaction was observed ($P < 0.05$) for plasma insulin but not for blood glucose, blood lactate, or glucose-to-insulin ratio. Blood glucose and blood lactate (**Figure 3-7B**) concentrations did not differ among experimental groups, but were greater ($P < 0.05$) during hyperglycemia than under basal conditions. Basal plasma insulin concentrations (**Figure 3-7A**) did not differ among groups, but glucose-stimulated insulin secretion was lower ($P < 0.05$) in unsupplemented IUGR lambs compared to controls and clenbuterol-supplemented IUGR lambs. Glucose-to-insulin ratios were increased ($P < 0.05$) for unsupplemented and clenbuterol-

supplemented IUGR lambs compared to controls, regardless of glycemic conditions (**Figure 3-7C)**. They were also reduced ($P < 0.05$) under hyperglycemic conditions compared to basal conditions, regardless of experimental group (**Figure 3-7D**).

### *Hindlimb Glucose Metabolism*

Hindlimb glucose uptake rates and blood lactate concentrations were not different among experimental groups under basal conditions but both were greater ($P < 0.05$) in clenbuterol-supplemented IUGR lambs than controls or unsupplemented IUGR lambs under HEC conditions (**Figure 3-8A and B**). Insulin sensitivity for glucose uptake was also not different among experimental groups (**Figure 3-9A**). Hindlimb glucose oxidation tended to be reduced ($P = 0.10$) under basal conditions and was reduced ($P < 0.05$) under HEC conditions for unsupplemented IUGR lambs compared to controls and clenbuterol-supplemented IUGR lambs (**Figure 3-8C**). Insulin sensitivity for glucose oxidation was increased ($P < 0.05$) in unsupplemented IUGR lambs compared to controls but did not differ between clenbuterol-supplemented IUGR lambs and controls (**Figure 3-8D**).

### *Ex Vivo Skeletal Muscle Glucose Metabolism*

Glucose uptake rates were less *(*$P < 0.05$) for FDS muscle from unsupplemented and clenbuterol-supplemented IUGR lambs than FDS from controls in all media conditions (**Figure 3-10A**). Basal glucose oxidation rates were less ($P < 0.05$) for FDS and soleus muscles from unsupplemented IUGR lambs and for FDS from clenbuterol-supplemented IUGR lambs compared to those from controls. Basal oxidation in soleus muscle from clenbuterol-supplemented IUGR lambs was intermediate between controls

and unsupplemented IUGR lambs (**Figure 3-10B**). When incubated in insulin-spiked media, glucose oxidation rates were less ($P < 0.05$) for FDS and soleus from unsupplemented IUGR lambs and soleus from clenbuterol-supplemented IUGR lambs compared to those from controls (**Figure 3-10B**). When incubated in TNFα-spiked media, glucose oxidation rates were lower *(*$P < 0.05$) for soleus from unsupplemented IUGR lambs and for FDS and soleus from clenbuterol-supplemented IUGR lambs compared to those from (**Figure 3-10B**).

## DISCUSSION

The results of this study demonstrate that muscle-specific deficits in glucose metabolism caused by placental insufficiency-induced IUGR continue to be exhibited by juvenile-aged offspring, despite improvement in whole-body oxidative metabolism between the neonatal and juvenile stages. *In vivo* and *ex vivo* metabolic studies indicated that impaired hindlimb glucose metabolism in addition to deficits in pancreatic β cell function persisted in juvenile lambs that were born IUGR. These results parallel our previous findings in the neonate in which hindlimb glucose metabolism was restricted by PI-IUGR, resulting in reduced hindlimb and primary skeletal muscle glucose oxidation under basal and insulin-stimulated conditions (Cadaret et al., 2019c). As with fetal and neonatal stages (Limesand et al., 2007b; Cadaret et al., 2019c), the deficits we observed in glucose oxidative metabolism at the juvenile stage appeared to be independent of glucose uptake. They also appeared to be associated with abhorrent insulin and cytokine sensitivity in muscle tissues. Despite the continuance of metabolic deficits in IUGR-born

offspring beyond early life, this study also showed that some metabolic deficits can be improved through daily treatment of the β2 adrenergic agonist, clenbuterol.

*In vivo* assessment of skeletal muscle glucose metabolism revealed that IUGR fetal adaptions continued to reduce hindlimb glucose oxidation through 2 mo. of age. Similar to our previous studies in the neonate (Cadaret et al., 2019c; Posont et al., 2019; Yates et al., 2019b), reductions in hindlimb glucose oxidation were independent of glucose uptake. Clenbuterol was particularly effective in recovering diminished hindlimb glucose metabolism, which was reflected in the recovery of both basal and insulin-stimulated glucose oxidation. In fact, clenbuterol reduced blood lactate levels during hyperinsulinemia, increased basal $CO_2$-bound hemoglobin, and reduced basal blood pH, all of which are consistent with the increase in oxidative metabolism. In addition to improvements in skeletal muscle glucose oxidation, clenbuterol also increased glucose uptake by the hindlimb tissues of our IUGR lambs beyond the rates observed in our normal lambs. The recovery of normal hindlimb glucose oxidation coupled with increased hindlimb glucose uptake rates and reduced blood lactate concentrations suggest that increasing the β2 adrenergic activity in our IUGR-born lambs helped to correct their muscle-specific deficits in glucose metabolism. This also further validates our long-standing speculation that β adrenergic dysfunction is prevalent in IUGR skeletal muscle (Yates et al., 2011b; Yates et al., 2012b; Yates et al., 2018a; Posont and Yates, 2019).

Our *ex vivo* analysis demonstrated the muscle-specific nature of the IUGR-associated deficits in glucose uptake and oxidation in two muscles of the hindlimb with very different metabolic phenotypes. Interestingly, the benefits of clenbuterol on glucose metabolism that were observed *in vivo* were not recapitulated in *ex vivo* primary skeletal

muscle glucose uptake and oxidation. This leads us to believe that β adrenergic modifiers may lose their effect once the muscle is no longer being exposed to them and thus they may require continuous administration to improve IUGR deficits long term. In addition, clenbuterol supplementation further diminished TNFα-stimulated glucose oxidation in IUGR lambs, which further represents the adrenergic system's inhibitory effect on inflammatory cytokine action.

Indicators of whole-body total oxidative metabolism were reduced in our IUGR-born lambs when assessed during the neonatal stage, but these differences had disappeared by 60 d of age, which suggests that total oxidative metabolism improves as neonates grow and mature into the juvenile stage, despite persistent reductions skeletal muscle glucose oxidation. We speculate that this improvement is likely the result of compensatory increases in protein and lipid oxidation and/or greater non-muscular glucose oxidation that offset the known reduction in glucose oxidative capacity of IUGR skeletal muscle.

This study also showed that pancreatic β cell response under hyperglycemic conditions continued to be impaired in IUGR-born offspring at the juvenile stage. Much like in the fetus and neonate (Cadaret et al., 2019a; Cadaret et al., 2019c), insulin secretion was not altered under resting glycemic conditions, suggesting that it is the stimulus-secretion coupling for insulin that is disrupted. Interestingly, proper insulin secretion and islet sensitivity to glucose were achieved by increasing β2 adrenergic activity with daily clenbuterol supplementation, despite insulin secretion being primarily modulated by α2 adrenoceptor binding (Limesand and Rozance, 2017a). In addition, glucose-to-insulin ratios were increased for both unsupplemented and clenbuterol-

supplemented IUGR lambs. This along with no differences in insulin sensitivity for glucose uptake suggests that peripheral tissue responsiveness to insulin stimulation might be impaired in the 60-d IUGR-born lamb in addition to β-cell function, as previously observed in the IUGR fetus (Limesand et al., 2007a).

From the results of this study, we can conclude that IUGR fetal adaptions continue to pose consequences for skeletal muscle glucose metabolism and pancreatic β cell function as offspring advance to the juvenile stage. However, these adaptive programming mechanisms appear to be at least partially recovered by daily treatment with the β2 agonist, clenbuterol. This study further demonstrates that IUGR-born offspring are restricted by β adrenergic dysfunction, which disrupts important regulatory mechanisms that are necessary for proper skeletal muscle glucose oxidation and insulin responses. In addition, this study provides evidence that postnatal treatment of metabolic deficits associated with IUGR is on target to prevent or reduce the risk of later life metabolic disease.

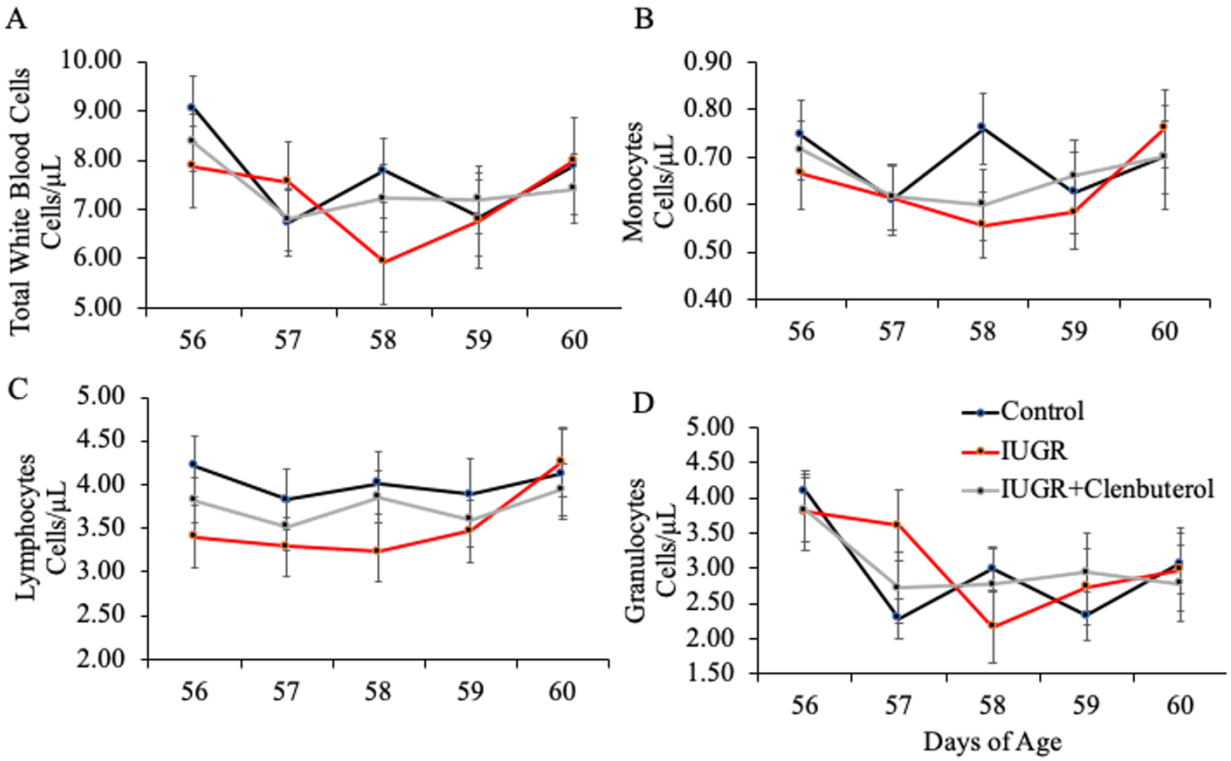


**Figure 3-1.** Daily total white blood cell (A), monocyte (B), lymphocyte (C), and granulocyte (D) concentrations from Control (n=11), IUGR (n=5), and IUGR+Clenbuterol (n=7) juvenile lambs.

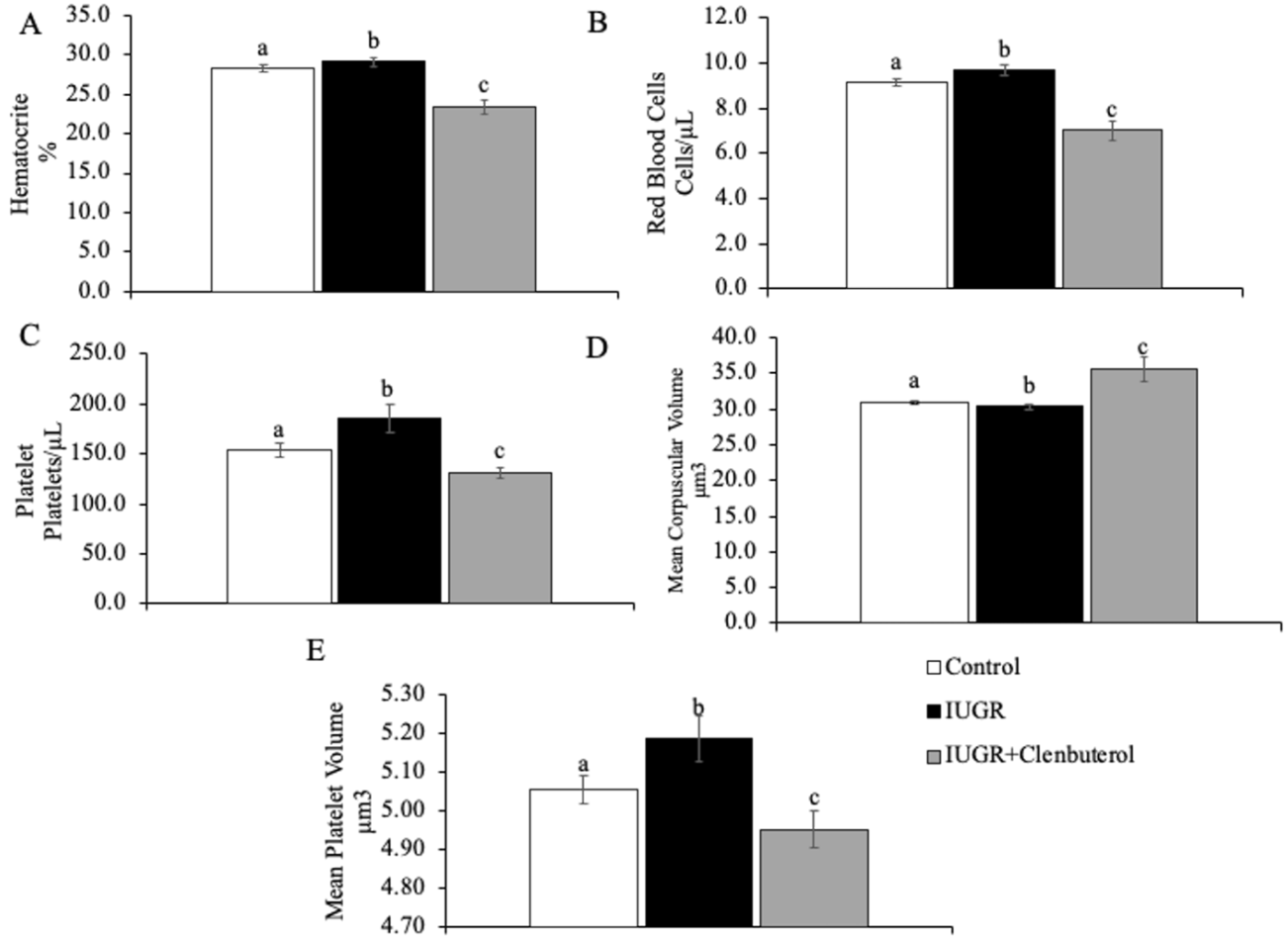


**Figure 3-2.** Daily hematocrit percentage (A), red blood cell concentration (B), platelet concentration (C), and mean corpuscular volume (D) from Control (n=11), IUGR (n=5), and IUGR+Clenbuterol (n=7) juvenile lambs. a,b means with differing superscripts differ ($P<0.05$).

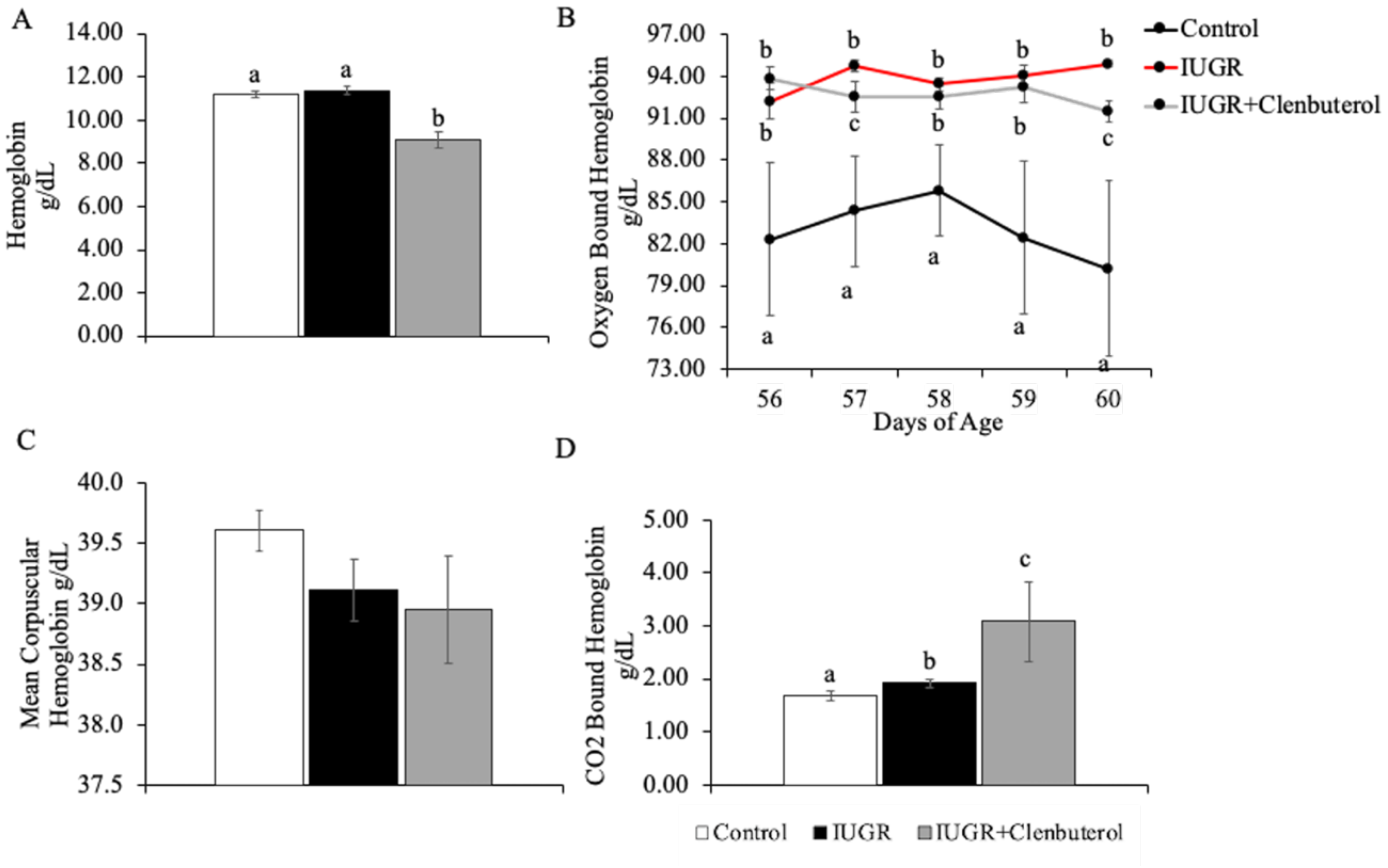


**Figure 3-3.** Daily hemoglobin (A), oxygen bound hemoglobin (B), mean corpuscular hemoglobin, and carbon dioxide bound hemoglobin (D) concentrations from Control (n=11), IUGR (n=5), and IUGR+Clenbuterol (n=7) juvenile lambs. a,b means with differing superscripts differ (P<0.05).

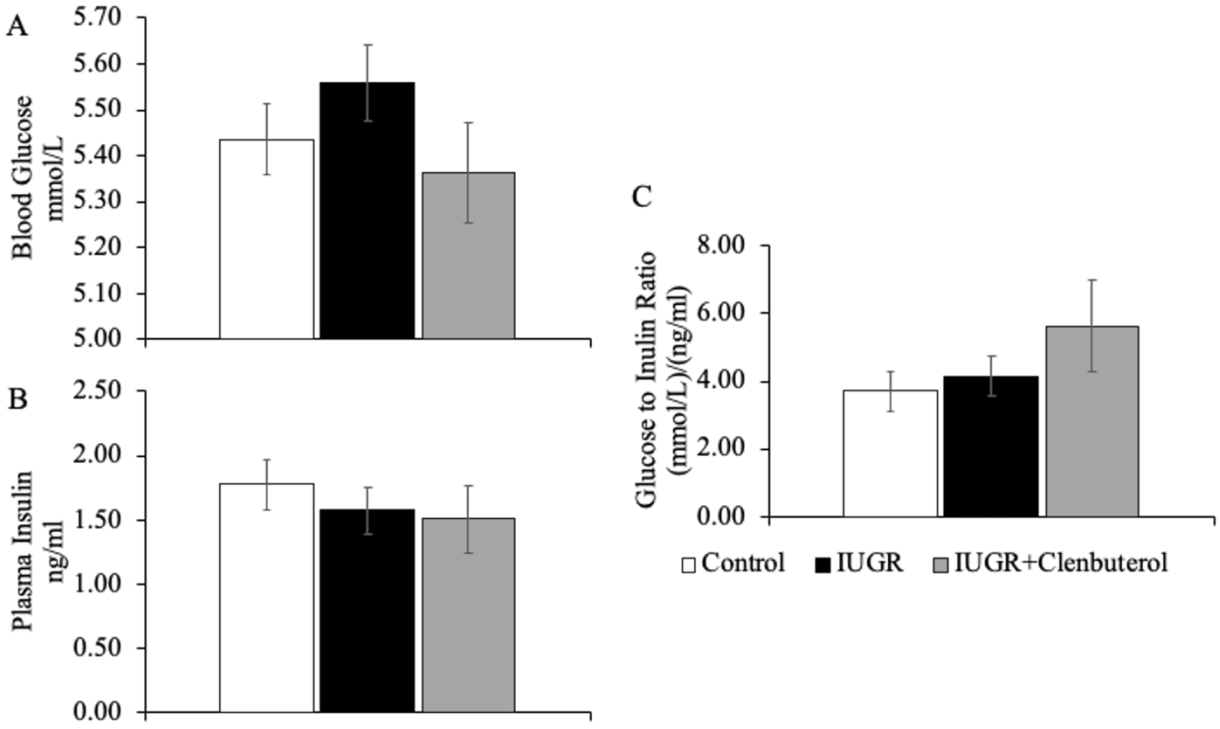


**Figure 3-4.** Daily blood glucose (A), plasma insulin concentration (B), and glucose-to-insulin ratio (C) from Control (n=11), IUGR (n=5), IUGR+Clenbuterol (n=7) juvenile lambs.

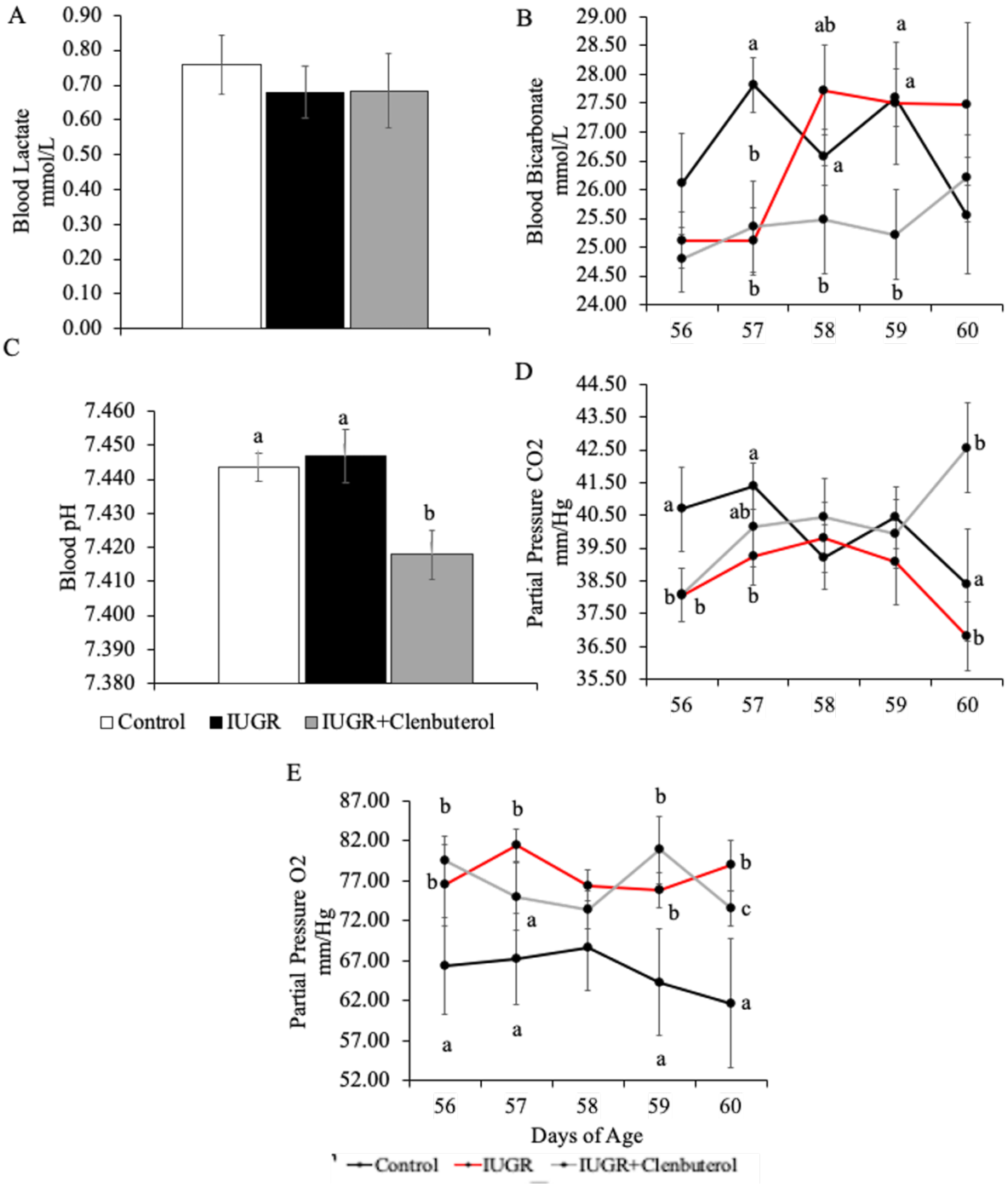


**Figure 3-5.** Daily blood lactate (A), blood bicarbonate (B), blood pH (C), partial pressure carbon dioxide (D), and partial pressure oxygen (E) concentrations from Control (n=11), IUGR (n=5), and IUGR+Clenbuterol (n=7) juvenile lambs. a,b means with differing superscripts differ (P<0.05).

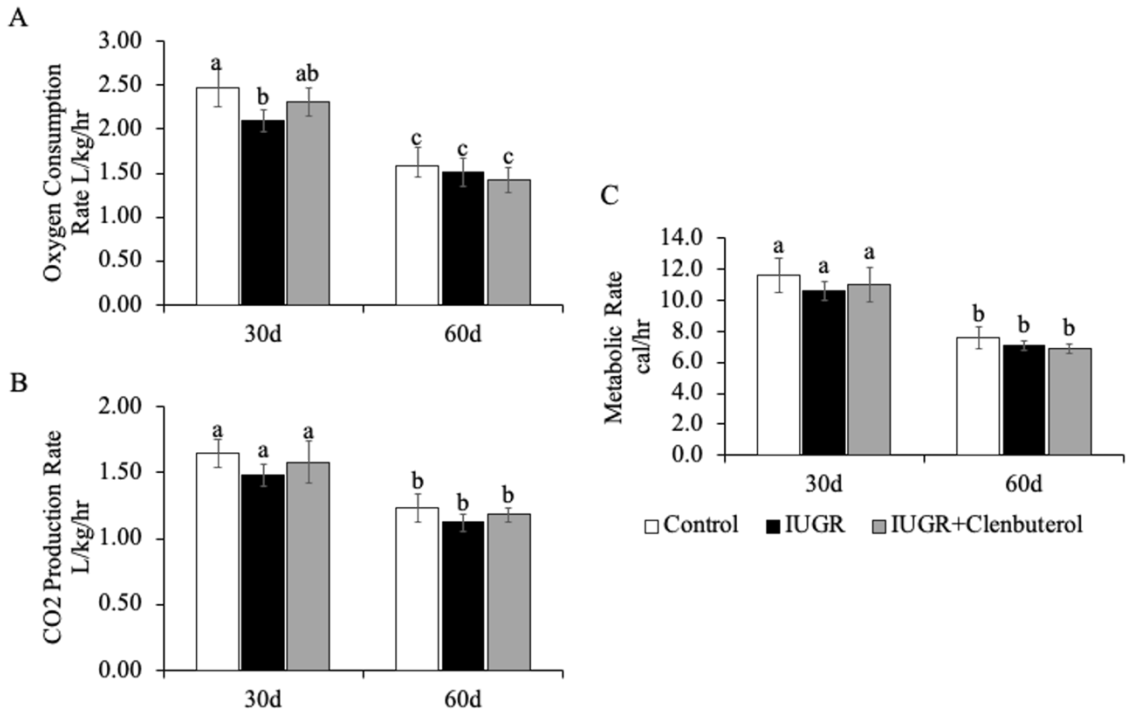


**Figure 3-6.** Whole body oxidative metabolism measured by oxygen consumption rate (A), carbon dioxide production rate (B), and metabolic rate (C) from Control (n=11), IUGR (n=6), and IUGR+Clenbuterol (n=7) juvenile lambs. a,b means with differing superscripts differ ($P<0.05$).

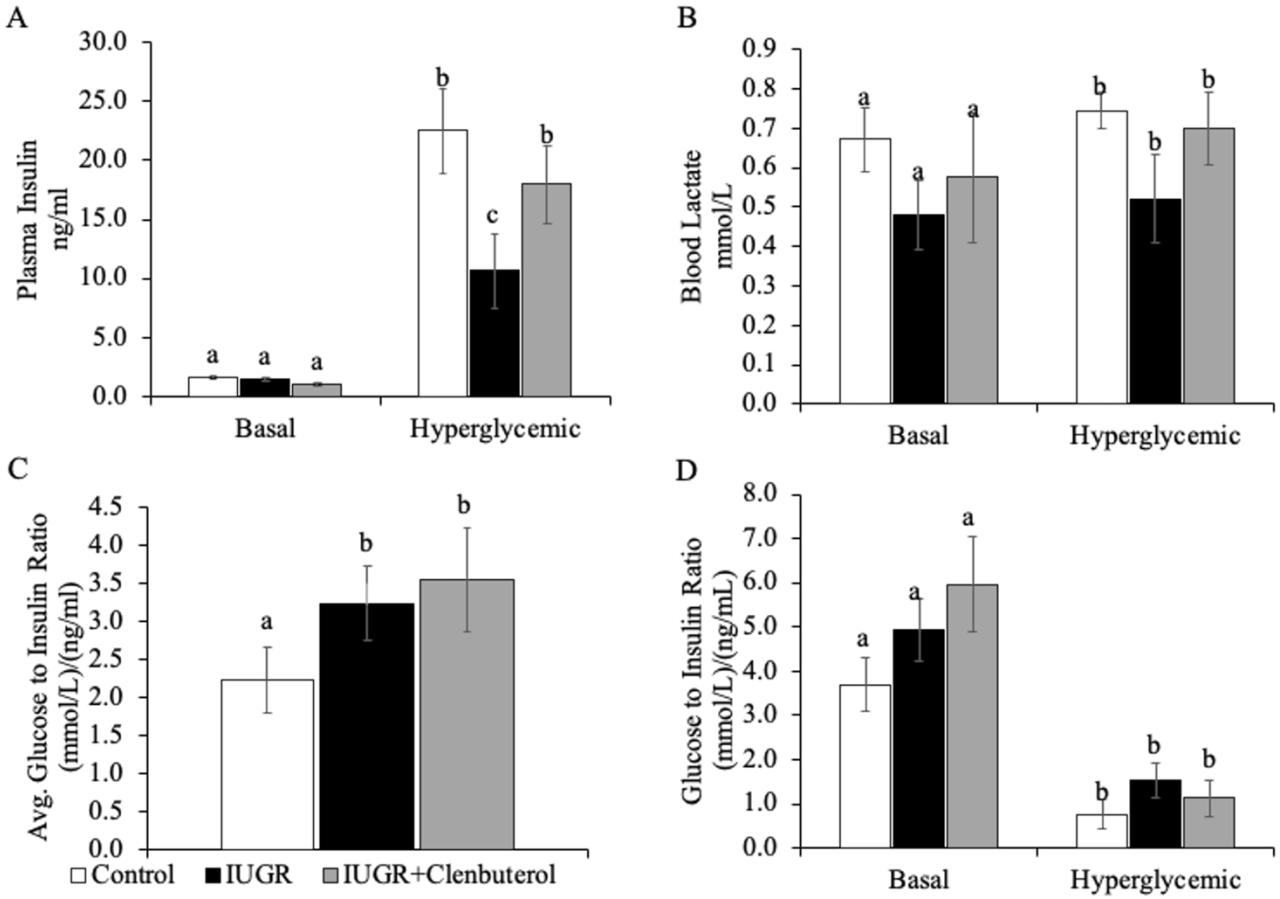


**Figure 3-7.** Plasma insulin concentration (A), blood lactate concentration (B), and glucose-to-insulin ratio (D) under basal and hyperglycemic conditions. Average glucose-to-insulin ratio (C) was measured over both periods from Control (n=11), IUGR (n=5), and IUGR+Clenbuterol (n=6) juvenile lambs. a,b means with differing superscripts differ ($P<0.05$).

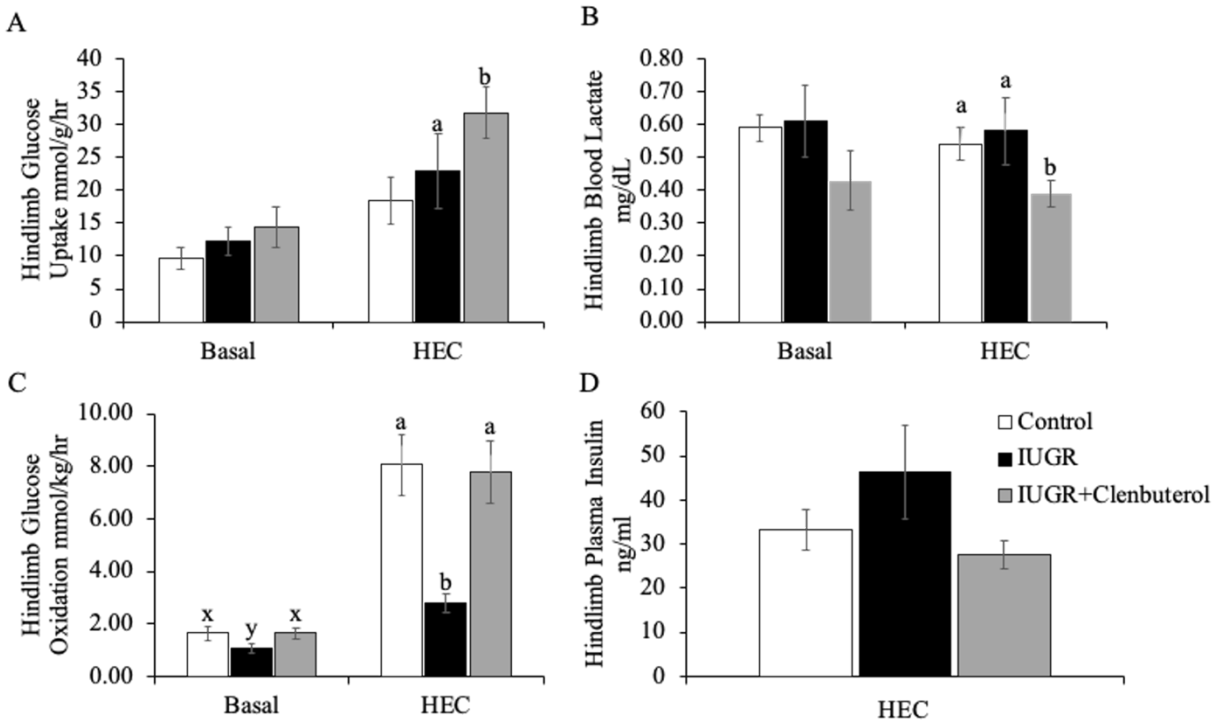


**Figure 3-8.** Hindlimb glucose uptake (A), hindlimb blood lactate (B), and hindlimb glucose oxidation (C) under basal and hyperinsulinemic-euglycemic conditions measured by an *in vivo* Hyperinsulinemic-Euglycemic Clamp study. Hindlimb plasma insulin concentrations during steady-state hyperinsulinemia was measured by Bovine ELISA for Control (n=8), IUGR (n=5), and IUGR+Clenbuterol (n=6) juvenile lambs. a,b means with differing superscripts differ ($P<0.05$).

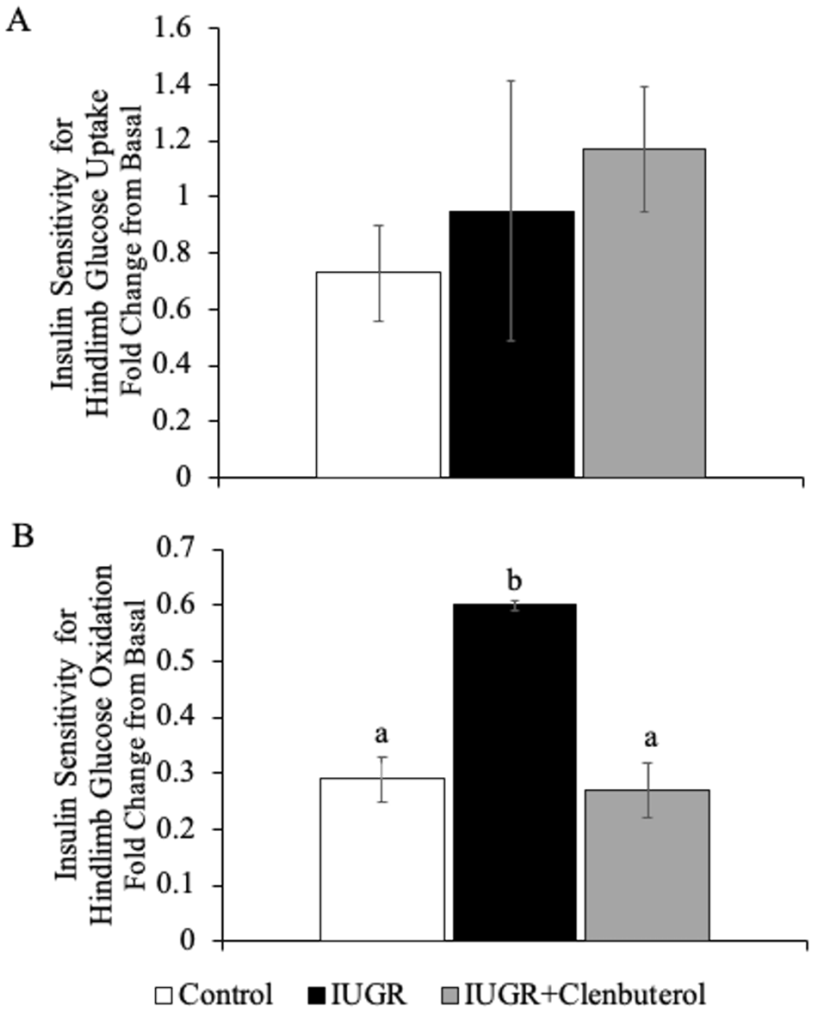


**Figure 3-9.** Insulin sensitivity for hindlimb glucose uptake (A) and hindlimb glucose oxidation (B) during steady-state hyperinsulinemia measured by fold change percentage between basal and hyperinsulinemic-euglycemic conditions. Data shown are from Control (n=8), IUGR (n=5), and IUGR+Clenbuterol (n=6) juvenile lambs. a,b means with differing superscripts differ ($P<0.05$).

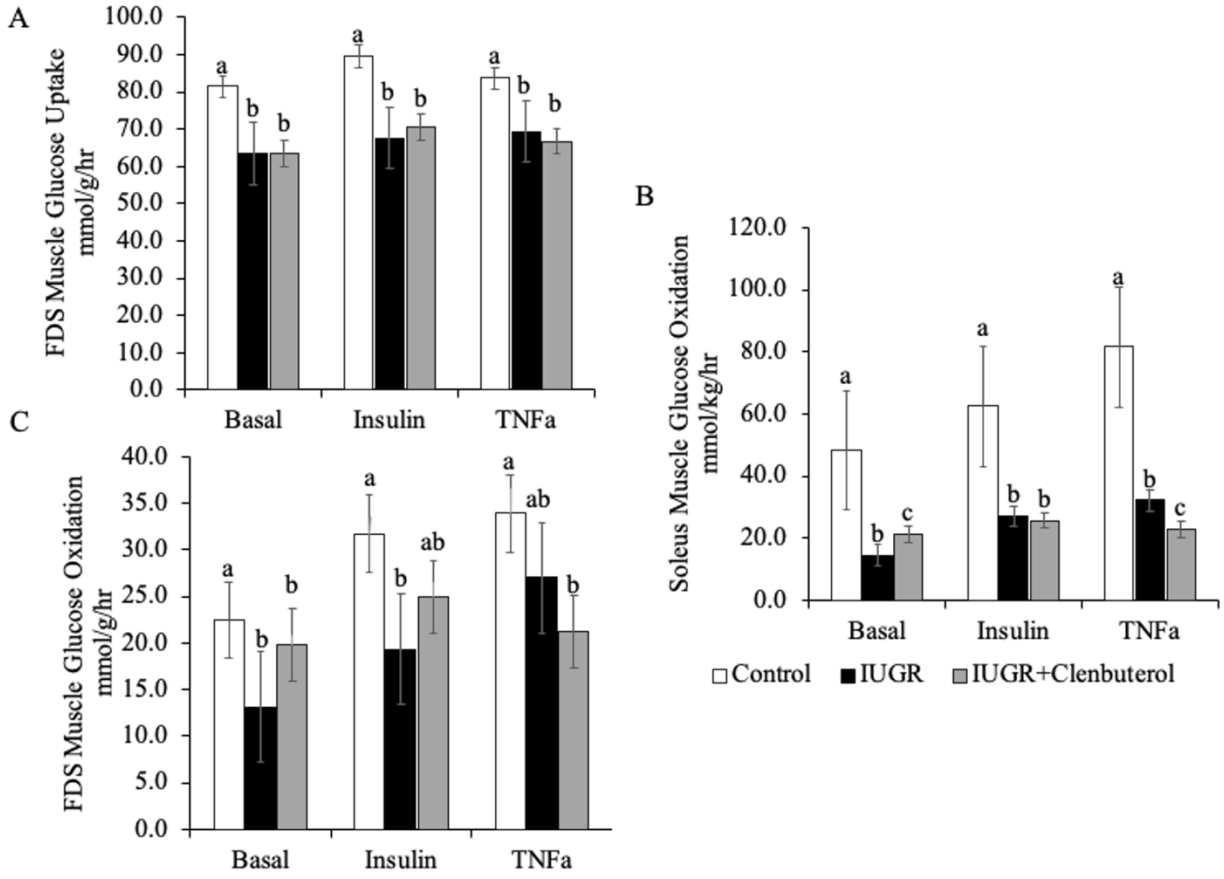


**Figure 3-10.** *Ex vivo* glucose metabolism by primary skeletal muscle collected at 60d of age from Control (n=11), IUGR (n=5), and IUGR+Clenbuterol (n=7). Data are shown for juvenile flexor digitorum superfalisis muscle glucose uptake rates (A.), solues muscle glucose oxidation rates (B.) and flexor digitorum superfalisis muscle glucose oxidation rates (C.) after incubation in media without (basal), with 5mU/ml insulin or 10ng/ml TNFα. a,b means with differing superscripts differ ($P<0.05$).

# Chapter 4

## Body composition estimated by bioelectrical impedance analyses (BIA) is diminished by prenatal stress in neonatal lambs and by heat stress in feedlot wethers.[2]

[2]A version of this chapter containing minimal modification was previously published in *Translational Animal Science*: 2019 Dec;3(Suppl 1):1691-1695. doi: 10.1093/tas/txz059.


## ABSTRACT

Stress during postnatal growth or during critical windows of prenatal development reduce muscle mass and alter body composition. Lean-to-fat proportion is indicative of wellbeing, performance, and value in livestock. Bioelectrical impedance analysis (**BIA**) is an accurate and objective tool for assessing body composition in humans. Our objective was to determine the impact of stress on BIA-estimated body composition in neonatal lambs exposed to *in utero* stress and in heat-stressed feedlot wethers. In Exp.1 of this study, intrauterine growth-restricted (IUGR) lambs were produced by maternal hyperthermia-induced placental insufficiency (PI-IUGR) or bacterial endotoxin-induced maternal inflammation (MI-IUGR). A 2$^{nd}$ group of PI-IUGR ewes were supplemented with 100% $O_2$ (10L/min, endotracheal) for the last 3 wk of gestation (PI-IUGR+$O_2$). BIA was performed at d 3 and 25 after birth. Bodyweight (**BW**) at d 3 and 25 was lower ($P <$ 0.05) in PI-IUGR and MI-IUGR lambs but not PI-IUGR+$O_2$ lambs compared to controls. At 3 d, BIA did not detect differences among groups for fat-free mass (**FFM**) or carcass components, and estimates were inconsistent and unrealistic. At 25 d, however, BIA

indicated that FFM/BW, moisture content, and fat content were reduced ($P < 0.05$) and protein content tended to be reduced ($P < 0.10$) in PI-IUGR and MI-IUGR lambs compared to PI-IUGR+$O_2$ and controls. In Exp.2 of this study, feedlot wethers were exposed to heat stress (40°C, 35% RH) or thermoneutral conditions for 30 d, and BIA was performed on d 0 and 14 in the live animal and on d 30 in the un-chilled carcass. Average daily gain tended to be less ($P < 0.08$) in heat-stressed wethers. At d 0 and 14, BIA did not detect differences for any body composition estimates. At d 30, postmortem FFM/BW in heat-stressed wethers was ~6.6% less ($P < 0.05$) and FFST/BW was ~6.5% less ($P < 0.05$) than control wethers. Carcass components did not differ between groups. From these studies, we conclude that BIA reasonably estimates stress-induced changes in body composition in lambs, except in very young animals.

## INTRODUCTION

In livestock, body composition plays an intricate role in productivity and profitability. Previous research has shown that carcass traits are highly heritable, thus the benefit of estimating body composition in the live animal is substantial (Berg et al., 1994). Bioelectrical impedance analysis (BIA) is used in humans to assess body composition (Khlaed et al., 1988) but is used less in livestock. BIA outputs for electrical flow through tissues are fit to regression equations that predict fat-free mass (FFM) or fat-free soft tissue (FFST) (Lukaski et al.,1985), which estimate the amount of lean body mass relative to fat. FFM and FFST indicate value for food animal producers. Poor body composition (high fat, less lean mass) can be caused by stress in growing lambs (Lukaski et al.,1985; Jenkins et al., 1988) and *in utero,* which has detrimental effects on muscle

growth and metabolic function of offspring later in life (DeBlasio et al., 2007; Barker and Hales, 1992). Intrauterine growth restriction (IUGR) is caused by placental insufficiency, and heat stress is a leading cause of placental insufficiency in livestock (Chen et al. 2010). In animal models, it restricts fetal growth by 30 to 60% (Brown et al., 2015; Macko et al., 2016). Maternal inflammation, another common stress factor in both humans and animals, restricts growth by 24% (Cadaret et al., 2018). IUGR increases perinatal mortality and morbidity and is characterized in offspring by low birthweight and asymmetrical body composition due to impaired muscle growth (Yates et al., 2018). The objective of this study was to determine whether BIA measurements can predict changes to body composition in live sheep for use in the food production industry as well as to determine if BIA measurements reflect stress-induced changes.

## MATERIALS & METHODS

### *Animals and Experimental Design*

The following experiments were approved by the Institutional Animal Care and Use Committee at the University of Nebraska-Lincoln. Studies were conducted at the University of Nebraska-Lincoln Animal Science Complex, which is accredited by AAALAC International.

*Expetriment 1.* Maternal inflammation-induced IUGR (MI-IUGR; n = 8) lambs were produced from time-mated Polypay ewes administered E.*coli* O55:B5 bacterial lipopolysaccharide (0.1μg/kg, i.v.; Sigma-Aldrich) every 3$^{rd}$ day from the 100$^{th}$ to the 115$^{th}$ day of gestation (dGA), as previously described (Cadaret et al., 2019). Placental insufficiency-induced IUGR (PI-IUGR; n = 7) lambs were produced from ewes exposed

to 40°C and 35% RH from dGA 40 to dGA 90, as previously described (Yates et al., 2019). A second group of PI-IUGR lambs was produced from ewes that were also supplemented with maternal $O_2$ through an endotracheal catheter for 8 h/d from dGA 131 until parturition (PI-IUGR+$O_2$; n = 9). Controls were maintained at thermoneutral conditions and injected with saline carrier only (n = 16). Lambs were weaned at birth and hand reared on milk replacer fed *ad libitum.* BIA was performed on all lambs at 3 d and 25 d of age.

*Experiment 2.* Suffolk crossbred wethers (approximately 5 mo of age, 43.1 ±0.6 kg) were commercially purchased. Wethers were stratified by bodyweight (BW) and randomly assigned to be individually penned under thermoneutral (controls; n = 14) or heat-stress (n = 12) conditions. Heat stress (35°C x 12 h/d and 40°C x 12 h/d, 35% RH) was induced for 30 d following a 2-d temperature step-up. Controls were maintained at 25°C and 15% humidity. Ractopamine HCl was supplemented to half of each group in a 2 x 2 factorial but had no effect on the results of this study, so it was removed from the model. Additional data from these lambs has been published elsewhere (Swanson et al., 2020).

### *Bioimpedance Analysis*

In Experiment 1, BIA was performed in the live lambs at 3 and 25 d of age. In Experiment 2, BIA was performed in the live wethers on d 0 and d 14 of the study period and in the hot carcasses at necropsy. We utilized a four-terminal Quantum V impedance apparatus, (RJL Systems, Detroit, MI) that measures reactance (Xc), resistance (Rs), and

phase angle (PA). This machine utilizes two sets of spaced electrode-terminals that transmit an electrical current through the tissues, which is detected by electrodes placed at another location on the body. Aluminum 20G MONOJECT$^{TM}$ needles (Covidien llc, Mansfield, MA) were placed SQ in the live animal and IM in the hot carcass and connected to the electrodes. The two sets of electrode-terminals (one red and one black) were placed 2.5 cm apart from each other. In live animals, one set was placed at the upper back, approximately 10 cm from the point of the scapula. The 2$^{nd}$ set was placed at the lower back, approximately 5 cm from the tail head. Both sets were placed dorsally, approximately 1 cm off the midline. Measurements were recorded for 30 consecutive seconds, with one measurement every 5 seconds, resulting in six total measurements. These were averaged and used in estimation equations outlined in **Table 4-1** for live animal mass and nutrient composition. For wether carcasses, electrodes were placed in the same approximate location as in the live animal. Body composition was estimated using the previously-determined equations in **Table 4-1**.

***Proximate Analysis***

Proximate analysis was performed on the longissimus dorsi (i.e. loin muscle) of wethers in Experiment 2 by Midwest Laboratories (Omaha, NE) to determine moisture, fat, and protein content. These were compared to BIA-estimated values.

***Statistical Analysis***

All data were analyzed by ANOVA using the mixed procedure of SAS. For BIA data, age of the animal was treated as a repeated measure. Lamb was considered the

experimental unit for Experiment 1 and wether for Experiment 2. Mean FFM and FFST were calculated from the average of their respective equations. Data are presented as means ± standard error.

## RESULTS

### *Experiment 1.*

BIA-estimated body composition and nutrient content for neonatal lambs are presented in **Table 2**. At 3 and 25 d of age, BW was less ($P < 0.05$) for MI-IUGR and PI-IUGR lambs than for controls and PI-IUGR+$O_2$ lambs. BW was also less ($P < 0.05$) in PI-IUGR lambs than MI-IUGR lambs at 3 d of age but not at 25 d of age. At 3 d of age, BW/body length (BL) was less ($P < 0.05$) in PI-IUGR lambs than controls, MI-IUGR lambs, and PI-IUGR+$O_2$ lambs. At 25 d of age, BW/BL was less ($P < 0.05$) in PI-IUGR+$O_2$ and MI-IUGR lambs than controls and PI-IUGR lambs. BIA-estimated moisture content was less ($P < 0.05$) for PI-IUGR and MI-IUGR lambs than for controls and PI-IUGR+$O_2$ lambs at 3 and 25 d of age. Estimated moisture was also less ($P < 0.05$) in PI-IUGR lambs than in MI-IUGR lambs at 3 d but not 25 d. Estimated protein content was not different among groups and estimated fat content could not be estimated at 3 d, but both were less ($P < 0.05$) in PI-IUGR and MI-IUGR lambs than in controls and PI-IUGR+$O_2$ lambs at 25 d. Estimated moisture content/BW and protein content/BW did not differ among groups at either day. Estimated fat content/BW was less ($P < 0.05$) in PI-IUGR lambs than in controls, PI-IUGR+$O_2$, and MI-IUGR at 25 d of age. BIA-estimated FFM was not different among groups at 3 d but tended to be less ($P < 0.10$) in PI-IUGR and MI-IUGR lambs than controls at 25 d. FFM was also less ($P < 0.05$) in PI-IUGR

lambs than in PI-IUGR+$O_2$ lambs. FFM/BW was less ($P < 0.05$) in PI-IUGR lambs than in controls, PI-IUGR+$O_2$, and MI-IUGR lambs at 25 d of age.

***Experiment 2.***

BIA-estimated body composition measured in the live animal is presented in **Table 3** and that measured at necropsy is presented in **Table 4**. There were no differences between controls and heat-stressed wethers for any BIA-estimated body composition variables (FFM, FFST, muscle yield) on d 0 or d 14 of the study. Average daily gain (ADG) between d 0 and d 14 and between d 0 and d 30 (Tables 3 and 4, respectively) tended to be less ($P < 0.10$) in heat-stressed weathers than in controls. None of the four equations for FFM or three equations for FFST detected differences between groups at d 0 or d 14. Likewise, no differences were observed for FFM/BW or FFST/BW. At necropsy, there were no differences between control and heat-stressed wethers for 3 of 4 FFM equations and for 2 of 3 FFST equations. However, the FFM4 equation, the FFST2 equation, and the mean for FFM and FFST detected reductions ($P < 0.05$) or tendencies for reductions ($P < 0.10$) in heat-stressed wethers compared to controls. Moreover, FFM/BW and FFST/BW were reduced ($P < 0.05$) in heat-stressed wethers compared to controls for all equations as well as the respective means of the equations. Estimated sum of the leg, sirloin, rack, shoulder, neck, riblets, shank, and lean trim mass (SUM), the sum of leg, sirloin, loin, rack, and shoulder mass (LSRLS), and the sum of leg, sirloin, and loin mass (LSL) were not different between groups. Nutrient composition (moisture, protein, fat, lean mass) estimated for heat-stressed wethers at d 0 and d 14 is presented in **Table 5**. No differences between controls and heat-stressed wethers were observed at either day.

## DISCUSSION

Our findings show that the impact of prenatal stress on body composition in offspring was detectable at 25 d of age but not at 3 d of age. Reduced lean tissue mass is a hallmark characteristic of IUGR and is often coupled with increased fat deposition during early postnatal growth (Yates et al., 2018). The reduced fat mass estimated in IUGR lambs at 25 d of age shows that they had not yet undergone postnatal catchup growth. This is further indicated by their lighter BW at 25 d. We speculate that our inability to effectively detect the impact of prenatal stress on body composition at 3 d of age is likely due to the decreased body mass of young lambs. In addition, we believe body composition estimates are more accurately represented as percentages of BW due to variability in lamb size and genetic potential.

Our findings in wethers show that BIA estimates can also detect the impact of heat stress on body composition in rapidly-growing animals. Heat stress reduced average daily gain in wethers, as expected (Morrision et al., 1983), and our BIA-estimated lean mass values would indicate that this is due to a reduction in muscle growth, although equations estimating the collective mass of specific muscle groups were not able to detect heat stress-induced differences. It is worth noting that the moderate nature of heat stress-induced effects in the present study was likely due to pair feeding of controls and thus differences represent direct effects of the heat stress itself. From these findings, we conclude that BIA estimates for FFM and FFST reasonably reflect stress-induced changes in body composition.

## IMPLICATIONS

Accurate live-animal body composition estimates will increase product uniformity and potentially reduce the risk of costly discounts that producers take at harvest for carcasses with low quality and low yield. BIA appears to be a potential tool for estimating carcass characteristics in live animals. Its relative simplicity and consistency mean that it could be adapted for use in livestock to improve efficiency and increase profits. Further studies will better optimize estimation equations for nutrient and body composition to increase precision and accuracy.

**Table 4-1.** Equations for carcass traits estimated from bioelectrical impedance analyses (BIA) in heat-stressed wethers and intrauterine growth-restricted (IUGR) neonatal lambs.

| Estimate | Equation | Citation |
|---|---|---|
| | Live Animal BIA | |
| FFM1 | = (0.585*BW) - (0.28*Rs) + (0.578*Xc) + 16.35 | Berg & Marchello, '94 |
| FFM2 | = (0.578*BW) - (0.293*Rs) + (0.039*L) +18.771 | Berg & Marchello, '94 |
| FFM3 | = (0.596*BW) - (0.286*Rs) + 19.711 | Berg & Marchello, '94 |
| FFM4 | = (0.643*BW) + (0.624*Xc) - 2.701 | Berg & Marchello, '94 |
| | | Berg & Marchello, '94 |
| FFST1 | = (0.555*BW) - (0.247*Rs) + (0.390*Xc) + 16.260 | Berg & Marchello, '94 |
| FFST2 | = (0.542*BW) - (0.259*Rs) + (0.044*L) + 17.470 | Berg & Marchello, '94 |
| FFST3 | = (0.562*BW) - (0.251*Rs) + 18.529 | Berg & Marchello, '94 |
| SUM | = 1.7 + 0.338*BW - 0.0531*Rs + 0.0494*L | Slanger et al. '94 |
| LSLRS | = 1.7 + 0.237*BW - 0.0396*Rs + 0.0308*L | Slanger et al. '94 |
| LSL | = 0.95 + 0.147*BW - 0.0329*Rs + 0.0222*L | Slanger et al. '94 |
| Moisture | = 0.66 + 0.94*XcD + 0.09*V | Moro et al. '19 |
| Protein | = -0.70 + 0.05*RsD + 0.03*V + 0.07*PA | Moro et al. '19 |
| Fat | = -2.11 + 0.10*RsD + 0.04*V | Moro et al. '19 |
| Lean | = -1.90 + 0.11*V + 0.18*RsD + 0.31*PA | Moro et al. '19 |
| | Hot Carcass | |
| FFM1 | = (0.454*BW) - (0.134*Rs) + (0.217*Xc) - (0.244*T) + 26.609 | Berg & Marchello, '94 |
| FFM2 | = (0.396*BW) - (0.106*Rs) + 20.216 | Berg & Marchello, '94 |
| FFM3 | = (0.437*BW) - (0.130*Rs) + (0.229*Xc) + 16.950 | Berg & Marchello, '94 |
| | | Berg & Marchello, '94 |
| FFST1 | = (0.433*BW) + (0.124*L) - (0.114*Rs) + (0.175*Xc) - (0.211*T)+17.811 | Berg & Marchello, '94 |
| FFST2 | = (0.393*BW) - (0.089*Rs) + 17.773 | Berg & Marchello, '94 |
| FFST3 | = (0.419*BW) - (0.111*Rs) + (0.188*Xc) + (0.111*L) + 10.051 | Berg & Marchello, '94 |
| SUM | = -4.5 + 0.598*BW - 0.0297*Rs + 0.096*Xc + 0.114*L + 0.103*T | Slanger et al. '94 |
| LSLRS | = -3.6 + 0.440*BW - 0.0214*Rs + 0.0880*Xc + 0.0527*L + 0.0939*T | Slanger et al. '94 |
| LSL | = -2.4 + 0.256*BW - 0.0142*Rs + 0.0521*Xc + 0.0327*L + 0.0748*T | Slanger et al. '94 |

FFM, fat-free mass (kg); FFST, fat-free soft tissue (kg); SUM, sum of leg, sirloin, rack, shoulder, neck, riblets, shank, and lean trim (kg); LSLRS, sun of leg, sirloin, loin, rack, and shoulder; LSL, sum of leg, sirloin, and loin (kg); BW, bodyweight (kg); Rs, resistance (Ω); Xc, reactance (Ω); L, length between electrodes (cm); XcD, resistive density ($kg^2$/ ($cm^2$* Ω)); V, biometrical volume ($cm^2$/ Ω); RsD, reactive density ($kg^2$/ ($cm^2$* Ω)); PA, phase angle (°); T, temperature (°C).

**Table 4-2.** Live animal composition estimated from bioelectrical impedance analysis (BIA) in intrauterine growth restricted lambs (IUGR) at 3 d and 25 d of age.

| Variables | Control | PI-IUGR | PI-IUGR+$O_2$ | MI-IUGR | *P*-value |
|---|---|---|---|---|---|
| **3 d of age** | | | | | |
| BW, kg | 5.0 ± 0.2[a] | 2.6 ± 0.2[b] | 4.6 ± 0.1[a] | 3.9 ± 0.4[c] | 0.02 |
| BW/BL, kg/cm | 0.018 ± 0.001[a] | 0.011 ± 0.001[b] | 0.017 ± 0.001[a] | 0.017 ± 0.002[a] | 0.009 |
| FFM, kg | 6.7 ± 0.3 | 7.1 ± 3.2 | 8.0 ± 1.7 | 6.9 ± 2.1 | NS |
| FFM/BW, kg/kg | 1.4 ± 0.3 | 1.8 ± 0.3 | 1.7 ± 0.3 | 1.2 ± 0.3 | NS |
| Moisture, kg | 6.1 ± 0.3[a] | 3.2 ± 0.9[b] | 6.3 ± 0.5[a] | 4.7 ± 0.5[c] | 0.008 |
| Protein, kg | 1.52 ± 0.09 | 1.48 ± 0.65 | 1.87 ± 0.41 | 1.53 ± 0.45 | NS |
| Fat, kg | - | - | - | - | - |
| Moisture/BW, kg/kg | 1.301 ± 0.091 | 1.362 ± 0.503 | 1.343 ± 0.105 | 1.226 ± 0.068 | NS |
| Protein/BW, kg/kg | 0.321 ± 0.021 | 0.583 ± 0.206 | 0.398 ± 0.083 | 0.491 ± 0.238 | NS |
| Fat/BW, kg/kg | - | - | - | - | - |
| **25 d of age** | | | | | |
| BW, kg | 11.8 ± 0.5[a] | 9.1 ± 0.8[b] | 11.4 ± 0.4[a] | 9.2 ± 0.6[b] | 0.002 |
| BW/BL, kg/cm | 0.024 ± 0.001[a] | 0.024 ± 0.002[a] | 0.023 ± 0.002[b] | 0.021 ± 0.001[b] | 0.02 |
| FFM, kg | 8.7 ± 0.6[a] | 6.4 ± 0.7[b] | 8.6 ± 0.8[ac] | 7.4 ± 0.4[bc] | 0.1 |
| FFM/BW, kg/kg | 0.82 ± 0.04[a] | 0.7 ± 0.04[b] | 0.82 ± 0.04[a] | 0.81 ± 0.04[a] | 0.03 |
| Moisture, kg | 7.4 ± 0.3[a] | 5.9 ± 0.5[b] | 7.9 ± 0.7[a] | 6.7 ± 0.3[b] | 0.04 |
| Protein, kg | 2.04 ± 0.16[a] | 1.48 ± 0.19[b] | 2.09 ± 0.23[a] | 1.76 ± 0.13[b] | 0.1 |
| Fat, kg | 0.97 ± 0.1[a] | 0.31 ± 0.2[b] | 1.23 ± 0.3[a] | 0.65 ± 0.2[b] | 0.03 |
| Moisture/BW, kg/kg | 0.653 ± 0.042 | 0.662 ± 0.045 | 0.702 ± 0.059 | 0.739 ± 0.038 | NS |
| Protein/BW, kg/kg | 0.187 ± 0.026 | 0.164 ± 0.013 | 0.185 ± 0.019 | 0.193 ± 0.011 | NS |
| Fat/BW, kg/kg | 0.086 ± 0.012[a] | 0.031 ± 0.021[b] | 0.108 ± 0.022[a] | 0.069 ± 0.016[a] | 0.08 |

Values are expressed as means ± SE; BW, bodyweight (kg); BL, body length (cm); FFM, fat-free mass (kg); PI-IUGR, placental insufficiency intrauterine growth restriction; MI-IUGR, maternal inflammation intrauterine growth restriction; NS, not significant;

**Table 4-3.** Live animal composition estimated from bioelectrical impedance analysis (BIA) in heat-stressed wethers on d14.

| Variables | Control | Heat Stress | *P*-value |
|---|---|---|---|
| **d 14** | | | |
| BW, kg | 47.4 ± 0.9 | 47.7 ± 0.9 | NS |
| ADG, kg | 0.18 ± 0.02 | 0.13 ± 0.02 | 0.07 |
| | | | |
| FFM1, kg | 36.6 ± 0.5 | 36.2 ± 0.8 | NS |
| FFM2, kg | 39.2 ± 0.5 | 38.8 ± 0.7 | NS |
| FFM3, kg | 39.6 ± 0.5 | 39.2 ± 0.7 | NS |
| FFM4, kg | 28.7 ± 0.5 | 28.4 ± 0.9 | NS |
| **FFM, kg** | 36.0 ± 0.5 | 35.7 ± 0.7 | NS |
| FFM1/BW | 0.767 ± 0.009 | 0.770 ± 0.016 | NS |
| FFM2/BW | 0.822 ± 0.009 | 0.823 ± 0.014 | NS |
| FFM3/BW | 0.831 ± 0.008 | 0.832 ± 0.012 | NS |
| FFM4/BW | 0.601 ± 0.008 | 0.603 ± 0.028 | NS |
| **FFM/BW** | 0.700 ± 0.008 | 0.757 ± 0.017 | NS |
| | | | |
| FFST1, kg | 35.8 ± 0.4 | 35.0 ± 0.7 | NS |
| FFST2, kg | 37.4 ± 0.4 | 36.9 ± 0.7 | NS |
| FFST3, kg | 37.9 ± 0.4 | 37.4 ± 0.7 | NS |
| **FFST, kg** | 37.0 ± 0.4 | 36.6 ± 0.7 | NS |
| FFST1/BW | 0.751 ± 0.008 | 0.754 ± 0.014 | NS |
| FFST2/BW | 0.783 ± 0.008 | 0.786 ± 0.013 | NS |
| FFST3/BW | 0.794 ± 0.008 | 0.796 ± 0.011 | NS |
| **FFST/BW** | 0.776 ± 0.008 | 0.778 ± 0.016 | NS |
| | | | |
| SUM | 18.2 ± 0.2 | 17.9 ± 0.4 | NS |
| LSLRS | 13.1 ± 0.2 | 12.9 ± 0.3 | NS |
| LSL | 7.8 ± 0.1 | 7.7 ± 0.2 | NS |
| SUM/BW | 0.382 ± 0.002 | 0.382 ± 0.002 | NS |
| LSLRS/BW | 0.274 ± 0.001 | 0.274 ± 0.003 | NS |
| LSL/BW | 0.165 ± 0.001 | 0.165 ± 0.001 | NS |

Values are expressed as means ± SE; FFM, fat-free mass (kg); FFST, fat-free soft tissue (kg); SUM, sum of leg, sirloin, rack, shoulder, neck, riblets, shank, and lean trim (kg); LSLRS, sum of leg, sirloin, loin, rack, and shoulder; LSL, sum of leg, sirloin, and loin (kg); BW, bodyweight (kg); NS, not significant;

**Table 4-4.** Carcass characteristics estimated from bioelectrical impedance analysis (BIA) in heat-stressed wethers at necropsy.

| Variables | Control | Heat Stress | *P*-value |
|---|---|---|---|
| **Necropsy** | | | |
| BW, kg | 48.1 ± 0.8 | 48.3 ± 1.1 | NS |
| ADG, kg | 0.11 ± 0.01 | 0.08 ± 0.01 | 0.08 |
| | | | |
| FFM1, kg | 25.9 ± 0.5 | 24.9 ± 0.8 | NS |
| FFM2, kg | 20.7 ± 0.5 | 19.4 ± 0.8 | NS |
| FFM3, kg | 21.9 ± 0.5 | 20.9 ± 0.7 | NS |
| FFM4, kg | 23.1 ± 0.5 | 20.1 ± 0.9 | 0.01 |
| **FFM, kg** | 22.9 ± 0.4 | 21.4 ± 0.8 | 0.1 |
| FFM1/BW | 1.063 ± 0.009 | 1.026 ± 0.017 | 0.03 |
| FFM2/BW | 0.850 ± 0.010 | 0.798 ± 0.015 | 0.004 |
| FFM3/BW | 0.900 ± 0.009 | 0.861 ± 0.013 | 0.02 |
| FFM4/BW | 0.948 ± 0.009 | 0.829 ± 0.030 | <0.001 |
| **FFM/BW** | 0.940 ± 0.008 | 0.878 ± 0.018 | 0.003 |
| | | | |
| FFST1, kg | 23.1 ± 0.4 | 22.1 ± 0.7 | NS |
| FFST2, kg | 21.7 ± 0.3 | 19.2 ± 1.1 | 0.05 |
| FFST3, kg | 19.8 ± 0.4 | 18.7 ± 0.7 | NS |
| **FFST, kg** | 21.5 ± 0.4 | 20.1 ± 0.7 | 0.08 |
| FFST1/BW | 0.949 ± 0.008 | 0.912 ± 0.015 | 0.04 |
| FFST2/BW | 0.900 ± 0.012 | 0.789 ± 0.045 | 0.04 |
| FFST3/BW | 0.811 ± 0.008 | 0.774 ± 0.012 | 0.01 |
| **FFST/BW** | 0.883 ± 0.008 | 0.825 ± 0.017 | 0.004 |
| | | | |
| SUM | 16.3 ± 0.2 | 16.2 ± 0.4 | NS |
| LSLRS | 11.2 ± 0.1 | 11.2 ± 0.3 | NS |
| LSL | 6.6 ± 0.1 | 6.6 ± 0.2 | NS |
| SUM/BW | 0.667 ± 0.002 | 0.668 ± 0.002 | NS |
| LSLRS/BW | 0.454 ± 0.001 | 0.460 ± 0.003 | NS |
| LSL/BW | 0.270 ± 0.001 | 0.272 ± 0.001 | NS |

Values are expressed as means ± SE; FFM, fat-free mass (kg); FFST, fat-free soft tissue (kg); SUM, sum of leg, sirloin, rack, shoulder, neck, riblets, shank, and lean trim (kg); LSLRS, sun of leg, sirloin, loin, rack, and shoulder; LSL, sum of leg, sirloin, and loin (kg); BW, bodyweight (kg); NS, not significant;

**Table 4-5**. Nutrient composition estimated from bioelectrical impedance analysis (BIA) in heat-stressed wethers at trial day 0 and 14.

| Variables | Control | Heat Stress | *P*-value |
|---|---|---|---|
| **d 0** | | | |
| Moisture, kg | 7.4 ± 0.3 | 7.9 ± 0.5 | NS |
| Protein, kg | 3.1 ± 0.1 | 3.0 ± 0.1 | NS |
| Fat, kg | 3.9 ± 0.2 | 3.7 ± 0.2 | NS |
| Lean, kg | 12.0 ± 0.4 | 11.9 ± 0.4 | NS |
| Moisture/BW | 0.159 ± 0.005 | 0.177 ± 0.1 | NS |
| Protein/BW | 0.067 ± 0.001 | 0.068 ± 0.001 | NS |
| Fat/BW | 0.086 ± 0.002 | 0.083 ± 0.001 | NS |
| Lean/BW | 0.260 ± 0.004 | 0.267 ± 0.005 | NS |
| **d 14** | | | |
| Moisture, kg | 7.2 ± 0.5 | 7.4 ± 0.7 | NS |
| Protein, kg | 3.3 ± 0.1 | 3.3 ± 0.1 | NS |
| Fat, kg | 4.4 ± 0.2 | 4.1 ± 0.2 | NS |
| Lean, kg | 12.8 ± 0.4 | 12.8 ± 0.4 | NS |
| Moisture/BW | 0.151 ± 0.009 | 0.157 ± 0.014 | NS |
| Protein/BW | 0.069 ± 0.001 | 0.069 ± 0.001 | NS |
| Fat/BW | 0.091 ± 0.002 | 0.088 ± 0.001 | NS |
| Lean/BW | 0.267 ± 0.005 | 0.272 ± 0.006 | NS |

Values are expressed as means ± SE; BW, bodyweight; NS, not significant;

**References**

Adams, G., and F. Haddad. 1996. The relationships among IGF-1, DNA content, and protein accumulation during skeletal muscle hypertrophy. Journal of Applied Physiology 81(6):2509-2516.

Ahlquist, R. P. 1948. A study of the adrenotropic receptors. American Journal of Physiology-Legacy Content 153(3):586-600.

Alexander, G., J. Hales, D. Stevens, and J. Donnelly. 1987. Effects of acute and prolonged exposure to heat on regional blood flows in pregnant sheep. Journal of developmental physiology 9(1):1-15.

Anthony, W. N., and H. L. Henry. 2015. Hormones 3ed. Academic Press, Elsvier.

Avril, D. H., C. Lallo, V. Mlambo, and G. Bourne. 2013. The application of bioelectrical impedance analysis in live tropical hair sheep as a predictor of body composition upon slaughter. Tropical animal health and production 45(8):1803-1808.

Barker, D. J., K. M. Godfrey, P. D. Gluckman, J. E. Harding, J. A. Owens, and J. S. Robinson. 1993. Fetal nutrition and cardiovascular disease in adult life. The Lancet 341(8850):938-941.

Baschat, A., U. Gembruch, and C. Harman. 2001. The sequence of changes in Doppler and biophysical parameters as severe fetal growth restriction worsens. Ultrasound in Obstetrics and Gynecology 18(6):571-577.

Bauer, D. C., E. S. Orwoll, K. M. Fox, T. M. Vogt, N. E. Lane, M. C. Hochberg, K. Stone, and M. C. Nevitt. 1996. Aspirin and NSAID use in older women: effect on bone mineral density and fracture risk. Journal of bone and mineral research 11(1):29-35.

Beard, J. K., J. T. Mulliniks, and D. T. Yates. 2018. Function and dysfunction of fatty acid mobilization: a review Diabesity 5

Beede, K. A., S. W. Limesand, J. L. Petersen, and D. T. Yates. 2019. Real supermodels wear wool: summarizing the impact of the pregnant sheep as an animal model for adaptive fetal programming. Animal Frontiers 9(3):34-43. doi: 10.1093/af/vfz018

Beermann, D. 2002. Beta-adrenergic receptor agonist modulation of skeletal muscle growth. Journal of Animal Science 80(E-suppl_1):E18-E23.

Bentzinger, C. F., Y. X. Wang, and M. A. Rudnicki. 2012. Building muscle: molecular regulation of myogenesis. Cold Spring Harbor perspectives in biology 4(2):a008342.

Berg, E., M. Neary, J. Forrest, D. Thomas, and R. Kauffman. 1996. Assessment of lamb carcass composition from live animal measurement of bioelectrical impedance or ultrasonic tissue depths. Journal of Animal Science 74(11):2672-2678.

Bertacca, A., A. Ciccarone, P. Cecchetti, B. Vianello, I. Laurenza, M. Maffei, C. Chiellini, S. Del Prato, and L. Benzi. 2005. Continually high insulin levels impair Akt phosphorylation and glucose transport in human myoblasts. Metabolism 54(12):1687-1693.

Bhide, A., O. Vuolteenaho, M. Haapsamo, T. Erkinaro, J. Rasanen, and G. Acharya. 2016. Effect of hypoxemia with or without increased placental vascular resistance on fetal left and right ventricular myocardial performance index in chronically instrumented sheep. Ultrasound in medicine & biology 42(11):2589-2598.

Bodine, S. C., T. N. Stitt, M. Gonzalez, W. O. Kline, G. L. Stover, R. Bauerlein, E. Zlotchenko, A. Scrimgeour, J. C. Lawrence, and D. J. Glass. 2001. Akt/mTOR pathway is a crucial regulator of skeletal muscle hypertrophy and can prevent muscle atrophy in vivo. Nature cell biology 3(11):1014-1019.

Bohuslavek, Z., P. Pipek, and J. Maly. 2002. Use of BIA method for the estimation of beef carcass composition-weight of Iongissimus lumborum muscle, ratio of muscle tissue and fat in loin cross-section. CZECH JOURNAL OF ANIMAL SCIENCE 47(9):387-394.

Boleman, S. L., S. J. Boleman, W. W. Morgan, D. S. Hale, D. B. Griffin, J. W. Savell, R. P. Ames, M. T. Smith, J. D. Tatum, T. G. Field, G. C. Smith, B. A. Gardner, J. B. Morgan, S. L. Northcutt, H. G. Dolezal, D. R. Gill, and F. K. Ray. 1998. National Beef Quality Audit-1995: survey of producer-related defects and carcass quality and quantity attributes. J. Anim. Sci. 76(1):96-103. doi: 10.2527/1998.76196x

Bollrath, J., and F. R. Greten. 2009. IKK/NF-κB and STAT3 pathways: central signalling hubs in inflammation-mediated tumour promotion and metastasis. EMBO reports 10(12):1314-1319.

Bradford, P. G. 2013. Curcumin and obesity. Biofactors 39(1):78-87.

Brown, L. D. 2014. Endocrine regulation of fetal skeletal muscle growth: impact on future metabolic health. J Endocrinol 221(2):R13-29.

Brown, L. D., A. S. Green, S. W. Limesand, and P. J. Rozance. 2011. Maternal amino acid supplementation for intrauterine growth restriction. Frontiers in bioscience (Scholar edition) 3:428.

Brown, L. D., and W. W. Hay Jr. 2016. Impact of placental insufficiency on fetal skeletal muscle growth. Molecular and cellular endocrinology 435:69-77.

Brown, L. D., P. J. Rozance, J. L. Bruce, J. E. Friedman, W. W. Hay Jr, and S. R. Wesolowski. 2015. Limited capacity for glucose oxidation in fetal sheep with intrauterine growth restriction. American Journal of Physiology-Regulatory, Integrative and Comparative Physiology 309(8):R920-R928.

Buckingham, M., and F. Relaix. 2015. PAX3 and PAX7 as upstream regulators of myogenesis. In: Seminars in cell & developmental biology. p 115-125.

Cadaret, C. N., K. A. Beede, H. E. Riley, and D. T. Yates. 2017. Acute exposure of primary rat soleus muscle to zilpaterol HCl (β2 adrenergic agonist), TNFα, or IL-6 in culture increases glucose oxidation rates independent of the impact on insulin signaling or glucose uptake. Cytokine 96:107-113. doi: 10.1016/j.cyto.2017.03.014

Cadaret, C. N., E. M. Merrick, T. L. Barnes, K. A. Beede, R. J. Posont, J. L. Petersen, and D. T. Yates. 2018. Sustained maternal inflammation during the early third trimester yields fetal adaptations that impair subsequent skeletal muscle growth and glucose metabolism in sheep. Translational animal science 2(suppl_1):S14-S18.

Cadaret, C. N., E. M. Merrick, T. L. Barnes, K. A. Beede, R. J. Posont, J. L. Petersen, and D. T. Yates. 2019a. Sustained maternal inflammation during the early third-trimester yields intrauterine growth restriction, impaired skeletal muscle glucose metabolism, and diminished beta-cell function in fetal sheep1,2. J Anim Sci 97(12):4822-4833. doi: 10.1093/jas/skz321

Cadaret, C. N., R. J. Posont, K. A. Beede, H. E. Riley, J. D. Loy, and D. T. Yates. 2019b. Maternal inflammation at midgestation impairs subsequent fetal myoblast function

and skeletal muscle growth in rats, resulting in intrauterine growth restriction at term. Translational animal science 3(2):867-876.

Cadaret, C. N., R. J. Posont, R. M. Swanson, J. K. Beard, T. L. Barnes, K. A. Beede, J. L. Petersen, and D. T. Yates. 2019c. Intermittent maternofetal O2 supplementation during late gestation rescues placental insufficiency-induced intrauterine growth restriction and metabolic pathologies in the neonatal lamb. Translational Animal Science 3(Supplement_1):1696-1700.

Camacho, L. E., X. Chen, W. W. Hay Jr, and S. W. Limesand. 2017. Enhanced insulin secretion and insulin sensitivity in young lambs with placental insufficiency-induced intrauterine growth restriction. American Journal of Physiology-Regulatory, Integrative and Comparative Physiology 313(2):R101-R109.

Carey, A. L., G. R. Steinberg, S. L. Macaulay, W. G. Thomas, A. G. Holmes, G. Ramm, O. Prelovsek, C. Hohnen-Behrens, M. J. Watt, and D. E. James. 2006. Interleukin-6 increases insulin-stimulated glucose disposal in humans and glucose uptake and fatty acid oxidation in vitro via AMP-activated protein kinase. Diabetes 55(10):2688-2697.

Carr, D. J., R. P. Aitken, J. S. Milne, A. L. David, and J. M. Wallace. 2012. Fetoplacental biometry and umbilical artery Doppler velocimetry in the overnourished adolescent model of fetal growth restriction. American journal of obstetrics and gynecology 207(2):141. e146-141. e115.

Caton, J., and B. Hess. 2010. Maternal plane of nutrition: Impacts on fetal outcomes and postnatal offspring responses. In: Proc. 4th Grazing Livestock Nutrition Conference. BW Hess, T. DelCurto, JGP Bowman and RC Waterman (eds.) West. Sect. Am. Soc. Anim. Sci., Champaign, Ill. p 104-122.

Cettour-Rose, P., S. Samec, A. P. Russell, S. Summermatter, D. Mainieri, C. Carrillo-Theander, J.-P. Montani, J. Seydoux, F. Rohner-Jeanrenaud, and A. G. Dulloo. 2005. Redistribution of glucose from skeletal muscle to adipose tissue during catch-up fat: a link between catch-up growth and later metabolic syndrome. Diabetes 54(3):751-756.

Cheema, R., M. Dubiel, and S. Gudmundsson. 2006. Fetal brain sparing is strongly related to the degree of increased placental vascular impedance. Journal of perinatal medicine 34(4):318-322.

Chen, L., H. Deng, H. Cui, J. Fang, Z. Zuo, J. Deng, Y. Li, X. Wang, and L. Zhao. 2018. Inflammatory responses and inflammation-associated diseases in organs. Oncotarget 9(6):7204.

Chen, X., A. C. Kelly, D. T. Yates, A. R. Macko, R. M. Lynch, and S. W. Limesand. 2017. Islet adaptations in fetal sheep persist following chronic exposure to high norepinephrine. The Journal of endocrinology 232(2):285.

Cho, J.-W., K.-S. Lee, and C.-W. Kim. 2007. Curcumin attenuates the expression of IL-1β, IL-6, and TNF-α as well as cyclin E in TNF-α-treated HaCaT cells; NF-κB and MAPKs as potential upstream targets. International journal of molecular medicine 19(3):469-474.

Chow, J. C., D. W. Young, D. T. Golenbock, W. J. Christ, and F. Gusovsky. 1999. Toll-like receptor-4 mediates lipopolysaccharide-induced signal transduction. Journal of Biological Chemistry 274(16):10689-10692.

Cianfarani, S., D. Germani, and F. Branca. 1999. Low birthweight and adult insulin resistance: the “catch-up growth” hypothesis. Archives of Disease in Childhood-Fetal and Neonatal Edition 81(1):F71-F73.

Ciccarelli, M., D. Sorriento, E. Coscioni, G. Iaccarino, and G. Santulli. 2017. Adrenergic receptors, Endocrinology of the Heart in Health and Disease. Elsevier. p. 285-315.

Clarke, L., M. J. Bryant, M. A. Lomax, and M. E. Symonds. 1997. Maternal manipulation of brown adipose tissue and liver development in the ovine fetus during late gestation. British Journal of Nutrition 77(6):871-883.

Collins, C. A., I. Olsen, P. S. Zammit, L. Heslop, A. Petrie, T. A. Partridge, and J. E. Morgan. 2005. Stem cell function, self-renewal, and behavioral heterogeneity of cells from the adult muscle satellite cell niche. Cell 122(2):289-301.

Cui, Y., L. Huang, F. Elefteriou, G. Yang, J. M. Shelton, J. E. Giles, O. K. Oz, T. Pourbahrami, C. Y. Lu, and J. A. Richardson. 2004. Essential role of STAT3 in body weight and glucose homeostasis. Molecular and cellular biology 24(1):258-269.

da Justa Pinheiro, C. H., L. R. Silveira, R. T. Nachbar, K. F. Vitzel, and R. Curi. 2010. Regulation of glycolysis and expression of glucose metabolism-related genes by reactive oxygen species in contracting skeletal muscle cells. Free Radical Biology and Medicine 48(7):953-960.

De Blasio, M. J., K. L. Gatford, J. S. Robinson, and J. A. Owens. 2007. Placental restriction of fetal growth reduces size at birth and alters postnatal growth, feeding activity, and adiposity in the young lamb. American Journal of Physiology-Regulatory, Integrative and Comparative Physiology 292(2):R875-R886.

De Diego, A., L. Gandia, and A. Garcia. 2008. A physiological view of the central and peripheral mechanisms that regulate the release of catecholamines at the adrenal medulla. Acta physiologica 192(2):287-301.

del Aguila, L. F., K. P. Claffey, and J. P. Kirwan. 1999. TNF-α impairs insulin signaling and insulin stimulation of glucose uptake in C2C12muscle cells. American Journal of Physiology-Endocrinology And Metabolism 276(5):E849-E855.

Desai, M., and M. G. Ross. 2011. Fetal programming of adipose tissue: effects of intrauterine growth restriction and maternal obesity/high-fat diet. In: Seminars in reproductive medicine. p 237-245.

Du, M., J. Tong, J. Zhao, K. Underwood, M. Zhu, S. Ford, and P. Nathanielsz. 2010. Fetal programming of skeletal muscle development in ruminant animals. Journal of animal science 88(suppl_13):E51-E60.

Edmondson, D. G., and E. N. Olson. 1993. Helix-loop-helix proteins as regulators of muscle-specific transcription. Journal of Biological Chemistry 268(2):755-758.

Enthoven, W. T., P. D. Roelofs, R. A. Deyo, M. W. van Tulder, and B. W. Koes. 2016. Non-steroidal anti-inflammatory drugs for chronic low back pain. Cochrane Database of Systematic Reviews (2)

Faure, E., L. Thomas, H. Xu, A. E. Medvedev, O. Equils, and M. Arditi. 2001. Bacterial lipopolysaccharide and IFN-γ induce Toll-like receptor 2 and Toll-like receptor 4 expression in human endothelial cells: role of NF-κB activation. The Journal of Immunology 166(3):2018-2024.

Galan, H. L., R. V. Anthony, S. Rigano, T. A. Parker, B. de Vrijer, E. Ferrazzi, R. B. Wilkening, and T. R. Regnault. 2005. Fetal hypertension and abnormal Doppler velocimetry in an ovine model of intrauterine growth restriction. American journal of obstetrics and gynecology 192(1):272-279.

García, A. G., A. M. García-De-Diego, L. Gandía, R. Borges, and J. García-Sancho. 2006. Calcium signaling and exocytosis in adrenal chromaffin cells. Physiological reviews 86(4):1093-1131.

Gardner, B., H. Dolezal, F. Owens, L. Bryant, J. Nelson, B. Schutte, and R. Smith. 1998. Impact of health on profitability of feedlot steers. Okla. Agr. Exp. Sta. Res. Rep P-965 102

Gatford, K., R. Simmons, M. De Blasio, J. Robinson, and J. Owens. 2010. Placental programming of postnatal diabetes and impaired insulin action after IUGR. Placenta 31:S60-S65.

Gemmell, R., A. Bell, and G. Alexander. 1972. Morphology of adipose cells in lambs at birth and during subsequent transition of brown to white adipose tissue in cold and in warm conditions. American Journal of Anatomy 133(2):143-163.

Ghosh, N., N. Patel, K. Jiang, J. E. Watson, J. Cheng, C. E. Chalfant, and D. R. Cooper. 2007. Ceramide-activated protein phosphatase involvement in insulin resistance via Akt, serine/arginine-rich protein 40, and ribonucleic acid splicing in L6 skeletal muscle cells. Endocrinology 148(3):1359-1366.

Ghosh, S. S., T. W. Gehr, and S. Ghosh. 2014. Curcumin and chronic kidney disease (CKD): major mode of action through stimulating endogenous intestinal alkaline phosphatase. Molecules 19(12):20139-20156.

Gibbs, R. L., C. N. Cadaret, R. M. Swanson, K. A. Beede, R. J. Posont, T. B. Schmidt, J. L. Petersen, and D. T. Yates. 2019. Body composition estimated by bioelectrical impedance analyses is diminished by prenatal stress in neonatal lambs and by heat stress in feedlot wethers. Translational Animal Science 3(Supplement_1):1691-1695.

Gibbs, R. L., R. M. Swanson, J. K. Beard, T. B. Schmidt, J. L. Petersen, and D. Yates. 2020. Deficits in growth, muscle mass, and body composition following placental insufficiency-induced intrauterine growth restriction persisted in lambs at 60 d of age but were improved by daily clenbuterol supplementation. Translational Animal Science doi: txaa097

Gibson, M. C., and E. Schultz. 1983. Age-related differences in absolute numbers of skeletal muscle satellite cells. Muscle & Nerve: Official Journal of the American Association of Electrodiagnostic Medicine 6(8):574-580.

Glund, S., A. Deshmukh, Y. C. Long, T. Moller, H. A. Koistinen, K. Caidahl, J. R. Zierath, and A. Krook. 2007. Interleukin-6 directly increases glucose metabolism in resting human skeletal muscle. Diabetes 56(6):1630-1637.

Gollnick, P., B. Timson, R. Moore, and M. Riedy. 1981. Muscular enlargement and number of fibers in skeletal muscles of rats. Journal of Applied Physiology 50(5):936-943.

Gondret, F., L. Lefaucheur, I. Louveau, B. Lebret, X. Pichodo, and Y. Le Cozler. 2005. Influence of piglet birth weight on postnatal growth performance, tissue lipogenic capacity and muscle histological traits at market weight. Livestock Production Science 93(2):137-146.

Gonzales, A. M., and R. A. Orlando. 2008. Curcumin and resveratrol inhibit nuclear factor-kappaB-mediated cytokine expression in adipocytes. Nutrition & metabolism 5(1):17.

Gooch, K., B. F. Culleton, B. J. Manns, J. Zhang, H. Alfonso, M. Tonelli, C. Frank, S. Klarenbach, and B. R. Hemmelgarn. 2007. NSAID use and progression of chronic kidney disease. The American journal of medicine 120(3):280. e281-280. e287.

Greenwood, P., A. Hunt, J. Hermanson, and A. Bell. 2000. Effects of birth weight and postnatal nutrition on neonatal sheep: II. Skeletal muscle growth and development. J. Anim. Sci. 78(1):50-61.

Greenwood, P. L., A. S. Hunt, J. W. Hermanson, and A. W. Bell. 1998. Effects of birth weight and postnatal nutrition on neonatal sheep: I. Body growth and composition, and some aspects of energetic efficiency. Journal of animal science 76(9):2354-2367.

Grimmer, N. M., R. P. Gimbar, A. Bursua, and M. Patel. 2016. Rhabdomyolysis secondary to clenbuterol use and exercise. The Journal of emergency medicine 50(2):e71-e74.

Gunn, H. 1989. Heart weight and running ability. Journal of anatomy 167:225.

Hadari, T., J. Warms, I. Rose, and A. Hershko. 1992. A ubiquitin C-terminal isopeptidase that acts on polyubiquitin chains. Role in protein degradation. Journal of Biological Chemistry 267(2):719-727.

Haldar, M., G. Karan, P. Tvrdik, and M. R. Capecchi. 2008. Two cell lineages, myf5 and myf5-independent, participate in mouse skeletal myogenesis. Developmental cell 14(3):437-445.

Hales, C. N., and D. J. Barker. 1992. Type 2 (non-insulin-dependent) diabetes mellitus: the thrifty phenotype hypothesis. Diabetologia 35(7):595-601.

Hales, C. N., D. J. Barker, P. M. Clark, L. J. Cox, C. Fall, C. Osmond, and P. Winter. 1991. Fetal and infant growth and impaired glucose tolerance at age 64. Bmj 303(6809):1019-1022.

Han, J. M., S. J. Jeong, M. C. Park, G. Kim, N. H. Kwon, H. K. Kim, S. H. Ha, S. H. Ryu, and S. Kim. 2012. Leucyl-tRNA synthetase is an intracellular leucine sensor for the mTORC1-signaling pathway. Cell 149(2):410-424.

Hegarty, P., and C. Allen. 1978. Effect of pre-natal runting on the post-natal development of skeletal muscles in swine and rats. Journal of Animal Science 46(6):1634-1640.

Hinkle, R. T., K. M. Hodge, D. B. Cody, R. J. Sheldon, B. K. Kobilka, and R. J. Isfort. 2002. Skeletal muscle hypertrophy and anti-atrophy effects of clenbuterol are mediated by the β2-adrenergic receptor. Muscle & Nerve: Official Journal of the American Association of Electrodiagnostic Medicine 25(5):729-734.

Jensen, J., P. I. Rustad, A. J. Kolnes, and Y.-C. Lai. 2011. The role of skeletal muscle glycogen breakdown for regulation of insulin sensitivity by exercise. Frontiers in physiology 2:112.

Johnson, B., F. Ribeiro, and J. Beckett. 2013. Application of growth technologies in enhancing food security and sustainability. Animal frontiers 3(3):8-13.

Johnson, B. J., S. B. Smith, and K. Y. Chung. 2014. Historical overview of the effect of β-adrenergic agonists on beef cattle production. Asian-Australasian journal of animal sciences 27(5):757.

Kaur, J., M. D. Spranger, R. L. Hammond, A. C. Krishnan, A. Alvarez, R. A. Augustyniak, and D. S. O'Leary. 2014. Muscle metaboreflex activation during dynamic exercise evokes epinephrine release resulting in β2-mediated vasodilation. American Journal of Physiology-Heart and Circulatory Physiology 308(5):H524-H529.

Kim, K. M., H. C. Jang, and S. Lim. 2016. Differences among skeletal muscle mass indices derived from height-, weight-, and body mass index-adjusted models in assessing sarcopenia. The Korean journal of internal medicine 31(4):643.

Kostromina, E., N. Gustavsson, X. Wang, C.-Y. Lim, G. K. Radda, C. Li, and W. Han. 2010. Glucose intolerance and impaired insulin secretion in pancreas-specific signal transducer and activator of transcription-3 knockout mice are associated with microvascular alterations in the pancreas. Endocrinology 151(5):2050-2059.

Kostromina, E., X. Wang, and W. Han. 2013. Altered islet morphology but normal islet secretory function in vitro in a mouse model with microvascular alterations in the pancreas. PLoS One 8(7)

Lafontan, M., and D. Langin. 2009. Lipolysis and lipid mobilization in human adipose tissue. Progress in lipid research 48(5):275-297.

Lai, K.-M. V., M. Gonzalez, W. T. Poueymirou, W. O. Kline, E. Na, E. Zlotchenko, T. N. Stitt, A. N. Economides, G. D. Yancopoulos, and D. J. Glass. 2004. Conditional activation of akt in adult skeletal muscle induces rapid hypertrophy. Molecular and cellular biology 24(21):9295-9304.

Lang, U., R. S. Baker, J. Khoury, and K. E. Clark. 2000. Effects of chronic reduction in uterine blood flow on fetal and placental growth in the sheep. American Journal of Physiology-Regulatory, Integrative and Comparative Physiology 279(1):R53-R59.

Langen, R. C., A. M. Schols, M. C. Kelders, E. F. Wouters, and Y. M. Janssen-Heininger. 2001. Inflammatory cytokines inhibit myogenic differentiation through activation of nuclear factor-κB. The FASEB Journal 15(7):1169-1180.

Lawrence, T. 2009. The nuclear factor NF-κB pathway in inflammation. Cold Spring Harbor perspectives in biology 1(6):a001651.

Leclercq, I. A., G. C. Farrell, C. Sempoux, A. dela Peña, and Y. Horsmans. 2004. Curcumin inhibits NF-κB activation and reduces the severity of experimental steatohepatitis in mice. Journal of hepatology 41(6):926-934.

Lee, J.-Y., and L. Hennighausen. 2005. The transcription factor Stat3 is dispensable for pancreatic β-cell development and function. Biochemical and biophysical research communications 334(3):764-768.

Lelliott, C., and A. Vidal-Puig. 2004. Lipotoxicity, an imbalance between lipogenesis de novo and fatty acid oxidation. International journal of obesity 28(4):S22-S28.

Lemley, C. O., A. M. Meyer, L. E. Camacho, T. L. Neville, D. J. Newman, J. S. Caton, and K. A. Vonnahme. 2011. Melatonin supplementation alters uteroplacental hemodynamics and fetal development in an ovine model of intrauterine growth restriction. American Journal of Physiology-Regulatory, Integrative and Comparative Physiology 302(4):R454-R467.

Leos, R. A., M. J. Anderson, X. Chen, J. Pugmire, K. A. Anderson, and S. W. Limesand. 2010. Chronic exposure to elevated norepinephrine suppresses insulin secretion in fetal sheep with placental insufficiency and intrauterine growth restriction.

American Journal of Physiology-Endocrinology and Metabolism 298(4):E770-E778.

Li, Z., M. Mericskay, O. Agbulut, G. Butler-Browne, L. Carlsson, L.-E. Thornell, C. Babinet, and D. Paulin. 1997. Desmin is essential for the tensile strength and integrity of myofibrils but not for myogenic commitment, differentiation, and fusion of skeletal muscle. The Journal of cell biology 139(1):129-144.

Limesand, S. W., L. E. Camacho, A. C. Kelly, and A. T. Antolic. 2018. Impact of thermal stress on placental function and fetal physiology.

Limesand, S. W., J. Jensen, J. C. Hutton, and W. W. Hay Jr. 2005. Diminished β-cell replication contributes to reduced β-cell mass in fetal sheep with intrauterine growth restriction. American Journal of Physiology-Regulatory, Integrative and Comparative Physiology 288(5):R1297-R1305.

Limesand, S. W., and P. J. Rozance. 2017a. Fetal adaptations in insulin secretion result from high catecholamines during placental insufficiency. J Physiol 595(15):5103-5113. doi: 10.1113/JP273324

Limesand, S. W., and P. J. Rozance. 2017b. Fetal adaptations in insulin secretion result from high catecholamines during placental insufficiency. The Journal of physiology 595(15):5103-5113.

Limesand, S. W., P. J. Rozance, D. Smith, and W. W. Hay Jr. 2007a. Increased insulin sensitivity and maintenance of glucose utilization rates in fetal sheep with placental insufficiency and intrauterine growth restriction. American Journal of Physiology-Endocrinology and Metabolism 293(6):E1716-E1725.

Limesand, S. W., P. J. Rozance, D. Smith, and W. W. Hay, Jr. 2007b. Increased insulin sensitivity and maintenance of glucose utilization rates in fetal sheep with placental insufficiency and intrauterine growth restriction. Am J Physiol Endocrinol Metab 293(6):E1716-1725. doi: 10.1152/ajpendo.00459.2007

Limesand, S. W., P. J. Rozance, G. O. Zerbe, J. C. Hutton, and W. W. Hay. 2006. Attenuated insulin release and storage in fetal sheep pancreatic islets with intrauterine growth restriction. Endocrinology 147(3):1488-1497.

Lin, G., X. Wang, G. Wu, C. Feng, H. Zhou, D. Li, and J. Wang. 2014. Improving amino acid nutrition to prevent intrauterine growth restriction in mammals. Amino Acids 46(7):1605-1623.

Lorenzo, M., S. Fernández-Veledo, R. Vila-Bedmar, L. Garcia-Guerra, C. De Alvaro, and I. Nieto-Vazquez. 2008. Insulin resistance induced by tumor necrosis factor-α in myocytes and brown adipocytes. Journal of animal Science 86(suppl_14):E94-E104.

Macko, A. R., D. T. Yates, X. Chen, L. A. Shelton, A. C. Kelly, M. A. Davis, L. E. Camacho, M. J. Anderson, and S. W. Limesand. 2016a. Adrenal demedullation and oxygen supplementation independently increase glucose-stimulated insulin concentrations in fetal sheep with intrauterine growth restriction. Endocrinology 157(5):2104-2115.

Macko, A. R., D. T. Yates, X. Chen, L. A. Shelton, A. C. Kelly, M. A. Davis, L. E. Camacho, M. J. Anderson, and S. W. Limesand. 2016b. Adrenal Demedullation and Oxygen Supplementation Independently Increase Glucose-Stimulated Insulin

Concentrations in Fetal Sheep With Intrauterine Growth Restriction. Endocrinol. 157(5):2104-2115. doi: 10.1210/en.2015-1850

Maclennan, P. A., and R. Edwards. 1989. Effects of clenbuterol and propranolol on muscle mass. Evidence that clenbuterol stimulates muscle β-adrenoceptors to induce hypertrophy. Biochemical Journal 264(2):573-579.

McLaughlin, T., C. Lamendola, A. Liu, and F. Abbasi. 2011. Preferential fat deposition in subcutaneous versus visceral depots is associated with insulin sensitivity. The Journal of Clinical Endocrinology & Metabolism 96(11):E1756-E1760.

Mellor, D. 1983. Nutritional and placental determinants of foetal growth rate in sheep and consequences for the newborn lamb. British Veterinary Journal 139(4):307-324.

Mellor, D., and L. Murray. 1982. Effects of long term undernutrition of the ewe on the growth rates of individual fetuses during late pregnancy. Research in veterinary science 32(2):177-180.

Miller, M., D. Garcia, M. Coleman, P. Ekeren, D. Lunt, K. Wagner, M. Procknor, T. Welsh Jr, and S. Smith. 1988. Adipose tissue, longissimus muscle and anterior pituitary growth and function in clenbuterol-fed heifers. J. Anim. Sci. 66(1):12-20.

Miyazaki, Y., and R. A. DeFronzo. 2009. Visceral fat dominant distribution in male type 2 diabetic patients is closely related to hepatic insulin resistance, irrespective of body type. Cardiovascular diabetology 8(1):44.

Morrison, J. L. 2008. Sheep models of intrauterine growth restriction: fetal adaptations and consequences. Clinical and Experimental Pharmacology and Physiology 35(7):730-743.

Mostyn, A., J. Bispham, S. Pearce, Y. Evens, N. Raver, D. H. KEISLER, R. Webb, T. Stephenson, and M. E. Symonds. 2002. Differential effects of leptin on thermoregulation and uncoupling protein abundance in the neonatal lamb. The FASEB Journal 16(11):1438-1440.

Mostyn, A., S. Pearce, H. Budge, M. Elmes, A. Forhead, A. Fowden, T. Stephenson, and M. Symonds. 2003. Influence of cortisol on adipose tissue development in the fetal sheep during late gestation. Journal of Endocrinology 176(1):23-30.

Nelson, D. L., and M. M. Cox. 2008. Glycolysis, gluconeogenesis, and the pentose phosphate pathway. Lehninger principles of biochemistry 4:521-559.

Nonogaki, K. 2000. New insights into sympathetic regulation of glucose and fat metabolism. Diabetologia 43(5):533-549.

Oh, W., K. Omori, C. J. Hobel, A. Erenberg, and G. C. Emmanouilides. 1975. Umbilical blood flow and glucose uptake in lamb fetus following single umbilical artery ligation. Neonatology 26(3-4):291-299.

Pan, D., S. Lillioja, A. Kriketos, M. Milner, L. Baur, C. Bogardus, A. B. Jenkins, and L. Storlien. 1997. Skeletal muscle triglyceride levels are inversely related to insulin action. Diabetes 46(6):983-988.

Paul, A. C., and N. Rosenthal. 2002. Different modes of hypertrophy in skeletal muscle fibers. The Journal of cell biology 156(4):751-760.

Pette, D., and R. S. Staron. 1990. Cellular and molecular diversities of mammalian skeletal muscle fibers, Reviews of Physiology, Biochemistry and Pharmacology, Volume 116. Springer. p. 1-76.

Pette, D., and R. S. Staron. 1997. Mammalian skeletal muscle fiber type transitions, International review of cytology No. 170. Elsevier. p. 143-223.

Pirola, L., A. Johnston, and E. Van Obberghen. 2004. Modulation of insulin action. Diabetologia 47(2):170-184.

Pope, M., H. Budge, and M. Symonds. 2014. The developmental transition of ovine adipose tissue through early life. Acta Physiologica 210(1):20-30.

Posont, R. J. 2019. The Role of Inflammatory Pathways in Development, Growth, and Metabolism of Skeletal Muscle in IUGR Offspring; Blood Gene Expression of Inflammatory Factors as Novel Biomarkers for Assessing Stress and Wellbeing in Exotic Species.

Posont, R. J., K. A. Beede, S. W. Limesand, and D. T. Yates. 2018. Changes in myoblast responsiveness to TNFα and IL-6 contribute to decreased skeletal muscle mass in intrauterine growth restricted fetal sheep. Translational animal science 2(suppl_1):S44-S47.

Posont, R. J., C. N. Cadaret, K. A. Beede, J. K. Beard, R. M. Swanson, R. L. Gibbs, J. L. Petersen, and D. T. Yates. 2019. Maternal inflammation at 0.7 gestation in ewes leads to intrauterine growth restriction and impaired glucose metabolism in offspring at 30 d of age. Transl Anim Sci 3(Suppl 1):1673-1677. doi: 10.1093/tas/txz055

Posont, R. J., and D. T. Yates. 2019. Postnatal Nutrient Repartitioning due to Adaptive Developmental Programming. Vet Clin North Am Food Anim Pract 35(2):277-288. doi: 10.1016/j.cvfa.2019.02.001

Raghupathy, R., M. Al-Azemi, and F. Azizieh. 2011. Intrauterine growth restriction: cytokine profiles of trophoblast antigen-stimulated maternal lymphocytes. Clinical and Developmental Immunology 2012

Rawlings, J. S., K. M. Rosler, and D. A. Harrison. 2004. The JAK/STAT signaling pathway. Journal of cell science 117(8):1281-1283.

Ricks, C. A., R. Dalrymple, P. K. Baker, and D. Ingle. 1984. Use of a β-agonist to alter fat and muscle deposition in steers. Journal of Animal Science 59(5):1247-1255.

Rock, K. L., C. Gramm, L. Rothstein, K. Clark, R. Stein, L. Dick, D. Hwang, and A. L. Goldberg. 1994. Inhibitors of the proteasome block the degradation of most cell proteins and the generation of peptides presented on MHC class I molecules. Cell 78(5):761-771.

Rommel, C., S. C. Bodine, B. A. Clarke, R. Rossman, L. Nunez, T. N. Stitt, G. D. Yancopoulos, and D. J. Glass. 2001. Mediation of IGF-1-induced skeletal myotube hypertrophy by PI (3) K/Akt/mTOR and PI (3) K/Akt/GSK3 pathways. Nature cell biology 3(11):1009-1013.

Rozance, P. J., S. W. Limesand, J. S. Barry, L. D. Brown, and W. W. Hay. 2009. Glucose replacement to euglycemia causes hypoxia, acidosis, and decreased insulin secretion in fetal sheep with intrauterine growth restriction. Pediatric research 65(1):72.

Rozance, P. J., S. W. Limesand, J. S. Barry, L. D. Brown, S. R. Thorn, D. LoTurco, T. R. Regnault, J. E. Friedman, and W. W. Hay Jr. 2008. Chronic late-gestation hypoglycemia upregulates hepatic PEPCK associated with increased PGC1α

mRNA and phosphorylated CREB in fetal sheep. American Journal of Physiology-Endocrinology and Metabolism 294(2):E365-E370.

Rozance, P. J., L. Zastoupil, S. R. Wesolowski, D. A. Goldstrohm, B. Strahan, M. Cree-Green, M. Sheffield-Moore, G. Meschia, W. W. Hay, and R. B. Wilkening. 2018. Skeletal muscle protein accretion rates and hindlimb growth are reduced in late gestation intrauterine growth-restricted fetal sheep. The Journal of physiology 596(1):67-82.

Sadeghi, A., A. Rostamirad, S. Seyyedebrahimi, and R. Meshkani. 2018. Curcumin ameliorates palmitate-induced inflammation in skeletal muscle cells by regulating JNK/NF-kB pathway and ROS production. Inflammopharmacology 26(5):1265-1272.

Sako, Y., and V. E. Grill. 1990. A 48-Hour Lipid Infusion in the Rat Time-Dependently Inhibits Glucose-Induced Insulin-Secretion and B-Cell Oxidation through a Process Likely Coupled to Fatty-Acid Oxidation. Endocrinology 127(4):1580-1589. doi: DOI 10.1210/endo-127-4-1580

Saltiel, A. R., and C. R. Kahn. 2001. Insulin signalling and the regulation of glucose and lipid metabolism. Nature 414(6865):799-806.

Sandri, M., L. Barberi, A. Bijlsma, B. Blaauw, K. Dyar, G. Milan, C. Mammucari, C. Meskers, G. Pallafacchina, and A. Paoli. 2013. Signalling pathways regulating muscle mass in ageing skeletal muscle. The role of the IGF1-Akt-mTOR-FoxO pathway. Biogerontology 14(3):303-323.

Schiaffino, S., and C. Reggiani. 2011. Fiber types in mammalian skeletal muscles. Physiological reviews 91(4):1447-1531.

Schultz, E. 1989. Satellite cell behavior during skeletal muscle growth and regeneration. Medicine and science in sports and exercise 21(5 Suppl):S181-186.

Scott, W., J. Stevens, and S. A. Binder–Macleod. 2001. Human skeletal muscle fiber type classifications. Physical therapy 81(11):1810-1816.

Smith, G., J. Savell, H. Dolezal, T. Field, D. Gill, D. Griffin, D. Hale, J. Morgan, S. Northcutt, and J. Tatum. 1995. The final report of the national beef quality audit. Colorado State Univ., Fort Collins

Soto, S. M., A. C. Blake, S. R. Wesolowski, P. J. Rozance, K. B. Barthels, B. Gao, B. Hetrick, C. E. McCurdy, N. G. Garza, and W. W. Hay Jr. 2017. Myoblast replication is reduced in the IUGR fetus despite maintained proliferative capacity in vitro. The Journal of endocrinology 232(3):475.

Supramaniam, V., G. Jenkin, J. Loose, E. Wallace, and S. Miller. 2006. Basic science: Chronic fetal hypoxia increases activin A concentrations in the late-pregnant sheep. BJOG: An International Journal of Obstetrics & Gynaecology 113(1):102-109.

Swanson, R. M., R. G. Tait, B. M. Galles, E. M. Duffy, T. B. Schmidt, J. L. Petersen, and D. T. Yates. 2020. Heat stress-induced deficits in growth, metabolic efficiency, and cardiovascular function coincided with chronic systemic inflammation and hypercatecholaminemia in ractopamine-supplemented feedlot lambs. J Anim Sci 98(6)doi: 10.1093/jas/skaa168

Symonds, M., J. Bird, C. Sullivan, V. Wilson, L. Clarke, and T. Stephenson. 2000. Effect of delivery temperature on endocrine stimulation of thermoregulation in lambs born by cesarean section. Journal of Applied Physiology 88(1):47-53.

Symonds, M., M. Bryant, L. Clarke, C. Darby, and M. Lomax. 1992. Effect of maternal cold exposure on brown adipose tissue and thermogenesis in the neonatal lamb. The Journal of Physiology 455(1):487-502.

Thiruvenkadan, A., K. Karunanithi, J. Muralidharan, and R. N. Babu. 2011. Genetic analysis of pre-weaning and post-weaning growth traits of Mecheri sheep under dry land farming conditions. Asian-Australasian Journal of Animal Sciences 24(8):1041-1047.

Thoma, A., and A. P. Lightfoot. 2018. NF-kB and inflammatory cytokine signalling: role in skeletal muscle atrophy, Muscle Atrophy. Springer. p. 267-279.

Thorn, S. R., P. J. Rozance, L. D. Brown, and W. W. Hay. 2011. The intrauterine growth restriction phenotype: fetal adaptations and potential implications for later life insulin resistance and diabetes. In: Seminars in reproductive medicine. p 225-236.

Tornatore, L., A. K. Thotakura, J. Bennett, M. Moretti, and G. Franzoso. 2012. The nuclear factor kappa B signaling pathway: integrating metabolism with inflammation. Trends in cell biology 22(11):557-566.

USDA. 2017. Overview of U.S. Livestock, Poultry, and Aquaculture Production in 2017. National Agricultural Statistics Service-USDA, National Agricultural Statistics Service-USDA.

Vandenburgh, H. H., P. Karlisch, J. Shansky, and R. Feldstein. 1991. Insulin and IGF-I induce pronounced hypertrophy of skeletal myofibers in tissue culture. American Journal of Physiology-Cell Physiology 260(3):C475-C484.

Verhaegh, B., F. de Vries, A. Masclee, A. Keshavarzian, A. de Boer, P. Souverein, M. Pierik, and D. Jonkers. 2016. High risk of drug-induced microscopic colitis with concomitant use of NSAID s and proton pump inhibitors. Alimentary pharmacology & therapeutics 43(9):1004-1013.

Von Deutsch, D. A., I. K. Abukhalaf, L. E. Wineski, H. Y. Aboul-Enein, S. A. Pitts, B. A. Parks, R. A. Oster, D. F. Paulsen, and D. E. Potter. 2000. β-Agonist-induced alterations in organ weights and protein content: Comparison of racemic clenbuterol and its enantiomers. Chirality: The Pharmacological, Biological, and Chemical Consequences of Molecular Asymmetry 12(8):637-648.

Wallace, J. M., D. A. Bourke, R. P. Aitken, J. S. Milne, and W. W. Hay Jr. 2003. Placental glucose transport in growth-restricted pregnancies induced by overnourishing adolescent sheep. The Journal of physiology 547(1):85-94.

Wallace, L. 1948. The growth of lambs before and after birth in relation to the level of nutrition. The Journal of Agricultural Science 38(3):243-302.

Wang, Q. A., C. Tao, R. K. Gupta, and P. E. Scherer. 2013. Tracking adipogenesis during white adipose tissue development, expansion and regeneration. Nature medicine 19(10):1338-1344.

White, R. B., A.-S. Biérinx, V. F. Gnocchi, and P. S. Zammit. 2010. Dynamics of muscle fibre growth during postnatal mouse development. BMC developmental biology 10(1):21.

Wigmore, P., and N. Stickland. 1983. Muscle development in large and small pig fetuses. Journal of anatomy 137(Pt 2):235.

William Tank, A., and D. Lee Wong. 2011. Peripheral and central effects of circulating catecholamines. Comprehensive Physiology 5(1):1-15.

Wu, G., F. Bazer, J. Wallace, and T. Spencer. 2006. Board-invited review: intrauterine growth retardation: implications for the animal sciences. J. Anim. Sci. 84(9):2316-2337.

Yang, L.-K., and Y.-X. Tao. 2019. Physiology and pathophysiology of the β3-adrenergic receptor. Progress in molecular biology and translational science 161:91-112.

Yates, D., A. Green, and S. W. Limesand. 2011a. Catecholamines mediate multiple fetal adaptations during placental insufficiency that contribute to intrauterine growth restriction: lessons from hyperthermic sheep. Journal of pregnancy 2011

Yates, D., A. Macko, M. Nearing, X. Chen, R. Rhoads, and S. W. Limesand. 2012a. Developmental programming in response to intrauterine growth restriction impairs myoblast function and skeletal muscle metabolism. Journal of pregnancy 2012

Yates, D. T., C. N. Cadaret, K. A. Beede, H. E. Riley, A. R. Macko, M. J. Anderson, L. E. Camacho, and S. W. Limesand. 2016. Intrauterine growth-restricted sheep fetuses exhibit smaller hindlimb muscle fibers and lower proportions of insulin-sensitive Type I fibers near term. American Journal of Physiology-Regulatory, Integrative and Comparative Physiology 310(11):R1020-R1029.

Yates, D. T., L. E. Camacho, A. C. Kelly, L. V. Steyn, M. A. Davis, A. T. Antolic, M. J. Anderson, R. Goyal, R. E. Allen, and K. K. Papas. 2019a. Postnatal β2 adrenergic treatment improves insulin sensitivity in lambs with IUGR but not persistent defects in pancreatic islets or skeletal muscle. The Journal of physiology 597(24):5835-5858.

Yates, D. T., L. E. Camacho, A. C. Kelly, L. V. Steyn, M. A. Davis, A. T. Antolic, M. J. Anderson, R. Goyal, R. E. Allen, K. K. Papas, W. W. Hay, Jr., and S. W. Limesand. 2019b. Postnatal beta2 adrenergic treatment improves insulin sensitivity in lambs with IUGR but not persistent defects in pancreatic islets or skeletal muscle. J Physiol 597(24):5835-5858. doi: 10.1113/JP278726

Yates, D. T., D. S. Clarke, A. R. Macko, M. J. Anderson, L. A. Shelton, M. Nearing, R. E. Allen, R. P. Rhoads, and S. W. Limesand. 2014. Myoblasts from intrauterine growth-restricted sheep fetuses exhibit intrinsic deficiencies in proliferation that contribute to smaller semitendinosus myofibres. The Journal of physiology 592(14):3113-3125.

Yates, D. T., A. S. Green, and S. W. Limesand. 2011b. Catecholamines mediate multiple fetal adaptations during placental insufficiency that contribute to intrauterine growth restriction: lessons from hyperthermic sheep. Journal of pregnancy 2011

Yates, D. T., A. R. Macko, M. Nearing, X. Chen, R. P. Rhoads, and S. W. Limesand. 2012b. Developmental programming in response to intrauterine growth restriction impairs myoblast function and skeletal muscle metabolism. J Pregnancy 2012:631038. doi: 10.1155/2012/631038

Yates, D. T., J. L. Petersen, T. B. Schmidt, C. N. Cadaret, T. L. Barnes, R. J. Posont, and K. A. Beede. 2018a. ASAS-SSR Triennnial Reproduction Symposium: Looking Back and Moving Forward-How Reproductive Physiology has Evolved: Fetal origins of impaired muscle growth and metabolic dysfunction: Lessons from the heat-stressed pregnant ewe. J Anim Sci 96(7):2987-3002. doi: 10.1093/jas/sky164

Yates, D. T., J. L. Petersen, T. B. Schmidt, C. N. Cadaret, T. L. Barnes, R. J. Posont, and K. A. Beede. 2018b. ASAS-SSR Triennnial Reproduction Symposium: Looking

Back and Moving Forward—How Reproductive Physiology has Evolved: Fetal origins of impaired muscle growth and metabolic dysfunction: Lessons from the heat-stressed pregnant ewe. Journal of Animal Science 96(7):2987-3002.

Yuen, B. S. J., P. C. Owens, J. R. McFarlane, M. Symonds, L. J. Edwards, K. G. Kauter, and I. C. McMillen. 2002. Circulating leptin concentrations are positively related to leptin messenger RNA expression in the adipose tissue of fetal sheep in the pregnant ewe fed at or below maintenance energy requirements during late gestation. Biology of Reproduction 67(3):911-916.

Zammit, P. S., F. Relaix, Y. Nagata, A. P. Ruiz, C. A. Collins, T. A. Partridge, and J. R. Beauchamp. 2006. Pax7 and myogenic progression in skeletal muscle satellite cells. Journal of cell science 119(9):1824-1832.

Zhang, C., Y. Li, Y. Wu, L. Wang, X. Wang, and J. Du. 2013. Interleukin-6/signal transducer and activator of transcription 3 (STAT3) pathway is essential for macrophage infiltration and myoblast proliferation during muscle regeneration. Journal of Biological Chemistry 288(3):1489-1499.

Zhang, S., P. Barker, K. J. Botting, C. T. Roberts, C. M. McMillan, I. C. McMillen, and J. L. Morrison. 2016. Early restriction of placental growth results in placental structural and gene expression changes in late gestation independent of fetal hypoxemia. Physiological reports 4(23)

Zhang, Y., J. Nicholatos, J. R. Dreier, S. J. Ricoult, S. B. Widenmaier, G. S. Hotamisligil, D. J. Kwiatkowski, and B. D. Manning. 2014. Coordinated regulation of protein synthesis and degradation by mTORC1. Nature 513(7518):440-443.